MEDNARODNA PODIPLOMSKA ŠOLA JOŽEFA STEFANA
JOŽEF STEFAN INTERNATIONAL POSTGRADUATE SCHOOL

SKENDER KABASHI

DYNAMIC MODELING OF CLIMATE CHANGE IMPACTS OF GREENHOUSE GAS REDUCTION WITH RENEWABLE ENERGY IN KOSOVO

DOCTORAL DISSERTATION

LJUBLJANA, NOVEMBER 2008

DYNAMIC MODELING OF CLIMATE CHANGE IMPACTS OF GREENHOUSE GAS REDUCTION WITH RENEWABLE ENERGY IN KOSOVO

Doctoral Dissertation
Jožef Stefan International Postgraduate School
Ljubljana, Slovenia, November 2008

Supervisor: *Prof. Dr. Ivo Šlaus*

Co-supervisor: *Prof. Dr. Aleksander Zidanšek*

Evaluation Board:

Prof. Dr. Robert Blinc, Chairman, Jožef Stefan Institute and Jožef Stefan International Postgraduate School, Ljubljana, Slovenia

Prof. Dr. Lojze Sočan, Faculty of Social Sciences, University of Ljubljana, Ljubljana, Slovenia

Prof. Dr. Naim H. Afgan, Instituto Superior Técnico, Lisbon, Portugal

Skender Kabashi

DYNAMIC MODELING OF CLIMATE CHANGE IMPACTS OF GREENHOUSE GAS REDUCTION WITH RENEWABLE ENERGY IN KOSOVO

Doctoral Dissertation

DINAMIČNO MODELIRANJE ZNIŽANJA EMISIJ TOPLOGREDNIH PLINOV NA KOSOVEM – VPLIV NA KLIMATSKE SPREMEMBE

Doktorska disertacija

Supervisor: Prof. Dr. Ivo Šlaus

Co-Supervisor: Prof. Dr. Aleksander Zidanšek

November 2008

MEDNARODNA PODIPLOMSKA ŠOLA JOŽEFA STEFANA
JOŽEF STEFAN INTERNATIONAL POSTGRADUATE SCHOOL
Ljubljana, Slovenia

Index

Abstract

Atmospheric concentration of CO_2 and other greenhouse gases (GHG) is higher than any time in the last 400000 years and growing faster than at any time in the past 18000 years. The high concentration of GHG generates radiative forcing that contributes to climate change. Energy production from fossil fuels has central role in regard to the climate change. Harnessing of renewable energy sources is vital to constraining the extent of climate change in global and regional level and in Kosovo, because climate change is regionally driven with global consequences and the energy use and production from fossil fuels has a central role to global warming.

The main task of this thesis is the modeling of climate change impacts due to greenhouse gases reduction on various dynamic systems in Kosovo such as: Mobile source emission systems and Electric power emission systems. This means the reduction of GHG with continually increasing the renewable energy and gradual replacement in long term of the fossil fuels energy with renewable energy, mainly with solar energy in its various mode: biomass, wind, hydro and direct radiation (harnessing energy from Sun light).

Firstly the impact of renewable energy on GHG reduction in global level (zero dimensional modeling of GHG reduction) is modeled and it is shown that increasing the Earth surface temperature would stop if the GHG reduction in the next 50 years would be 80% due to renewable use and new technologies. Then, the modeling is carried out regionally for Kosovo for two dynamical systems which are the main emitters of GHG (CO_2, N_2O, CH_4, $HCFC_s$, CFS_s, etc), i.e. transportation and electricity generation emissions systems.

These models incorporate environment policies and new technologies including nanotechnology that achieve EU standards which would be compatible with GHG reduction requirements (IPCC, Kyoto Protocol) ensuring a sustainable Energy Demand–Supply for Kosovo, that becomes increasingly environmentally compatible.

As a result of the energy production from lignite we have as well emission of air pollutants SO_2, NO_x and aerosols. For these pollutants we develop a model for distribution pollutant transport and visibility near the TPP (Unit A and B). The purpose of the doctoral dissertation is modeling the various dynamical GHG emissions systems in Kosovo in STELLA software, in which model we will gradually replace the fossil fuels energy sources with renewable ones and we introduce the new technology for CO_2 sequestration and high energy efficiency in transport, and also, our models predict the significant reduction on GHG in long term prediction scenarios.

Povzetek

Koncentracija ogljikovega dioksida in drugih toplogrednih plinov v atmosferi je najvišja v zadnjih 400000 letih in raste najhitreje v zadnjih 18000 letih. Visoka koncentracija toplogrednih plinov vpliva na klimatske spremembe. Pri tem je zelo pomemben vpliv energije iz fosilnih goriv. Zato je pomembno, da omejimo rabo fosilnih goriv.

Glavna naloga te disertacije je modeliranje klimatskih sprememb in vpliva zmanjašanja emisij toplogrednih plinov zaradi mobilnih virov in proizvodnje električne energije na Kosovem, predvsem s sončno energijo v različnih oblikaj: biomasa, veter, hidroenergija in neposredno pridobivanje energije iz sončne svetlobe.

0-dimenzionalni model vpliva obnovljive energije na zmanjšanje emisij toplogrednih plinov je pokazal, da bi se dviganje povprečne površinske temperature na Zemlji ustavilo, če bi emisije toplogrednih plinov v 50 letih zmanjšali za 80% z rabo obnovljivih virov in novih tehnologij. Na Kosovu sem modeliral dva sistema, ki sta glavna vira emisij toplogrednih plinov, in sicer transport in proizvodnjo elektrike. Ti modeli upoštevajo okoljske politike in nove tehnologije, vključno z nanotehnologijo. Na ta način bi Kosovo izpolnilo mednarodne zaveze za znižanje emisij in zagotovilo trajnostno rabo energije.

Zaradi proizvodnje energije iz lignite so pomembne tudi emisije polutantov, kot so SO_2, NO_x in aerosoli. Za te polutante sem razvil model porazdelitve polutantov v bližini termoelektrarn. V disertaciji sem tudi modeliral različne dinamične sisteme emisij toplogrednih plinov s programom STELLA. V modelu sem upošteval postopno zamenjavo fosilnih goriv z obnovljivimi viri ter vpeljavo novih tehnologij za zajemanje CO_2 in večjo energijsko učinkovitost v transportu. Model tudi napove bistveno zmanjšanje emisij toplogrednih plinov v scenarijih dolgoročnih napovedi.

Abbreviations

Abbreviation	Explanation
GHG	Greenhouse Gases
IPCC	International Panel of Climate Change
ESTAP	Energy Sector Technical Assistance Project
MEM	Ministry of Energy and Mining
KOSTS	Kosovo Transmission System
KEK	Kosovo Electricity Corporate
TPP	Thermo Power Plant
HPP	Hydro Power Plant
IJS	Institute Josef Stefan
AU	Astronomical Unit
CFCs	Chlorofluorocarbons
HCFCs	Hydro chlorofluorocarbons
HFCs	Hydro fluorocarbons
PFCs	Per halocarbons
IEA	International Energy Agency
RD&D	Research, Development and Demonstration
UNFCCC	United Nations Framework Convention on Climate Change
CAFE	Corporate Average Fuel Economy
MVRAK	Motor Vehicle Registration Authority of Kosovo
EPCT	Energy Power Community Treaty

1 Introduction

The main task of this thesis is the modeling of climate change impacts due to greenhouse gases (GHG) reduction on various dynamic systems in Kosovo such as: Mobile source emission systems and Electric power emission systems. This means the reduction of green house gases (GHG) with continually increasing the renewable energy and gradual replacement in long term the fossil fuels of energy with renewable energy, mainly with solar energy in its various mods: biomass, wind, hydro and direct radiation (harnessing energy from Sun light).

Harnessing of renewable energy sources is vital to constraining the extent of climate change in global and regional level and in Kosovo, because climate change is regionally driven with global consequences and the energy use and production from fossil fuels has a central role to global warming.

Firstly the impact of renewable energy in GHG reduction on global level (zero dimensional modeling of GHG reduction) is modeled and it is shown that increasing the Earth surface temperature would stop if the GHG reduction the next 50 years would be 80% due to renewable use and new technologies. The initial time value for this model is taken year 2005. Then, the modeling is carried out regionally for Kosovo for two dynamical systems which are the main emitters of GHG (CO_2, N_2O, CH_4, $HCFC_s$, CFS_s, etc), i.e. transportation and electricity generation emissions systems.

These models incorporate environment policies and new technologies including nanotechnology that achieve EU standards which would be compatible with GHG reduction requirements (IPCC, Kyoto Protocol) ensuring a sustainable Energy Demand–Supply for Kosovo, that becomes increasingly environmentally compatible.

In Modeling the Dynamic Mobile Source Emission Systems in Kosovo, at first emissions of greenhouse gases and air pollution from two types of vehicles: light and heavy vehicles (cars, buses, tractors, vans, trailers, etc.), is calculated. The initial data values are taken from ESTAP (Energy Sector Technical Assistance Project) Kosovo and by the Motor Vehicle Registration Authority of Kosovo. For initial time we have taken the year 2000, and for age of vehicles we suppose that 90% of them are of the age >10 years. We have divided the vehicles in five groups according to the age: 0-2 years, 3-5 years, 6-8 years, 9-11 years and >11 years. For each cohort of vehicles we have input scrap page rate r_k factor (fraction of vehicles scraped while in the cohort) and increase rate factor while in cohort $1+p_j(t)$ (imported vehicles per year for each cohort). The time dependence change for average kilometers traveled, emission factor for each GHG, total number of vehicles and increasing rate factor while in cohort are the nonlinear functions and this nonlinearity depends on many factors (renewable energy potential, new technology and environmental policies in Kosovo), whereas the scrap factor does not depend on time. The initial value data for average kilometers traveled, emission factor for each of GHG and total number of vehicles are taken from sources: The IPPC Directive, The European Commission, 1996. See also: http://www.ec.europa.eu/environment/ipcc/index.htm
http://en.wikipedia.org/wiki/List_of_countries_by_carbon_dioxide_emissions_per_capita
http://enrin.grida.no/htmls/kosovo/SoE/energy.htm. MEM(Ministry of Energy and Mining) https://www.ks-gov.net/mem.Total emission of GHG is calculated for the year interval t=2000-2025

In Modeling the Electricity Demand–Supply and GHG reduction with renewable energy in Kosovo at first for developing the electricity demand forecast model for Kosovo we used the STELLA software. Historical data from KOSTT and KEK are the most important source for demand forecast.

For the yearly demand forecast a distinction is made between: residential demand, heavy industrial and light industrial demand and service demand.

We have considered the year 2000 as initial condition for demand-supply forecast model of Kosovo. For electricity emission system we develop two scenarios.

According to scenario 1, electric power is produced 95%-97% from the lignite and only 3-5% from renewable resources for the time period 2000-2025. As a result of the energy production from lignite we have an increase in emission of GHG.

According to scenario 2, the renewable energy will increase from the year 2015 to the year 2025 from 8% to 14% of total energy production in Kosovo and the reduction of GHG up to 20% in comparison with the year 2005. As a result of the energy production from lignite we have as well emission of air pollutants SO_2, NO_x and aerosols. For these pollutants we develop a model for distribution pollutant transport and visibility

near the TPP (Unit A and B). The purpose of the doctoral dissertation is modeling the various dynamical GHG emissions systems in Kosovo in STELLA software, in which model we will gradually replace the fossil fuels energy sources with renewable ones and we introduce the new technology for CO_2 sequestration and high energy efficiency in Transport, and also, our models predict the significant reduction on GHG in long term prediction scenarios.
This aim is achieved and it is documented by several scientific activities and publications.
This doctoral dissertation aims to open the road (perspective) in the future for other scientific studies. Continuing to make an integrated Energy-Climate model for Kosovo this model will incorporate environment policies and new technologies including nanotechnology, that achieve EU standards which would be compatible with GHG reduction requirements ensuring a sustainable Energy Demand–Supply for Kosovo that becomes increasingly environmentally compatible. Models that we did are the first ones, with original data and results, with the predictions which are regional, but accepted globally (IPCC 2007, Al Gore, *An Inconvenient Truth: The Planetary Emergency of Global Warming and What We Can Do About It*, the Nobel prize winner).Our models according to participation of renewable energy in total energy, predict high emission of GHG in short term from year 2000 to the year 2010, both in mobile source emission system-transport and electricity power emission system in Kosovo. Because participation of renewable energy in this period is only 2-4%, there are no policy options and no new technology options.
In middle term, 2010 to 2015,there is stabilization and slight decreases in GHG emission. From 2010 to 2015 renewable energy slightly increases from 5-8% in total electricity power production and in energy use in transport. Policy and technology options for reducing GHG and air pollution take place.
In long term from year 2015 to 2025 we will have gradual reduction in GHG by 20% in comparison with the year 2005. During this time renewable energy gradually increases to 14% of the overall energy. Policy and technology options for reducing GHG and air pollution achieve EU standards which would be compatible with GHG reduction requirements (IPCC, Kyoto Protocol) (see:The Kyoto protocol - A brief summary) ensuring a sustainable Energy Demand–Supply for Kosovo that becomes increasingly environmentally compatible. Emission of sulfur dioxide (SO_2) generated at coal power plants (unit A, B and from new TPP unit C) will be continually increasing till to the year 2013 and increased concentration of SO_2 due to the new source will potentially affect SO_3^- and SO_4^{2-} at the receptor site that ultimately transforms it into sulfuric acid (H_2SO_4) which is deposited as acid rain. After 2013 in our pollution-transport model we incorporate SO_2 control technology and policy that would reduce SO_2 emissions and as a result acid rains are less possible.
As a consequence of air pollutants and aerosols near coal power plants (unit A, B) until 2013, the visibility is less then in other localities in Kosovo. After 2017 when TPP unit A falls out of use and new TPP unit C due to the advanced technology replaces it, the emission of aerosols will gradually decrease and the visibility increase till to 2025.
Models presented here have a particular importance because these are the first models of this field for Kosovo and in addition they notify the public and political structures how and where to take into account the consequences that GHG and air pollutants on national, regional and global level.
From the results of these models, the variables that drive GHG and air pollutant reduction are identified. Modeling is made in STELLA software (STELLA. Copyright©1985-2007 by ISEE Systems, Inc. www.iseesystems.com)
Each of the systems which are modeled is nonlinear and the dynamical systems are presented with systems of nonlinear differential equations. Their solution is found by numerical methods, either Euler's method or Runge-Kutta method.

2 Physical Foundations

2.1 Climate and Energy

Climate is often defined as average weather (Peixoto, P. J and Oort.H. A. 1992).
Climate is usually described in terms of the mean and variability of temperature, precipitation and wind over a period of time, ranging from months to millions of years (the classical period is 30 years). The climate system evolves in time under the influence of its own internal dynamics and due to changes in external factors that affect climate (called 'forcings'). External forcings include natural phenomena such as volcanic eruptions and solar variations, as well as human-induced changes in atmospheric composition. Solar radiation powers the climate system.

2.1.1 The Climate System and its Components

The climate system **(S**) is a composite system consisting of five major interactive adjoin components: the atmosphere (**A)**, the hydrosphere (**H)** with the ocean (**O**), the cryosphere
(**C**),the lithosphere (**L**),and biosphere (**B**), i.e.,

$$\mathbf{S} \equiv \mathbf{A} \cup \mathbf{H} \cup \mathbf{C} \cup \mathbf{L} \cup \mathbf{B} \cup \mathbf{O} \qquad (1)$$

As shown schematically in Figure 1, all the subsystems are open and nonisolated system for energy, but a closed system for the exchange of matter with outer space. The atmosphere, hydrosphere, cryosphere, and biosphere act as a cascading system linked by complex physical processes involving fluxes of energy, momentum, and matter across the boundaries and generating numerous feedback mechanisms (Hansen et al., 1984). The components of the climatic system are heterogeneous thermo – hydrodynamical systems, which can be characterized by their chemical composition and their thermodynamic and mechanical states. The thermodynamic states are specified, in general, by certain intensive variables (e.g., temperature, pressure, specific humidity, specific energy, density, and salinity) (Holton, 1992) whereas the mechanical state are specified, in general, by certain intensive variables (e.g., temperature, pressure, specific humidity, specific energy, density, and salinity) whereas the mechanical state is defined by other intensive variables that characterize the motions (e,g., forces and velocities) (Hartmann, 1994)

2.1.1.1 Atmosphere

The Earth's atmosphere is a comparatively thin film of a gaseous mixture which is distributed almost uniformly over the surface of the Earth. In the vertical direction, more than 99% of the, mass of the atmosphere is found below an altitude of only 30 km. The Earth's dry atmosphere is composed mainly of nitrogen (N_2, 78.1% volume mixing ratio), oxygen (O_2, 20.9% volume mixing ratio, and argon (Ar, 0.93% volume mixing ratio) (Peixoto and Abraham, 1992). These gases have only limited interaction with the incoming solar radiation and they do not interact with the infrared radiation emitted by the Earth. However there are a number of trace gases, such as carbon dioxide (CO_2), methane (CH_4), nitrous oxide (N_2 O) and ozone (O_3), which do absorb and emit infrared radiation. These so called greenhouse gases, with a total volume mixing ratio in dry air of less than 0.1% by volume, play an essential role in the Earth's energy budget. Moreover the atmosphere contains water vapor (H_2O), which is also a natural greenhouse gas. Its volume mixing ratio is highly variable, but it is typically in the order of 1%. Because these greenhouse gases absorb the infrared radiation emitted by the Earth and emit infrared radiation up- and downward, they tend to raise the temperature near the Earth's surface. Water vapor, CO_2 and O_3 also absorb solar short-wave radiation. The atmospheric distribution of ozone and its role in the Earth's energy budget is unique. Ozone in the lower part of the atmosphere, the troposphere and lower stratosphere, acts as a greenhouse gas. Higher up in the stratosphere there is a natural layer of relatively high ozone concentration, which absorbs solar ultra-violet radiation. In this way this so-called ozone layer plays an essential role in the stratosphere's radiative balance, at the same time filtering out this potentially damaging form of radiation.

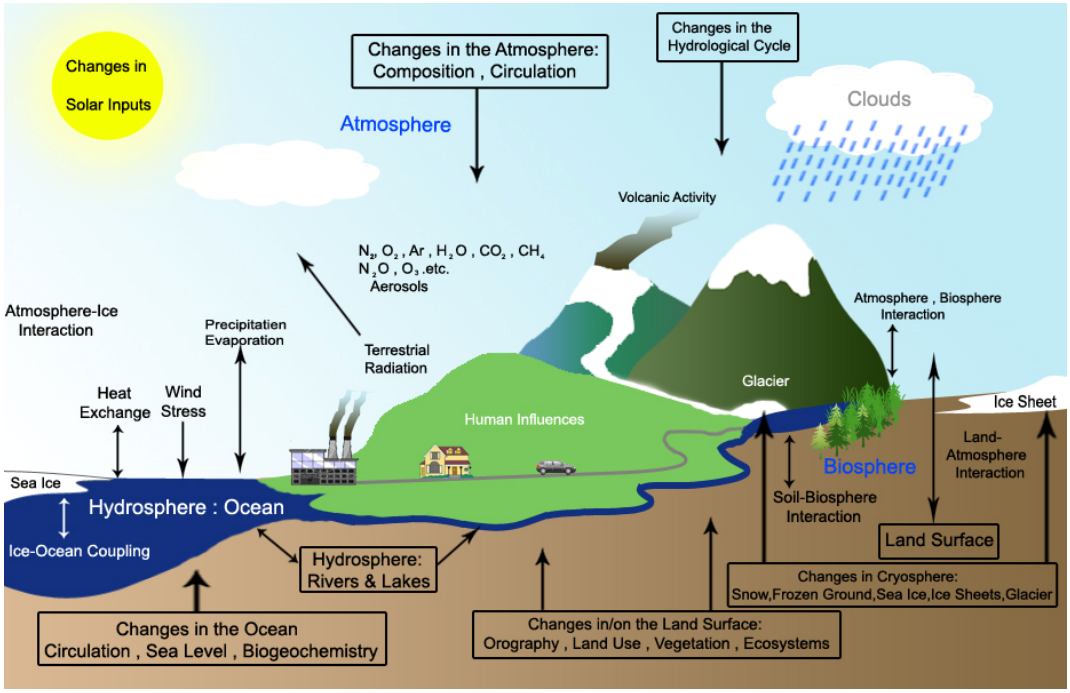

Figure 1: Schematic view of the components of the climate system, their processes and interactions

Beside these gases, the atmosphere also contains solid and liquid particles (aerosols) and clouds, which interact with the incoming and outgoing radiation in a complex and spatially very variable manner. The most variable component of the atmosphere is water in its various phases such as vapor, cloud droplets, and ice crystals. Water vapor is the strongest greenhouse gas. For these reasons and because the transition between the various phases absorb and release much energy, water vapor is central to the climate and its variability and change.

2.1.1.2 Hydrosphere

The hydrosphere is the component comprising all liquid surface and subterranean water, both fresh water, including rivers, lakes and aquifers, and saline water of the oceans and seas. Fresh water runoff from the land returning to the oceans in rivers influences the ocean's composition and circulation. The oceans cover approximately 70% of the Earth's surface. They store and transport a large amount of energy and dissolve and store great quantities of carbon dioxide. Their circulation, driven by the wind and by density contrasts caused by salinity and thermal gradients, is much slower than the atmospheric circulation. Mainly due to the large thermal inertia of the oceans, they damp vast and strong temperature changes and function as a regulator of the Earth's climate and as a source of natural climate variability, in particular on the longer time-scales.

2.1.1.3 Cryosphere

The cryosphere, including the ice sheets of Greenland and Antarctica, continental glaciers and snow fields, sea ice and permafrost, derives its importance to the climate system from its high reflectivity (albedo) for solar radiation, its low thermal conductivity, its large thermal inertia and, especially, its critical role in driving deep ocean water circulation. Because the ice sheets store a large amount of water, variations in their volume are a potential source of sea level variation

2.1.1.4 Lithosphere

The lithosphere includes the continents whose topography affects air motions and the ocean floor. There is a strong interaction of the lithosphere with the atmosphere with the atmosphere through the transfer of mass, angular momentum, and sensible heat, as well as through the dissipation of kinetic energy by friction in the atmosphere boundary layer. The transfer of mass occurs mainly in the form of water vapor, rain and snow, and to a lesser extent, in the form of other particles and dust. Volcanoes throw matter and energy from the lithosphere into the atmosphere, thereby increasing the turbidity of the air. The added particulate matter, as well as the ejected sulfur-bearing gases that may condense in the stratosphere, together forming what is called aerosol, may have an important effect on the radiation balance of the atmosphere and therefore on the Earth's climate There is also a large-scale transfer of angular momentum between the oceans presumably through the action of torques between the oceans and the continents.

2.1.1.5 Biosphere

The biosphere comprises the terrestrial, the continental fauna, and the flora and fauna of the oceans. The vegetation alters the surface roughness, surface albedo, evaporation, runoff, and field capacity of the soil. Furthermore, the biosphere influences the carbon dioxide balance in the atmosphere and oceans through photosynthesis and respiration. On the whole, the biosphere is sensitive changes in the atmospheric climate and it is through the signature of these changes in fossils, tree rings, pollen, etc., during past ages that we obtain information on paleoclimates of the Earth.

As this point we may mention the human interaction with the climatic system through such activities as agriculture, urbanization, industry, pollution, etc.

2.1.1.6 Climate variability

The climate system evolves in time under the influence of its own internal dynamics and due to changes in external factors that affect climate (called 'forcings'). External forcings include natural phenomena such as volcanic eruptions and solar variations, as well as human-induced changes in atmospheric composition. Solar radiation powers the climate system. There are three fundamental ways to change the radiation balance of the Earth:
1. By changing the incoming solar radiation (a) in the intensity of solar irradiance (Hays, J (ed.), 1997.) ;
(b) By changes in Earth's orbit (eccentricity of the orbit, axial precession and obliquity of the ecliptic) (Imbrie and Imbrie 1980) ;
(c) in the rate of rotation of the Earth or in the Sun itself; (Hays et al., 1976) ;
2. By changing the fraction of solar radiation that is reflected (albedo)
(a) variations in atmospheric composition (mixing rations of carbon dioxide and ozone, aerosol loading etc.) due to volcanic eruptions and human activity;
(b) variations of the land surface due to land use (deforestation, desertification, etc);
(c) long–term changes of tectonic factors such as continental drift, mountain -building processes, polar wandering, etc, and
3. By altering the long wave radiation from Earth back towards space (e.g., by changing greenhouse gas concentrations and by pollution).
For a linear system the externally forced variations would lead to a simple relationship of cause and effect, the forcing an oscillatory process the response of the system would have exactly the same frequency.
Climate variability results form complex interactions of forced and free variations because the climate system is a dissipative, highly nonlinear system with many sources of instabilities. The interactive and often nonlinear nature of the instabilities and the feedback mechanisms of the climatic system make it very difficult to obtain a straightforward interpretation of cause and effect.

2.1.2 Feedback processes in the climate system

Of particular importance in open systems such as the components of the climatic system is feedback.

2.1.2.1 Definition of Feedback

Feedback loop in a dynamic system can be defined (Deaton and Winebrake, 2000), as a closed-loop circle of cause and effect in which "conditions" in one part of the system cause "results" elsewhere in the system which in turn act on the original" conditions" to change them. This is represented schematically in Figure 2.

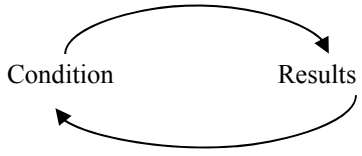

Figure 2: Feedback: A closed-loop circle of cause and effect

Feedback is very common in dynamic systems. There are two types of feedbacks loops that can occur. These are (1) positive feedback (also called reinforcing feedback) and (2) negative feedback (also called counteracting feedback). Both types are common in the environment.
In fact, being able to recognize and distinguish between these two types in a real-life environmental system can lead to significant understandings of how the system works.

2.1.2.2 Positive Feedback

Positive feedback (also called reinforcing feedback) exists whenever changes at one point on a feedback loop eventually work their way back to eventually run out of control. Many environmental problems are

closely associated with naturally occurring positive feedback loops whose influence on the overall system has been accentuated by changes due to human activity.
One example of a positive feedback loop can be found in models of global climate change. It is hypothesized that increases in carbon dioxide (CO_2) emissions into our atmosphere will cause the Earth's global temperature to rise. This in turn will reduce the ability of the Earth's oceans to hold gaseous CO_2 thereby causing the oceans to release additional CO_2 into the atmosphere. This additional increase in atmospheric CO_2 will lead to further warming, which will then lead to even more CO_2 released form the oceans, and so on. According to this theory, increased CO_2 levels (e.g., form the uses of fossil fuels) could lead to a "runaway" accumulation of CO_2 in the atmosphere, thereby leading to increased global temperatures and eventual breakdown of the world's ecosystems. The diagram this feedback loop is shown in Figure 3.

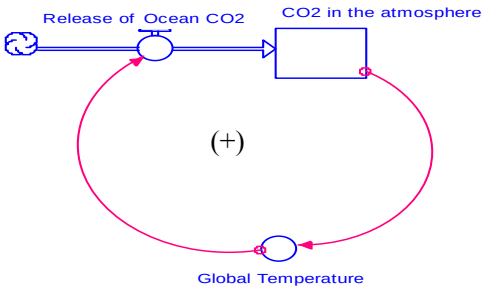

Figure 3: Global warming positive feedback loop

2.1.2.3 Negative Feedback

Negative feedback (also called counteracting feedback) exists whenever changes at one point on a feedback loop eventually work their way back through the system to counteract the original change. Such systems tend to be self-regulating and are not as prone to run out of control. Negative feedback loops help many environmental systems remain stable. In fact, some environmental problems can be attributed to the breakdown of naturally occurring negative feedback loops. Whenever these loops do break down, then the system can lose its stability and can begin to behave in ways that lead to an eventual collapse of the system. This concept is used in electrical engineering. The feedback mechanisms act as internal controls of the system and result from a special coupling or mutual adjustment among two or more subsystems. Part of the output returns to serve as an input again, so that the net response of the system is altered; the feedback mechanism may act either to amplify the final output (positive feedback) or to dampen it (negative feedback). There are a large number of such mechanisms operating within the various components of the climatic system and between the subsystems.

2.1.2.4 Feedback Effects

In addition to radiative forcing due to enhanced concentration of GHG, the modeling of global warming is further complicated because a rising surface temperature inevitably will cause secondary effects, called feedback effects. This can be expressed by the proportionality

$$\Delta T_s \infty \Delta\phi \ / \beta \tag{2}$$

Where ΔT_s is the rise of surface temperature, $\Delta\phi$ is radiative forcing due e.g. to GHG alone and β is a factor accounting for the feedback effect. If $\beta < 1$ the feedback is positive which will increase the surface temperature even more than by increasing greenhouse gas concentrations alone? If $\beta > 1$ the feedback is negative which will cause a smaller surface temperature increase? There are several feedback effects possible e.g.: water vapor, cloud, aerosol, ice-albedo, and ocean circulation feedbacks.

2.1.2.5 Ice-Albedo Feedback

As the Earth's surface warms due to increased GHG concentrations, the fringes of the Arctic and Antarctic ice caps may melt. Glaciers, which already are receding in this interglacial period, may recede even faster. Because ice has a higher albedo (reflects more sunlight) (Held, I.M and M.J Suarez, 1974) than water and land, the disappearance of ice will lead to a decrease in the Earth's albedo. This will cause the Earth's radiative temperature T_E, and concomitantly the surface temperature T_S, to increase slightly. The ice-albedo effect may add 20% to the GHG-caused surface warming $(\beta \approx 0.8)$.

Altogether, the various feedback effects may double the GHG-caused global warming.

The reflectivity (albedo) for solar radiation is a very important factor in the energy balance. The high albedo values of snow and ice make them a dominant factor in the climate mainly in the polar regions. The extent of ice and snow depends largely on the near-surface temperature of the air. If the temperature decreases for some reason the amount of snow and ice will generally increase or last longer, which will lead to an increase of the planetary albedo. Then more solar radiation will be reflected and less energy will be available to heat the atmosphere, and the temperature of the atmosphere-snow/ice system will further decrease.

On the other hand, suppose that the snow or ice cover decreases in extent, then because of the decreased albedo less solar radiation will be reflected and the temperature will increase leading to a further decrease of snow cover are examples of positive feedbacks (see Figure 3).

Changes in vegetation cover can also cause variations in the surface albedo leading to important local feedback effects, such as exemplified by progressive desertification

Another example of a positive feedback mechanism is the water vapor feedback.

2.1.2.6 Water Vapor Feedback

This mechanism may be the most important feedback effect. Water vapor is a strong infrared absorbing gas at wavelengths between 5 and 7 μm and above 10 μm. As the average Earth's surface temperature rises because of increasing GHG concentrations, more evaporation will occur from the vast ocean surfaces, hence the atmosphere will become laden with more water vapor; that is, the humidity will increase. This would result in stronger absorption of the outgoing far-IR radiation, thus a positive feedback. Radiative models predict that the water feedback effect may increase the GHG caused global warming by about 60% $(\beta \approx 0.6)$.An increase in surface temperature, in the absence of other changes, will cause the evaporation at the Earth's surface and the amount of water vapor in the atmosphere to increase as well. Since water vapor is a strong absorber of long-wave radiation more terrestrial radiation will be trapped, heating the lower atmosphere and leading to a further increase of temperature. If on the other hand, the temperature becomes lower due to some other reasons (e.g., ice-albedo feedback), the amount of water vapor decreases and the greenhouse effect becomes less effective.

Another way of expressing this same feedback mechanism is to accept that the time-mean relative humidity at a particular altitude tends to remain almost constant within a relatively large range of temperatures in the lower atmosphere. However while the relative humidity remains practically the same, the absolute humidity increases rapidly with temperature. Thus an increase of temperature at constant relative humidity increases the amount of water vapor in the air leading through the absorption of long-wave radiation to a further increase in the temperature at contact relative humidity increases the amount of water vapor in the air leading through the absorption of long-wave radiation to a further increase in the temperature. As an example of a negative internal feedback, we can consider the temperature-long-wave radiation coupling in the atmosphere. If the temperature-atmosphere will generally lose more long–wave radiation to space, thus reducing the temperature and attenuating the initial perturbation.

2.1.2.7 Cloud-Radiation Feedback

The feedback effect of clouds is complicated. Clouds can have both a negative and positive feedback effect. The negative effect is due to reflection by clouds can have both a negative and positive feedback to an increase of the Earth's albedo and this reducing the Earth surface temperature. The positive effect is due to the clouds reflecting the outgoing Earth's thermal radiation. The balance of the two effects is dependent on cloud characteristics, theirs altitude, and droplet or crystal size. In general, low, cumulus type clouds reflect solar radiation; a cooling effect. High-altitude cirrus type clouds reflect the Earth's radiation: a warming effect. Modeling a cloud feedback effects is highly uncertain. The cloud feedback effect will ad another 20% $(\beta \approx 0.8)$ to the surface temperature increase due to increasing GHG concentrations.

2.1.2.8 Aerosol Feedback

Similarly to clouds, natural and man-made small particles suspended in the air, called aerosols, can interfere with the incoming solar and outgoing terrestrial radiation. The average composition of aerosols is about one-third crystal material (fugitive dust from soil, sand, rocks and, shale), one-third sulfate (mainly from sulfur emissions associated with fossil fuel combustion), and one-third carbonaceous matter and nitrate (also from fossil fuel combustion). The diameter range of the aerosols is much less than a micrometer. This diameter range is more effective in scattering incoming solar radiation than in reflecting outgoing terrestrial; radiation. This, the aerosol feedback effect is thought to be negative reducing the GHG effect by 10-15% $(\beta \approx 1.1)$.The aerosols may also have an indirect feedback effect. Aerosols serve as condensation nuclei for clouds. The more aerosols in the air, the higher the probability of cloud formation. Depending on the formed cloud height, and droplet or crystal size, clouds may reflect incoming solar radiation or outgoing terrestrial radiation. This indirect effect is presently under intense study, and the resulting feedback cannot yet be assessed.

2.1.2.9 Ocean Circulation Feedback

Another possible feedback mechanism is the alteration of the ocean circulation and currents. In general, cold and highly saline water sinks to grater depth and warm, less saline water rises. The cold and larger-than-average saline waters are generated in the Arctic, as ice is formed at the surface. These waters sink to the ocean bottom and move toward the equator. There, warmer and less saline waters rise and move toward the poles completing a loop. With melting ice caps, along with an increase of precipitation at high latitudes the normal ocean circulation pattern may be altered with possible changes in the average global surface temperature. This feedback effect on average surface temperature is varying difficult to predict; it may be negative, positive, or neutral. The disruption of the ocean circulation may have other consequences, such as enhanced El Nino and changing storm system patterns.

2.1.2.10 Air-sea exchange

In this case, sea surface temperature anomalies tend to strongly affect the thermal structure of the lower atmosphere and eventually, through the atmospheric general circulation, they also affect the surface wind stresses. These anomalous wind stresses form the feedback mechanism from the atmosphere back to the oceans by generating changes in the general circulation in the oceans that, in turn, modify the sea surface temperature anomalies, closing the loop Figure 4, 5, 6, and 7.
As we have seen there are in nature many positive and negative feedback processes. However, it must be noted that a positive feedback process cannot proceed indefinitely because it would lead to runway situations that have not been observed on Earth but may have happened in the case of Venus. Therefore, compensation between positive and negative feedback processes must prevail in the mean. There is some geological evidence for catastrophic changes in the climatic state that could involve some runaway process and in which a change to a new and different climatic state occurred.

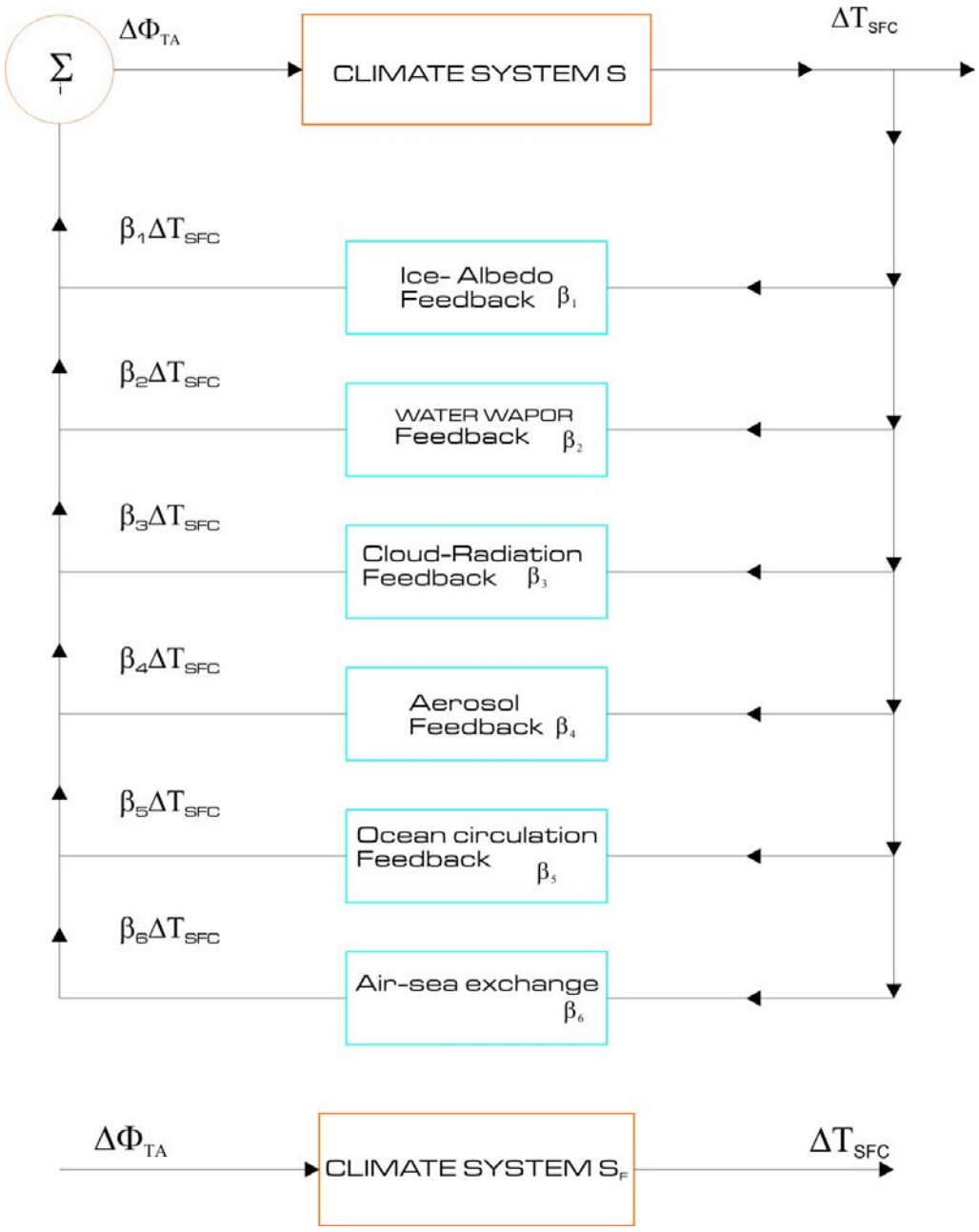

Figure 4: Examples of a set of possible feedback loops in the climate system.

Where the input is an imbalance in the net radiation at the top of the atmosphere $\Delta\Phi_{TA}$ and the output is the change in surface temperature of the Earth. The symbols S, β_1, β_2,..., β_6 and S_F represent the gain, feedback factors, and effective gain of the climate system, respectively.

Two of the feedback loops work through photosynthetic activity, as shown in Figure 5. Trees and other green plants may respond to warmer air temperature with accelerated growth. Green plant photosynthesis would lead to greater CO_2 absorption, less CO_2 in the atmosphere, less absorbed radiation and a reduction in air temperature. This is the outer loop in Figure 5. The inner loop involves an increase in air temperature followed by an increase in ocean temperature, which could lead to more rapid growth in algae phytoplankton, greater CO_2 absorption by the ocean, less CO_2 in the atmosphere, less absorbed radiation, and a reduction in air temperature.

The third loop involves the water vapor. An increase in air temperature could lead to more rapid evaporation, more water vapor in the air, and a more extensive cloud cover. A wider spread of bright white clouds leads to greater reflection of short-wave energy, a reduction in absorbed radiation, and a reduction in air temperature.
Figure 6, shows a positive loop that involves the increased water vapor that could occur with higher air temperatures. Increased water vapor could lead to greater long-wave absorption, greater total absorbed radiation, and still further increases in the air temperature.
Figure 7, shows two additional examples of positive feedback, both of which operate through the permafrost. Enormous amounts of methane are believed to be trapped in the Arctic permafrost. Methane is one of the most potent of the greenhouse gases, and scientists fear that a reduction in the area of the permafrost could release the methane into the atmosphere, where it would lead to an increase in absorbed radiation further increases in air temperature and still further reductions in the area of the permafrost. This is the outer loop in Figure 7. The inner loop in Figure 7 involves the reflective power of the permafrost. The ice sheets of the Arctic act to reflect incoming radiation. If sheets were to shrink due to higher air temperatures, we could see greater absorbed radiation, higher air temperatures and still further shrinkage of the ice sheets in the future.

.

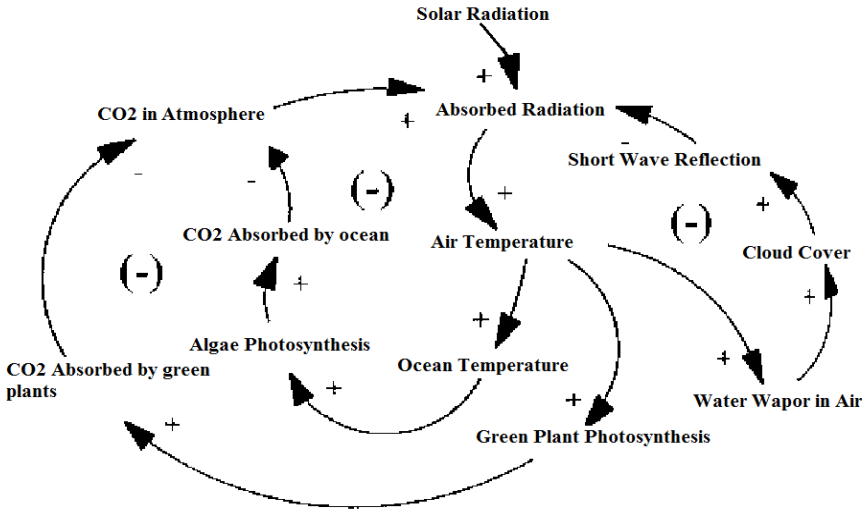

Figure 5: Three examples of negative feedback in the global warming system

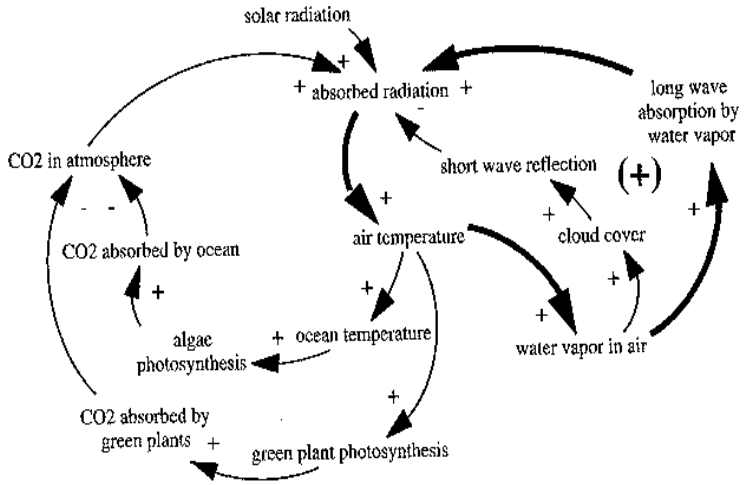

Figure 6: Positive feedback acting through long-wave absorption

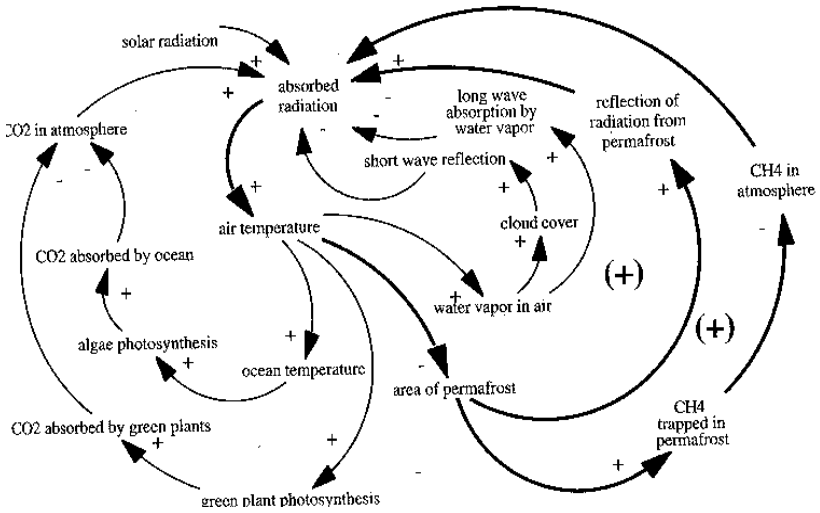

Figure 7: Additional positive loops acting through the permafrost

2.1.3 Nature of solar and terrestrial radiation

The major energy sources and skins for the Earth as a whole are the solar radiation and terrestrial radiation, respectively. The solar radiation (Hartmann, 1994), (Ramanathan et al., 1989), (Jose and Abraham, 1992), covers the entire electromagnetic spectrum form gamma and X rays, through ultraviolet, visible, and infrared radiation, to microwaves and radioactive energy transfer in the climate system range from the ultraviolet to the near infrared

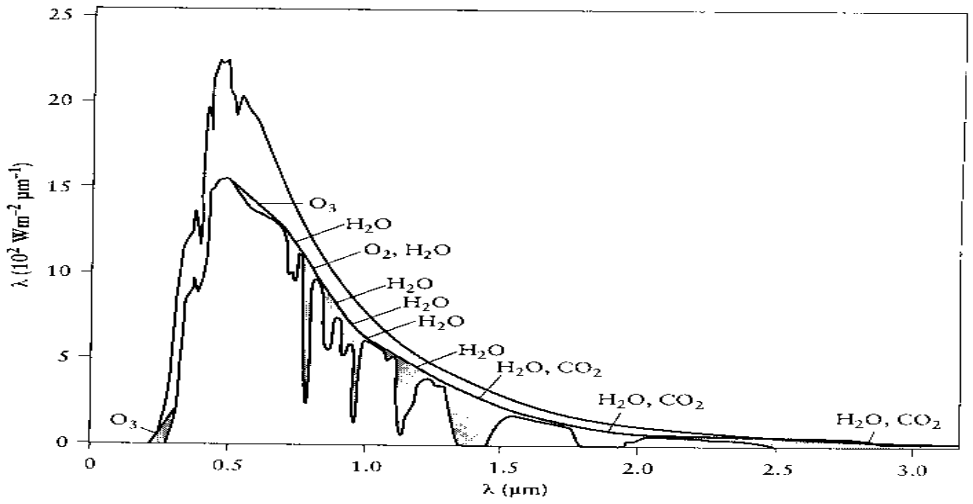

Figure 8: Spectral distribution of solar irradiation at the top of atmosphere and at sea level by average atmospheric conditions for the Sun at zenith (adapted from Gast, 1965).

The shaded areas in Figure 8 represent absorption by various atmospheric gasses. The un shaded are a between the two curves represents the portion of solar energy backscattered by the air, water vapor, dust and aerosols and reflected by clouds. For the curve at the top of the atmosphere the integral $\int_x^0 E_\lambda d\lambda = 1368 \frac{W}{m^2}$ represents the solar constant (adapted from Gast, 1965).

In order to maintain the Earth in its long-term observed state of quasi-equilibrium, the amount of absorbed energy is also in the form of radiant energy emitted by the Earth's surface and atmosphere. In fact, we know (based on Prevost's work in the late 18th century) that all bodies having a temperature above absolute zero K emit radiant energy over a large range of wavelength Figure 9. As we will see, the essentially all energy that enters the Earth's atmosphere comes from the Sun since the upward conduction of heat from the Earth's interior (due to radioactivity decay) is negligible. The incoming solar radiation is partly absorbed, partly scattered and partly reflected by the various gases of atmosphere, absorbed by oceans, lithosphere, cryosphere and biosphere and only a small part is reflected. According to the first law of thermodynamics the absorbed energy can be transformed into internal energy (heat) or it can be used to do work against the environment, appearing as potential or kinetic energy.

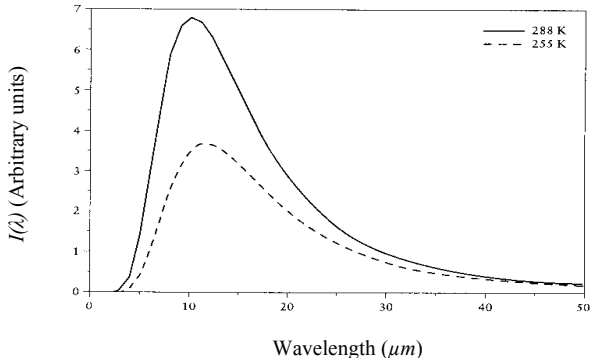

Figure 9: Radiation intensity versus wavelength for black bodies at 255 K (dashed curve) and 288 K (solid curve)

Higher the temperature of emitting body, the larger the amount of emitted energy and the shorted wavelength of its peak. Thus, due to the large difference in solar and terrestrial temperature, the incoming solar radiation terrestrial radiation has its peak in the visible range $0.5\mu m$, whereas the outgoing terrestrial radiation has its peak in the infrared portion of the spectrum $10\ \mu m$. Most of the solar energy of interest for the energetic of the climate system ranges from 0.1 to 2.0 μm in the ultraviolet visible and near infrared regions while most of outgoing terrestrial radiation to space is in the region between 4.0 and 60 μm well in the infrared range of the electromagnetic spectrum (see Figures 8, 9 and 10).This gives the rationale for breakdown of the radiant energy that heats the cools the climate system into two types: the short-wave or solar radiation with $\lambda < 4\mu m$ and the long-wave or terrestrial radiations with $\lambda > 4\mu m$ .We may add that the mathematical and physical treatments of the two types of radiation are also quite different.
Since the solar radiation comes from a very distant point-like source, the Sun, it can be treated as parallel unidirectional radiation. On the other hand, terrestrial radiation comes from all direction since each molecule acts as an individual "minuscule Sun" for thermal diffuse radiation. Furthermore, the terrestrial emission is negligible at the wavelengths of solar emission so that only absorption has to be considered. However, emission and absorption are equally important at the frequencies of terrestrial radiation and need to be considered simultaneously

2.1.3.1 Greenhouse Gas Spectral Overlaps and Their Significance

One of the difficulties in measuring the GWP (Global Warming Potential) of GHG is that GHG absorb infrared radiation at a variety of wavelengths. Some GHG have common absorption bands. Table.1 shows how the GHG absorption bands overlap. Water is the sole absorber in the windows from 0.5 μm to 2.0 μm and from 5.0 μm to 7.0 μm, ozone in the 8.0 μm to 10.0 μm window, carbon dioxide in the 14.7 μm to 16.5 μm window, and nitrous oxide in the 16.5 μm to 46.0 μm window. However, in some regions absorption frequencies of various GHG overlap; water, carbon dioxide, and carbon monoxide absorption bands overlap in the 2.0 μm to 3.0 μm region; water and methane absorption bands overlap in the 3.0 μm to 4.0 μm region; carbon dioxide and carbon monoxide by absorption bands overlap in the 4.0 μm to 5.0 μm region; nitrous oxide and methane absorption bands overlap in the 7.0 μm to 8.0 μm region; and carbon dioxide, ozone, and methane absorption bands overlap in the 13.7μm to 14.7 μm region. Methane does not have a separate and distinct absorption window for itself like other GHG. Current global warming calculations and some climate models include infrared absorption characteristics of GHG to a moderate extent. The infrared absorption spectrum of atmospheric greenhouse gases is very complex. The mono chromaticity (radiation of one wavelength) of most of its absorption bands of individual GHG is lost due to

pressure, temperature, aggregation, emission, and other factors. The infrared absorption spectrum of atmospheric GHG may also depend on latitude-longitude and altitude locations since GHG distributions other than carbon dioxide are not uniform. Partly because the infrared absorption bands of the various components of the atmosphere overlap, the contributions from individual absorbers do not add linearly. Clouds trap only 14 percent of the radiation with all other major species present, but would trap 50 percent if all other absorbers were removed (Table 1.). Carbon dioxide adds 12 percent to radiation trapping, which is less than the contribution from either water vapor or clouds. By itself, however, carbon dioxide is capable of trapping three times as much radiation as it actually does in the Earth's atmosphere. The overlap of carbon dioxide and water absorption bands in the infrared region. Given the present composition of the atmosphere, the contribution to the total heating rate in the troposphere is around 5 percent from carbon dioxide and around 95 percent from water vapor. In the stratosphere, the contribution is about 80 percent from carbon dioxide and about 20 percent from water vapor. It is important to remember, however, that it is currently believed that the impact of water vapor produced from surface sources such as fuel combustion on the atmospheric water vapor concentrations is minimal.

Table 1: Overlap of Absorption Bands of Greenhouse Gases

Greenhouse Gases	Absorption Bands(μm)
H_2O	0.5 – 2.0
H_2O, CO, and CO_2	2.0 – 3.0
H_2O and CH_4	3.0 – 4.0
CO and CO_2	4.0 – 5.0
H_2O	5.0 – 7.0
N_2O and CH_4	7.0 – 8.0
O_3	8.0 – 10.0
CO_2, CH_4, and O_3	13.7 – 14.7
CO_2	14.7 – 16.5
N_2O	16.5 – 46.0

Carbon dioxide absorbs infrared radiation wavelengths of 2.69 μm, 2.76 μm, 4.25 μm, 14 μm, and 15 μm. Carbon monoxide absorbs at 2.3 μm, and 4.7 μm Water vapor absorbs at 0.6 μm, 0.72 μm, 0.82 μm, 0.94m, 1.10 μm, 1.38 μm, 1.87 μm, 2.70 μm, 3.20 μm, and 6.30m. Methane absorbs at 3.4 μm, 7.4 μm, 7.58 μm, and 7.87m. Nitrous oxide absorbs at 7.83 μm, 16.98 μm, and 44.9 μm. Ozone absorbs at 9.0 μm, 9.6 μm, and 14.2 μm. (Sources: Snell-Ettre, Encyclopedia of Industrial Chemical) (Sedgwick, 1950)

Table 2: Efficiency of Heat Trapping by Greenhouse Gases and Clouds Source: (Ramanathan, 1978)

Species Removed	Percentage Heat Trapped	Percentage Heat Not Trapped
All[a]	0	100
H_2O, CO_2, O_3	50	50
H_2O	64	36
Clouds	86	14
CO_2	88	12
O_3	97	3
None	100	0

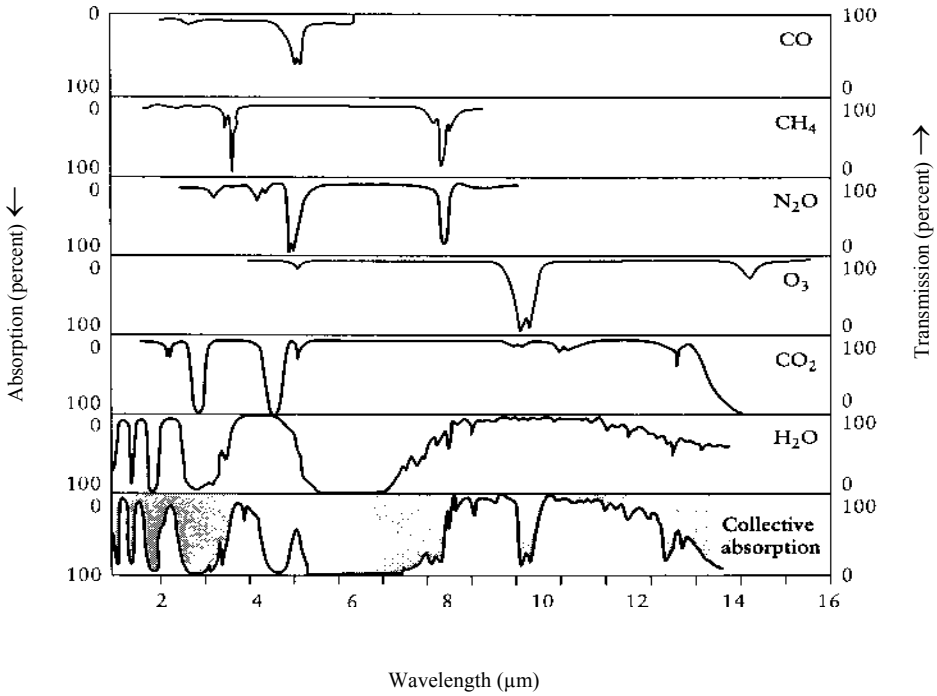

Figure 10: Absorption of some atmospheric gases in the infrared spectral region. Redrawn from Salby, 1996.

2.1.4 Physical radiation laws

2.1.4.1 Planck's law

A black body is e perfect absorber. It also emits the maximum possible amount of energy at a given temperature. The energy emitted by a black body are uniquely determined by its temperature as given action $E_\lambda(T)$ energy init time per unit area per unit solid per unit wavelength) emitted by a black body at temperature T is expressed by

$$E_\lambda(T)d\lambda = \frac{2hc^2}{\lambda^5\left[\exp(c\ h/k\lambda T)-1\right]}d\lambda \tag{3}$$

Where $h = 6.63\cdot10^{-34} J\ s$ the Planck constant $k = 1.38\cdot10^{-23}\ J\ K^{-1}$ is the Boltzmann constant. This law can also be written in terms of frequency using $\lambda = c/v$

$$E_\lambda(T)dv = \frac{2hv^3}{c^2\left[\exp(hv/kT)-1\right]}dv \tag{4}$$

The black body radiation is isotropic, i.e., the intensity is independent of the direction.

2.1.4.2 Stefan-Boltzmann law

The total radiance of a black body can be obtained by integrating the Planck law over the entire wavelength domain from 0 to ∞:

$$E(T) = \int_0^\infty E_\lambda(T) d\lambda \approx T^4 \tag{5}$$

This emission can be integrated over all angles of a hemisphere covering a horizontal surface, leading to the total flux (energy per unit time) coming from all angles at that surface:

$$\int E(T) \cos\theta \, d\omega \, dA = \sigma T^4 dA \tag{6}$$

where σ is the Stefan Boltzmann constant $\sigma = 5.670 \cdot 10^{-8} W m^{-2} K^{-4}$, θ is the angle between the incoming beam of solar radiation and the vertical, $d\omega = \sin\theta \, d\theta \, d\lambda$ is a solid angle element and dA is an element of surface area. Noting that $E(T)$ is independent of the direction, the integration of the left-hand side of Eq.(6) over the entire hemisphere leads to

$$2\pi E(T) \int_0^{\pi/2} \cos\theta \, d\theta = \pi E(T) \; = \pi E(T) = \sigma T^4 \tag{7}$$

Thus, the flux density (energy per unit area per unit time) emitted by a black body is proportional to the fourth power of the absolute temperature.

2.1.4.3 Wien displacement law

By setting the derivative of $E_\lambda(T)$ (with respect to λ in Eq.(3) equal to zero the wavelength of maximum emission $\lambda_{\max}$ can be obtained leading to the Wien displacement law.

$$\lambda_{\max} T = b = const. \tag{8}$$

When λ is in μm and T in K we find that $b = 2898 \mu m \, K$. The Wien displacement law states that for black body radiation the wavelength of maximum emission is inversely proportional to the absolute temperature. Using this relation the temperature black body can be determined from the wavelength of maximum monochromatic radiant. The law shows that in the infrared region of the spectrum. Of course the radiation emitted from the upper troposphere ($T \approx 225K$) peaks at a somewhat higher wavelength. Taking the observed value of $\lambda_{\max} = 0.474 \mu m$ for the solar radiation we find the Sun's surface temperature to be on the order of 6000 K (Figure 13).

2.1.4.4 Kirchhoff's law

The previous law deal essentially with the intensity emitted by a black body. However, in general, a medium will not only absorb but also reflect part of the incident radiant and transmit the remainder. Thus, in terms of the ratios of the absorbed, reflected, and transmitted radiation with respect to the monochromatic intensity of the radiation I_λ incident upon a layer, we may write.

$$a_\lambda + r_\lambda + \tau_\lambda = 1 \tag{9}$$

Where $a_\lambda = I_{\lambda a} / I_\lambda$ is the absorptivity $r_\lambda = I_{\lambda r} / I_\lambda$ the reflectivity and $\tau_\lambda = I_{\lambda t} / I_\lambda$ the transmissivity of the layer.
Kirchhoff's law states that in thermodynamic equilibrium and at a given wavelength the ratio of the intensity of emission I_λ to the absorptivity a_λ of any substance does not depend on the mature of the substance. It depends only on the temperature and the wavelength:

$$I_\lambda / a_\lambda = F(\lambda, T) \tag{10}$$

In case of a black body $a_\lambda = 1$ for all values of λ. Therefore, the ratio $F(\lambda, T)$ is equal to $E_\lambda(T)$ the black body intensity for a given temperature and wavelength. For any real body a_λ is less than 1, so that $I_\lambda < E_\lambda(T)$.
When we assume that a_λ is the same at all wavelengths we define what is known as a gray body.
In order for I_λ to be different from zero it is necessary that both $E_\lambda(T)$ and a_λ be different from zero. Thus, for a body to be able to emit energy at a given wavelength and at a given temperature it is necessary that a black body also emit energy at that temperature and that the body absorb it. Since the emissivity e_λ is defined as the ratio of the emitted intensity to the Planck function, Kirchhoff's law can also be expressed by $e_\lambda = a_\lambda$
So that any selective absorber of radiation at wavelength λ is also a selective emitter of radiation at the same wavelength.

2.1.4.5 Beer-Bouger-Lambert law

This law expresses change in radiation intensity I_λ due to the absorption of the radiation. Let us consider a parallel beam of radiation with intensity I_λ passing through an absorbing medium. The intensity of radiation after traversing a layer of thickness ds in the direction of propagation is $I_\lambda + dl_\lambda$ and

$$dl_\lambda = -k_{\lambda a} p \, ds \tag{11}$$

Where p is the density of the medium and $k_{\lambda a}$ is the absorption coefficient (absorption cross section in units of area or unit mass) for radiation of wavelength λ. Integration of this equation between s = 0 and $s = s_1$ yields the emergent intensity $I_\lambda(s_1)$ so that

$$I_\lambda(s_1) = I_\lambda(0) \exp\left(-\int_0^{s_1} k_{\lambda a} p \, ds \right) \tag{12}$$

Where $I_\lambda(0)$ is the density at s = 0.When the medium is homogeneous, $k_{\lambda a}$, is independent of s and Eq.(12) then expresses the Beer-Bouger-Lambert absorption law. A similar law is valid for the scattering of a parallel beam passing through the atmosphere. In this case we must use a scattering coefficient $k_{\lambda s}$.When absorption and scattering occur simultaneously we may write $k_\lambda = k_{\lambda a} + k_{\lambda s}$ where k_λ is called the extinction coefficient. The transmissivity τ_λ of the atmosphere at a given wave length is then given by

$$\tau_\lambda = I_\lambda / I_{\lambda 0} = \exp\left(-\int_0^{\infty} k_\lambda p \, ds \right) \tag{13}$$

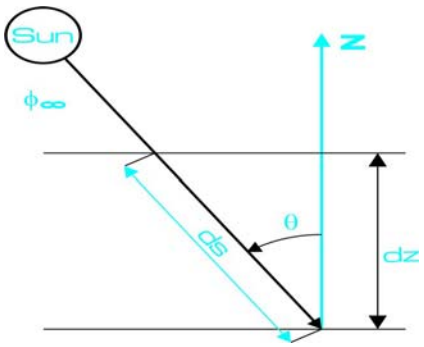

Figure 11: Diagram showing the extinction of solar beam through a plane-parallel atmosphere

Where k_λ is the extinction coefficient analog a slant path d in the direction of propagation through the atmosphere? If the zenith angle of the Sun is θ_s, $ds = dz \sec\theta_s$ (Figure 11) and Eq.(13) can be written as

$\tau_\lambda = I_\lambda / I_{\lambda 0} = \exp\left(-\sec\theta_s \int_0^\infty k_\lambda p\, dz\right) = \exp(-\sec\theta_s u)$, where the quantity

$$u = \int_0^\infty k_\lambda p\, dz \tag{14}$$

Is called the optical depth or optical thickness.

For normal incidence ($\theta_s = 0$) and when u = 1 we find $\tau = e^{-1} = 0.37$ which implies that the initial intensity $I_{\lambda 0}$ is decreased by 63%. If u = 2 we find $\tau = e^{-2} = 0.14$ or a decrease in intensity 86%. During normal atmospheric conditions the optical depth is much less than 1, but for very thick, dark clouds it can be much greater than 1.

2.1.5 Solar radiation

2.1.5.1 Solar spectrum and solar constant

Most solar radiation that affects the climate system is in the ultraviolet, visible, and near infrared regions of the spectrum (see Figure 8). Indeed, 99% of the solar energy reaching the Earth has a wavelength between 0.15 and 4.0 μm with 9% in the ultraviolet ($\lambda < 0.4\mu m$), 49% in the visible ($0.4 < \lambda < 0.8\mu m$) and on the infrared ($\lambda > 0.8\mu m$) (Houghton, 1985).

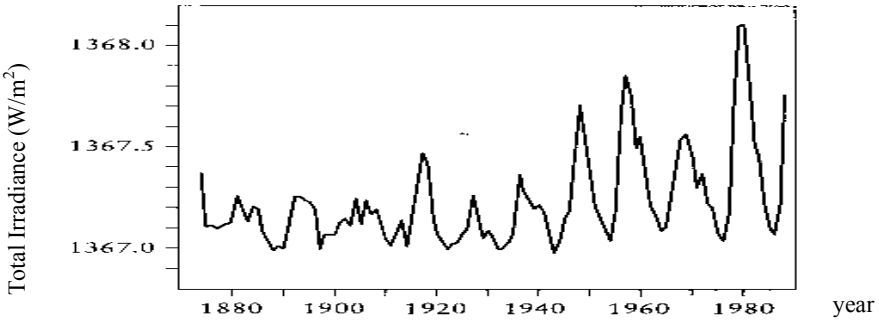

Figure 12: Reconstructed solar irradiance from 1874 to 1988, redrawn from Houghton, 1990.

Observations over many years show that the intensity of solar radiation has not changed substantially. For this reason we may introduce a quantity known as the solar constant S. The solar constant is defined as the

amount of solar radiation incident per unit area and per unit time on a surface normal to the direction of propagation and situated at the Earth's mean distance from the Sun. The value of the solar constant is about 1368 Wm^{-2} (Figure 13).

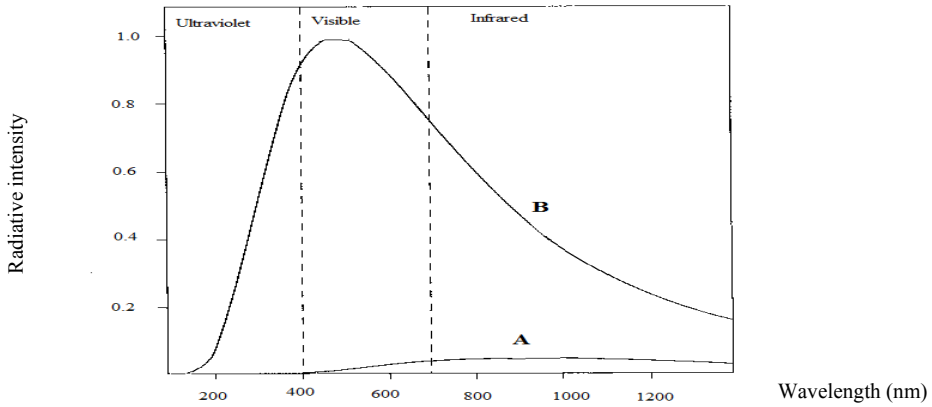

Figure 13: Distribution of energy from blackbody radiator at 330 K (curve A) and 6000 K (curve B)

Figure 13 gives the spectral distribution of the solar radiation both at the top of the atmosphere and at ground level. The spectrum at the top of the atmosphere closely resembles the spectrum given by Planck's law for a black body with a temperature of about 6000 K This radiation coming directly from the Sun received at the Earth's surface on a unit area normal to the solar beam is called direct solar radiation. The amount of scattered radiation coming from all angles, except for the solid angle subtended by the solar disk, is called diffuse solar radiation.
The sum of both components as received on a horizontal surface is called global solar radiation.

2.1.5.2 Distribution of the solar radiation at the top of the atmosphere

The distribution of solar radiation at the top of the atmosphere depends on the geometry of the globe, its elliptical orbit around the Sun (Figures 14 and 16). Thus it is a function of the tilt of the axis to the plane of the ecliptic, the eccentricity of the orbit, and the longitude of the perihelion. The mean distance between the Sun and the Earth is $1.496 \cdot 10^{11} m$ and is known as the Astronomical Unit (AU). The maximum distance (perihelion) is 1.034 AU, and minimum is 0.9646 AU.
The eccentricity of the Earth's orbit is defined by the ratio of the maximum deviation from a circular orbit and the mean radius. The eccentricity has a present value of 0.0167. The present value of the tilt or obliquity of the ecliptic is $23^{o}27'$.
As the solar radiation enters the atmosphere it is depleted by absorption and scattering. The absorbed radiation is directly added to the heat budget, whereas the scattered radiation is partly returned to space and partly continues its path through the atmosphere where it is subject to further scattering and absorption. Maximum depletion of the solar beam tends to occur at high latitudes were the path length through the atmosphere is longest, and minimum depletion in the inter tropical regions where the path length is shortest.
The irradiance Φ_{sw} on a horizontal surface depends on the Sun's zenith angle θ_s (Figure 15)

$$\Phi_{sw} = \Phi^{0}_{sw} \cos\theta_s \tag{15}$$

where Φ^{0}_{sw} is the irradiance normal to the solar beam (short waves flux). Applying spherical trigonometry to the so-called ZPS (zenith-pole-Sun) spherical triangle (See Figure 15), we find that

$$\cos\theta_s = \sin\phi \sin\delta + \cos\phi \cos\delta \cos h \tag{16}$$

or

$$\cos \ell = \tan\phi \tan\delta \tag{17}$$

and the length of day (in radian)

$$2\ell = 2\cos^{-1}(-\tan\phi \tan\delta) \tag{18}$$

The length of day $(24\ell/\pi \ hours)$ is uniquely defined by the latitude and the time of the year through the solar declination (see e.g., Iqbal, 1983).
The distribution of solar radiation incident on a horizontal plane at the top of the atmosphere depends, of course, not only on cosθ_s but also on the Earth-Sun distance through the inverse square law:

$$f(d) = (d_m / d)^2 \tag{19}$$

Where d is actual distance and d_m the mean distance between the Sun and the Earth. As we have seen before the term cos θ_s depends, depends the day of year, time of, day and latitude so that for a given instant

$$\Phi_{sw} = S(d_m / d)^2 \cos\theta_s \tag{20}$$

Where S is a solar constant
=

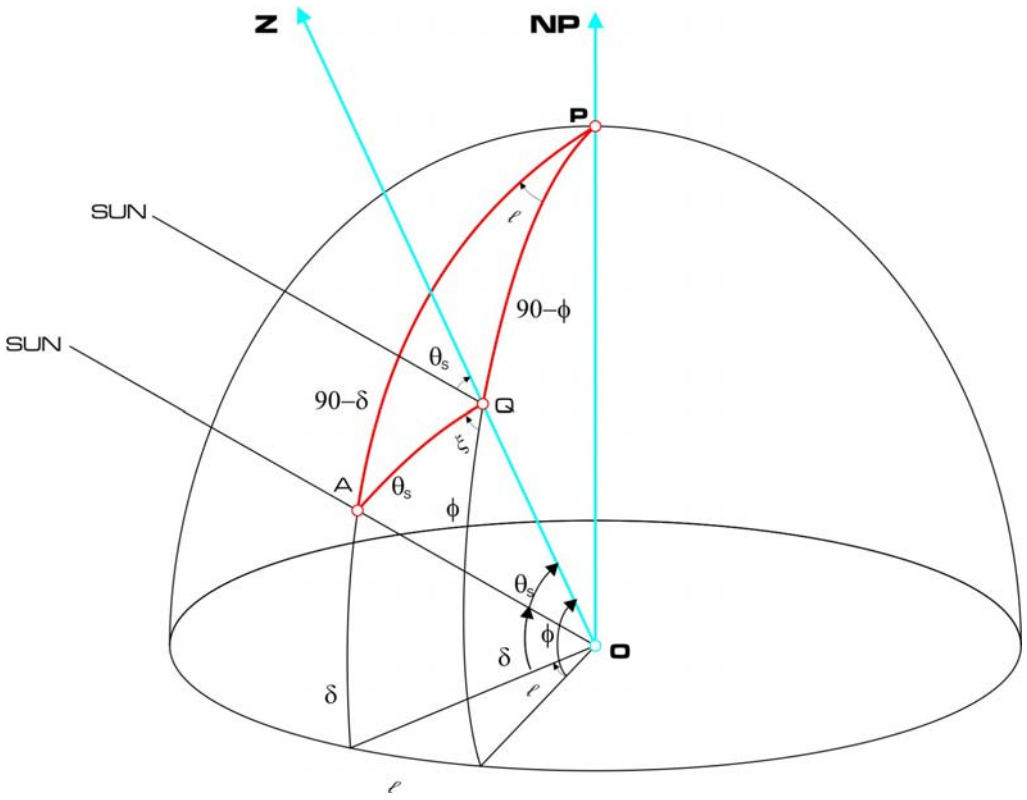

Figure 14: Spherical geometry for solar zenith angle calculation

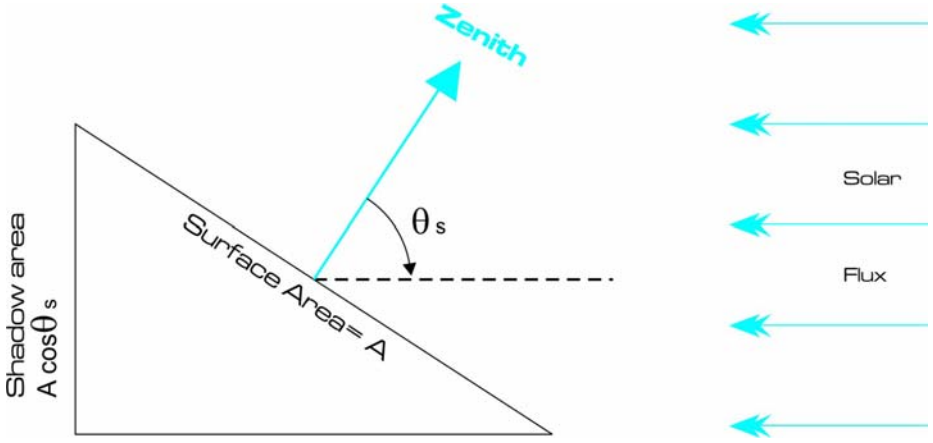

Figure 15: Diagram showing the relationship of solar zenith angle to insolation on a plane parallel to the Earth surface

Under present astronomical conditions the function f (d) reaches extreme values of 1.0344 in early January and 0.9646 in early July. Secular variations in the orbital parameters of the Earth may constitute a major case for climate changes as those experienced during the Pleistocene ice ages (Milankovitch, 1941; Berger, 1978; Imbrie and Imbrie, 1979), see Figure 16.

The total daily insulation at the top of the atmosphere can be determined by integration of Eq.(20) over a time then,

$$Q_0 = S(d_m, d)^2 \int_{time\ of\ sunrise}^{time\ of\ sunset} \cos\theta_S \, dt. \tag{21}$$

Using Eq.(16) and $dt = (12/\pi)d\ell$ Eq.(21) become

$$Q_0 = \frac{24}{\pi} S(d_m / d)^2 \left(\int_0^{\ell} \sin\phi \sin\delta \, d\ell + \int_0^{\ell} \cos\phi \cos\delta \cos\ell \, d\ell \right) \tag{22}$$

Again using Eq.(18) we find

$$Q_0 = \frac{24}{\pi} S(d_m / d)^2 \sin\phi \sin\delta \left(\ell - \tan\ell\right) \tag{23}$$

Where $Q_0, S,$ and ℓ are given in units of Wm^{-2} day, Wm^{-2} and radians, respectively (Iqbal, 1983).

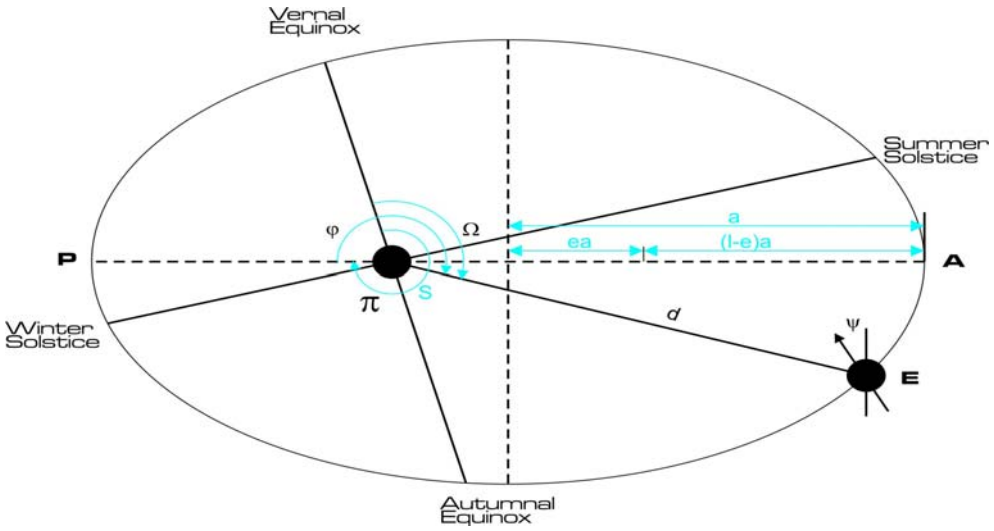

Figure 16: Schematic diagram of Earth's elliptical orbit about the Sun showing the critical parameters of eccentricity (e), obliquity (ψ), and longitude of perihelion (π) defined relative to the vernal equinox.

The size of the orbit is defined by the greatest distance between the ellipse and its center point, which is called the semi major axis length, a_0 .The Earth –Sun distance and any time (d), the angle between the position of Earth and perihelion that we call the true anomaly (φ), and the angle between the position of Earth and the vernal equinox (Ω) are also shown (Sources: Hartman, 1998.)

2.1.5.3 Radiative Effects of Atmospheric Aerosols

The Earth's energy balance requires that the flux of incoming energy from the Sun, most of which is in the visible part of the spectrum, must be balanced by an equal outgoing flux of infrared radiation. Any deviation on either side of this balance, incoming or outgoing, drives the Earth's climate to a new warmer or cooler equilibrium state so that the requirement for energy balance will again be satisfied. The rate at which the new equilibrium state is approached depends on magnitude of the imbalance and the inertia of the Earth s reservoirs of heat, especially the oceans. Greenhouse gases (GHG) intercept some of the outgoing radiation and thereby act to force the Earth s surface to come to a higher equilibrium temperature. In contrast to GHG, which act only on outgoing, infrared radiation, aerosol particles can influence both sides of the energy balance. Particles of diameters less than 1μm are highly effective at scattering incoming solar radiation, sending a portion of that scattered radiation back to space. In so doing, these particles reduce the amount of incoming solar energy as compared with that in their absence and consequently cool Earth. Over industrialized part of the world, sulphate particles produced by the oxidation by the antropogenically emitted SO_2 comprise much of this light-scattering aerosol. In the tropics, biomass burning of forests and savannas is dominant source of airborne particles, which consist mainly of organic matter and soot. Mineral dust from wind acting on soils is always present in the atmosphere to some degree, although human activities, such as disruption of soils by changing use of land in arid sub arid regions, can increase the loading of dust over that present naturally. Because of their size and composition, mineral dust particles can scatter and absorb both incoming and outgoing radiation.

Greenhouse gases such as CO_2, CH_4, N_2O, and the CFCs are virtually uniform globally, aerosols concentrations are highly variable in space and time. With lifetimes of about a week, sulphate aerosols are most abundant close to their sources in the industrialized areas. Biomass aerosols are emitted predominantly during the dray season in tropical areas. Mineral dust appears downwind of large arid regions.

Aerosols radiative effects depend in complicated way on the solar angle, relative humidity, particle size and composition, and the albedo of the underlying surface. Aerosol residence times in the troposphere are roughly 1 to 2 weeks. If all SO_2 sources were shut off today, climate forcing by the resulting sulphate aerosols would disappear from the planet in 2 weeks. By contrast, not only are GHG residence times measured in decades to centuries, but because of the great inertia of the climate system, the effect of GHG forcing takes decades to be fully transformed into equilibrium climate warming.

2.1.5.4 Scattering and absorption of light by small particles

When a beam of light impinges on a particle (Seinfled and Pandis, 1998), electrons in the particle are excited into oscillatory motion. The excited electrons reradiate energy in all directions and may convert a part of the incident radiation into thermal energy. The amount crossing an area of a detector perpendicular to its direction of propagation is its intensity, measured in units of Wm^{-2}. We give the incident intensity of radiation the symbol I_0.

The energy scattered per second by a particle is proportional to the incident intensity. $E_{scat} = k_{scat} I_0$

Where k_{scat}, in units of m^2, is the single-particle scattering cross section. For absorption, the energy absorbed is described analogously, $E_{abs} = k_{abst} I_0$

Where $k_{abs}(m^2)$ is the single-particle absorption cross section.

Conservation of energy requires that the light removed from the incident beam by the particle is accounted for by scattering in all directions and absorption in the particle. The combined effect of scattering and absorption is referred to as extinction, and an extinction cross section, k_{ext} can be defined by $k_{ext}=k_{scat}+k_{abs}$ k_{ext} has the units of area. The dimensionless extinction, scattering and absorption efficiency of particle respectively, are:

$Q_{ext} = k_{ext}/A$, $Q_{scat} = k_{scat}/A$ and $Q_{abs} = k_{abs}/A$, where A is the cross-sectional area of the particle. Then

$$Q_{ext}=Q_{scat}+Q_{abs} \tag{24}$$

The ratio of Q_{scat} to Q_{ext} is called the single scattering albedo,

$$a_{scat} = \frac{Q_{scat}}{Q_{ext}} = \frac{k_{scat}}{k_{ext}} \tag{25}$$

Thus the fraction of light extinction that is scattered by a particle is a_{scat}, and the fraction absorbed is $a_{abs}=1- a_{scat}$

Light scattering mechanisms of particles can be divided into three categories:

- Elastic scattering-the wavelength of the scattered light is the same as that of the incident beam λ_0
- Quasi-elastic scattering- the wavelength shifts due to Doppler effects and diffusion broadening.
- Inelastic scattering - the emitted radiation has a wavelength different from that of incident radiation.

Figure 17 depicts the various processes that can occur when radiation of wavelength λ_0 interacts with a particle. Inelastic scattering processes include Raman scattering and fluorescence. For the interaction of solar radiation with the atmospheric aerosols, elastic light scattering is the process of interest.

The absorption and elastic scattering of light by a spherical particle is a classical problem in physics, the mathematical formalism of which is called Mie Theory. Te key parameters that govern the scattering and absorption of light by a particle are:

(1) The wavelength λ_0 of the incident radiation,

(2) The size of particle, is expressed as a dimensionless size parameter- the ratio of the circumference of the particle to the wavelength of light

$$\alpha=2\pi r_p/\lambda \tag{26}$$

and

(3) The particle optical property relative to the surrounding medium, the complex refractive index $N=n+ik$

Both the real part n, and the imaginary part k, of the refractive index are functions of λ.

The real and imaginary parts of refractive index represent the nonabsorbing and absorbing components, respectively. Refractive index N is usually normalized by the refractive index of the medium, N_0, and denoted by m. $m=N/N_0$. Where the medium of interest to us is air. Since the refractive index of air is effectively unity, for example, N_0=1.00029+0i at λ = 589 nm, for all practical purposes N and m are identical. Henceforth the refractive index will be denoted as $m = n + ik$, with the understanding that is referenced to that of air.

Mie theory can serve as the basic of computational procedure to calculate the scattering and absorption of light by any sphere as a function of wavelength. There are, in addition, approximate expressions, valid in certain limiting cases that provide insight into the physics of the problem. Based on

the value of α. light scattering can be divided into three domains:

- α<<1 Rayleigh scattering (particles small compared to wavelength of light)
- α≈1 Mie scattering (particles of about the same size as the wavelength of light)
- α>>1 Geometric scattering (particles large compared to wavelength of light)

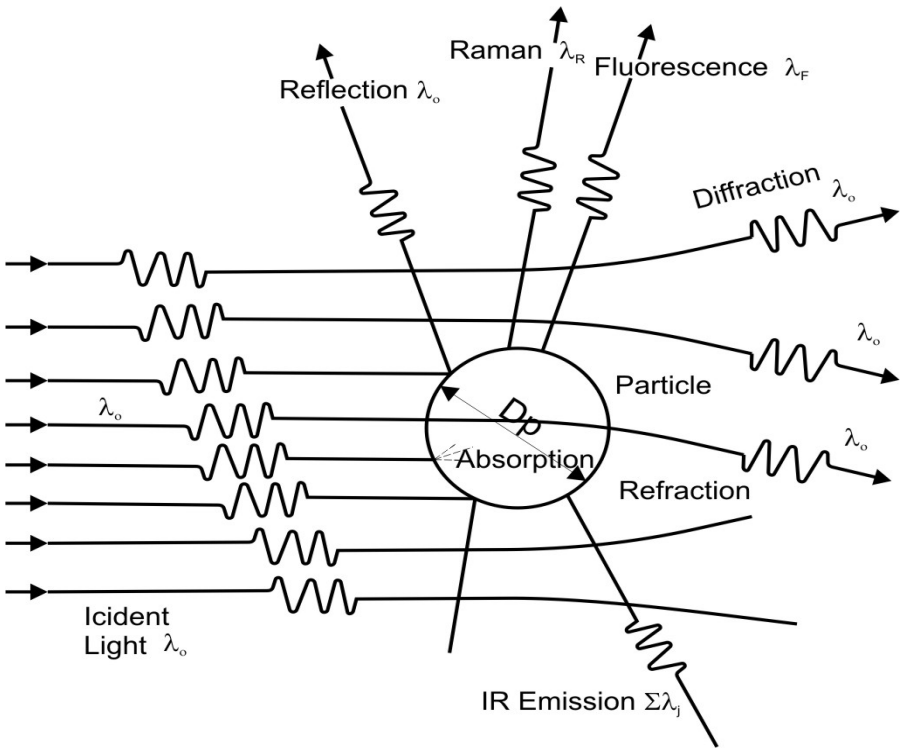

Figure 17: Mechanisms of interaction between incident radiation and particle (Sources: Seinfled. J.H., and Pandis.1998)

2.1.6 Terrestrial radiation

The absorption of short-wave solar radiation by the atmosphere and the Earth's surface leads to heating of the climate system. Thus, according to the Stefan-Boltzmann law Eq. (7) and the Wien law Eq. (8), all components of the climate system emit radiant energy in the long-wave region of the spectrum (infrared, microwave, etc.) This is why the terrestrial radiation is sometimes called thermal radiation. This has been stated already in the late 18th century by Prevost when he said that "all bodies have to lose energy." Today we would present the Prevost principle as follows: All bodies with a temperature above 0 K emit energy whose quality (in terms of υ and λ) depends on their temperature.
In the mean the short-wave solar radiation absorbed by the planet Earth must be returned to space as long-wave terrestrial radiation. Thus practically all exchange of energy between the Earth and outer space is through radioactive transfer.
All real bodies emit and absorb less radiant energy than a black body at the same temperature and wavelength. Their emissivities (or absorbivities) are less than 1 and vary with the wavelength (Kirchhoff's law). Gases in atomic from absorb (and emit) radiant energy only in very narrow distinct wavelength intervals that results from quantized changes in electronic states. They are called spectral absorption lines. However, molecular gases show spectral absorption bands, each one formed by a large number of very close lines. The location of the bands in the spectrum and their strength depend on the molecular structure of the gases. The absorptivities of the gases vary greatly with wavelength and the absorption spectra are highly irregular and discontinues.
Thermal vibrations and rotations of the molecules produce continuous emission (absorption) spectra with an emissivity slightly less than 1. It is therefore convenient to treat the radiant energy emission separately for the Earth's surface and the atmosphere.

2.1.6.1 Absorption and emission spectra of atmospheric gases

The absorption and emission of radiation in gases occurs at specific wavelengths according to their atomic and molecular structure. Isolated atoms and molecules, as we may consider the gases of the atmosphere to be, can only absorb and emit energy at certain discrete energy states and can only undergo discrete changes between these states. As predicted by quantum mechanics the energies involved in the transitions are quantized. Thus, the interaction of an atom or molecule with electromagnetic radiation (Figure 18) such as light, can only take place at well-defined frequencies that are characteristic of that molecule and of the corresponding pair of energy values between which the transition is taking place.
This can be expressed in quantum-mechanical terms by

$$E_i - E_k = h\nu, \tag{27}$$

Where E_i and E_k are the energies of an energetically higher and lower state, respectively, υ is the frequency of radiation, and h the Plank constant. In other words, the radiant energy has to be in resonance with energy gap in order to make the molecule "jump". If the molecule changes its energy from higher to a lower state, the energy emission of photons has the same value given by Eq. (27). Each chemical element or combination of elements has a characteristic absorption and emission spectrum showing the frequencies at which they absorb or emit radiation. The spectra are essentially discontinuous and consist of lines. The spectral distributions are explained by the fundamental principles of atomic physical and quantum mechanics, involving quantum- mechanical selection rules whose treatment is beyond the scope of this book. When an atom absorbs radiant energy, the electrons in the atom can go to a higher discrete orbit with some restrictions based on the selection rules and the conservation of angular momentum. When the electrons return to their original base state (ground state), they emit energy at frequency determined by the difference in the two orbits. In summary, we can say that an atom has certain preferred (natural) frequencies of emission based in its structure, just as a pendulum has a natural period depending on its length.
The atmospheric absorption spectra consist of many lines that correspond to electronic energy transitions characteristic of each particular atomic species. In the case of an atomic emission spectrum it is of course necessary that the higher energy states if the atom be populated, so that the atoms can emit energy when an electron moves to an orbit closer to the nucleus. Thus, the emission lines can result from either transition to

the ground state or from transitions between excited states. If radiation penetrating a gas cannot excite the atoms or molecules in the gas its energy will not be absorbed or emitted (Kirchhoff's law).
The absorption of a molecular gas occurs in bands which consist of a large number of closely spaced spectral lines. The molecular spectral bands in the ultraviolet and visible temperatures of the atmosphere and the Earth's surface electronic bands are not important because the higher energy states are not sufficiently populated.

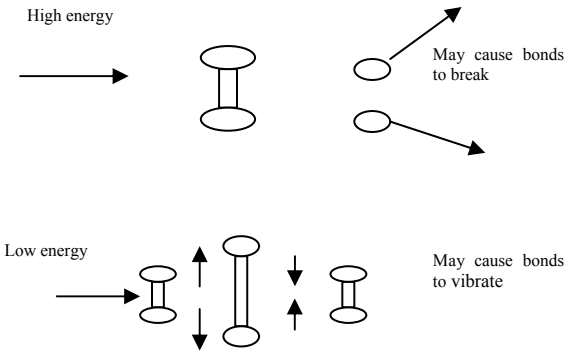

Figure 18: Results due to bombardment of molecules with electromagnetic radiation

2.1.6.2 Rotational and vibration bands

In this section, we give a simplified account of the infrared absorption (and emission) spectra of the principal absorbing gases of the atmosphere.
The emission spectra of molecules are usually more complex than those of individual atoms because they have more degrees of freedom. For example, the atoms of a diatomic molecule can rotate about a common axis leading to rotational energy. Another mode can occur when two or more atoms vibrate towards or away from each other. According to quantum mechanics there are certain preferred modes of behavior for each gas that give the specific emission characteristics for that gas. Although the energy amounts involved in the quantized vibrational and rotational energy transitions are much smaller than those in the electronic transitions, they are of paramount importance in the infrared and microwave regions of the spectrum that dominate the emission of terrestrial radiation.
Diatomic molecules can only have rotational or vibration spectra if the rotation or vibration results in an oscillating electric dipole moment. Because the most abundant molecules in the atmosphere, N_2 and O_2, have no electric dipoles due to their symmetric charge distribution, they show no vibrational or simple rotational spectra. Their absorption and emission spectra are caused by electronic transitions and are therefore in the ultraviolet and visible regions of the electromagnetic spectrum.
The principal atmospheric gases that are active in the long-wave range of the spectrum are H_2O, CO_2 and O_3. They are all triatomic. Their structure and their principal virbrational modes are shown schematically in Figure 19. The atoms of water vapor jade a triangular configuration with an oxygen atom at mass of the molecule with different moments of inertia about each axis. The combination of the rational and vibrational states leads to a very complex and irregular absorption spectrum for water vapor. Vibrational bands occur at higher energies (higher frequencies) than the rotational bands, and the energies of vibrational quant are two orders of magnitude larger than those of the rational quanta. Water vapor has a pure rotational band extending upward from 14µm and centered at 65 µm and has several vibrational- rotational bands in the 1-8µm region (see Figure 19).

Carbon dioxide is another important constituent of the atmosphere causing strong absorption in the far infrared. Because CO_2 is linear symmetric molecule, its rotation does not produce an oscillating dipole moment and it has no rotational bands. Its absorption spectrum shows maxima at 2,3 and 4 μm and in the 13-17 μm region.

Ozone, which is abundant in the stratosphere , contributes to the absorption of the terrestrial radiation mainly in one band centered at 9.6 μm which is of a vibrational-rotational nature (Figure 19). In the troposphere ozone is only a minor tracer and its influence in the radioactive exchanges can be disregarded. Therefore the principal absorbers in the troposphere are water vapor and carbon dioxide, whereas in the stratosphere all three are important.

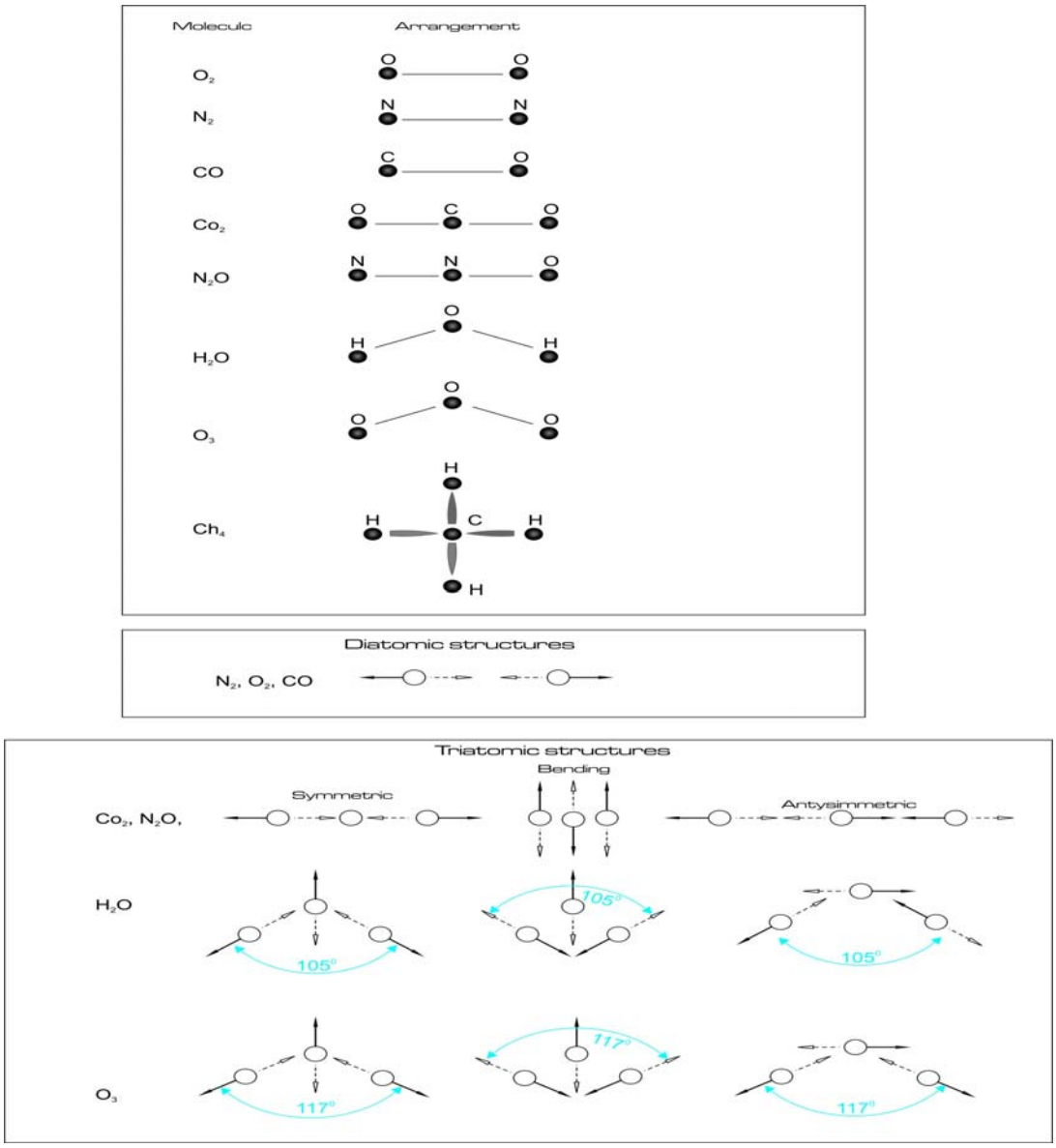

Figure 19: Schematic diagrams showing the vibrational modes of diatomic and triatomic molecules

2.1.7 Greenhouse Gases And Climate Change

2.1.7.1 Greenhouse Gases and Greenhouse Effect

Human activities contribute to climate change by causing changes in Earth's atmosphere in the amounts of greenhouse gases and cloudiness. The largest known contribution comes from the burning of fossil fuels (coal, oil and natural gas), which releases carbon dioxide gas to the atmosphere.

Greenhouse gases and aerosols affect climate by altering incoming solar radiation and outgoing infrared (thermal) radiation that are part of Earth's energy balance.

Changing the atmospheric abundance or properties of these gases and particles can lead to a warming or cooling of the climate system. Since the start of the industrial era (about 1750) the overall effect of human activities on climate has been a warming influence. The human impact on climate now is much larger than ever.

2.1.7.2 Greenhouse Gases

Human activities result in emissions of four principal gases
(see: http://www.epa.gov/otaq/greenhousegases.htm): carbon dioxide (CO_2), methane (CH_4), nitrous oxide (N_2O) and halocarbons (a group of gases containing fluorine, chlorine and bromine). These gases accumulate in the atmosphere, causing concentrations to increase with time. Significant increases in all of these gases have occurred in the industrial era (see Figure 21).

Carbon dioxide (CO_2) is most important anthropogenic greenhouse gas. The global atmospheric concentration of carbon dioxide has increased from a pre-industrial value of about 280 ppm to 380 ppm in 2007 (see: http://en.wikipedia.org/wiki/List_of_countries_by_carbon_dioxide_emissions_per_capita).

The atmospheric concentration of carbon dioxide in 2007 exceeds by far the natural range over the 650000 years (180-300 ppm) as determined from ice cores. The annual carbon dioxide concentration growth rate was larger during the last 15 years (1.9 ppm, current concentration 1.3 ppm per year, see Figure 20).

Carbon dioxide has increased from fossil fuel use in transportation, building heating and cooling and the manufacture of cement and other goods. Deforestation releases CO_2 and reduces its uptake by plants. Carbon dioxide is also released in natural processes such as the decay of plant matter.
Emissions of CO_2 (Figure 24) from fossil fuel combustion, with contributions from cement manufacture, are responsible for more than 75% of the increase in atmospheric CO_2 concentration since pre-industrial times.

The remainder of the increase comes from land use changes dominated by deforestation (and associated biomass burning) with contributions from changing agricultural practices. All these increases are caused by human activity.

The increase in atmospheric CO_2 concentration is known to be caused by human activities because the character of CO_2 in the atmosphere, in particular the ratio of its heavy to light carbon atoms, has changed in a way that can be attributed to addition of fossil fuel carbon. In addition, the ratio of oxygen to nitrogen in the atmosphere has declined as CO_2 has increased; this is as expected because oxygen is depleted when fossil fuels are burned. A heavy form of carbon, the carbon-13 isotope, is less abundant in vegetation and in fossil fuels that were formed from past vegetation, and is more abundant in carbon in the oceans and in volcanic or geothermal emissions. The relative amount of the carbon-13 isotope in the atmosphere has been declining, showing that the added carbon comes from fossil fuels and vegetation. Carbon also has a rare radioactive isotope, carbon-14, which is present in atmospheric CO_2 but absent in fossil fuels. Prior to atmospheric testing of nuclear weapons, decreases in the relative amount of carbon-14 showed that fossil fuel carbon was being added to the atmosphere.

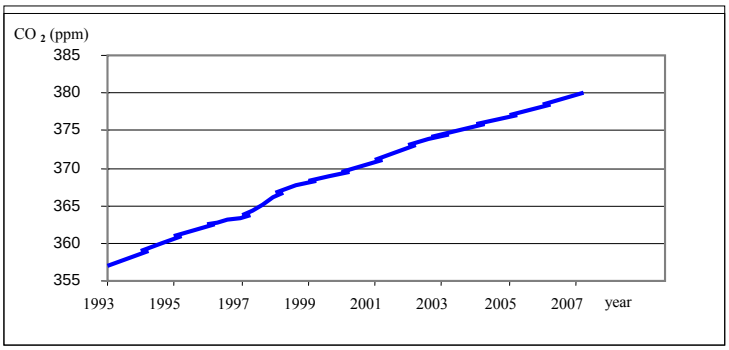

Figure 20: Carbon dioxide concentration growth rate during the last 14 years

Methane (CH_4) has increased as a result of human activities related to agriculture, natural gas distribution and landfills. Methane is also released from natural processes that occur, for example, in wetlands. The global atmospheric concentration of methane has increased from a pre-industrial value of about 715 ppb to 1732 ppb in the early 1990, and was 1774 ppb in 2005.The atmospheric concentration of methane in 2005 exceeds by far the natural range of the last 650000 years (320 to 790 ppb) as determined from ice cores. Growth rates have declined since the early 1990s. It is very likely that the observed increase in the methane concentration is due to anthropogenic activities, predominantly agriculture and fossil fuel use. The human activities that produce CH_4 include energy production from coal and natural gas, waste disposal in landfills, raising ruminant animals, rice agriculture and biomass burning. Once emitted, CH_4 remains in the atmosphere for approximately 8.4 years before removal, mainly by chemical oxidation in the troposphere. Minor sinks for CH_4 include uptake by soils and eventual destruction in the stratosphere

Nitrous oxide (N_2O) is also emitted by human activities such as fertilizer use and fossil fuel burning. Natural processes in soils and the oceans also release N_2O.Nitrous oxide (N_2O) sources to the atmosphere from human activities are approximately equal to N_2O sources from natural systems. Between 1960 and 1999 N_2O concentrations grew an average of at least two times faster than over any 40-year period of the two millennia before 1800. Natural sources of N_2O include oceans, chemical oxidation of ammonia in the atmosphere, and soils. Tropical soils are a particularly important source of N_2O to the atmosphere. Human activities that emit N_2O include transformation of fertilizer nitrogen into N_2O and its subsequent emission from agricultural soils, biomass burning, raising cattle and some industrial activities, including nylon manufacture. Once emitted, N_2O remains in the atmosphere for approximately 114 years before removal, mainly by destruction in the stratosphere.

Halocarbon gas concentrations have increased primarily due to human activities. Natural processes are a small source. Principal halocarbons include the chlorofluorocarbons (e.g., CFC-11 and CFC-12), which were used extensively as refrigeration agents and in other industrial processes before their presence in the atmosphere was found to cause stratospheric ozone depletion. The abundance of chlorofluorocarbon gases is decreasing as a result of international regulations designed to protect the ozone layer. Human activities are responsible for the bulk of long-lived atmospheric halogen-containing gas concentrations. Before industrialization, there were only a few naturally occurring halogen-containing gases, for example, methyl bromide and methyl chloride. The development of new techniques for chemical synthesis resulted in a proliferation of chemically manufactured halogen-containing gases during the last 50 years of the 20th century. Emissions of key halogen-containing gases produced by humans are shown in Figure 22. Atmospheric lifetimes range from 45 to 100 years for the chlorofluorocarbons (CFCs) plotted here, from 1 to 18 years for the hydro chlorofluorocarbons (HCFCs), and from 1 to 270 years for the hydro fluorocarbons (HFCs).

Concentrations of several important halogen-containing gases, including CFCs, are now stabilizing or decreasing at the Earth's surface as a result of the Montreal Protocol on Substances that Deplete the Ozone Layer and its Amendments. Concentrations of HCFCs, production of which is to be phased out by 2030, and of the Kyoto Protocol gases HFCs and PFCs, are currently increasing.

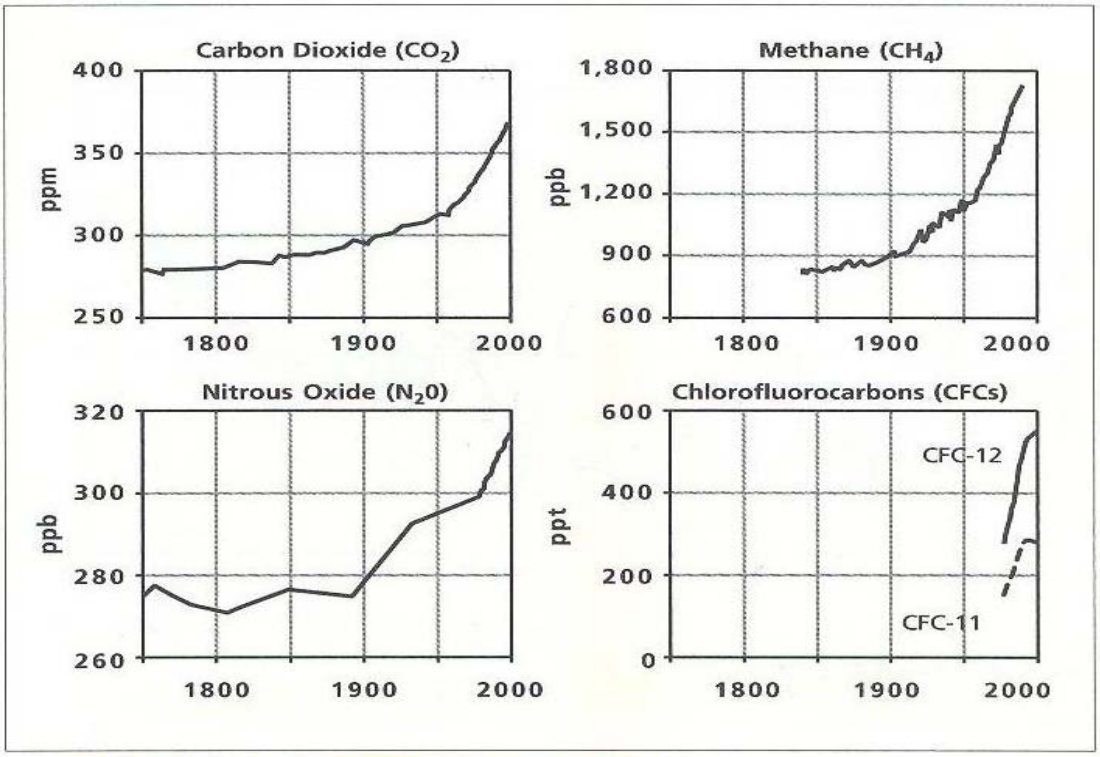

Figure 21: Global Greenhouse Gas Concentrations.

Carbon dioxide, methane, nitrous oxide, and chlorofluorocarbons all reduce emissions of heat from the Earth to outer space, thus increasing the temperature of the Earth. The atmospheric concentration of these gases –except for CFCs, which were first synthesized in the mid-1900s-has been increasing since the 1800s (Sources: CDIAC: UNEP)

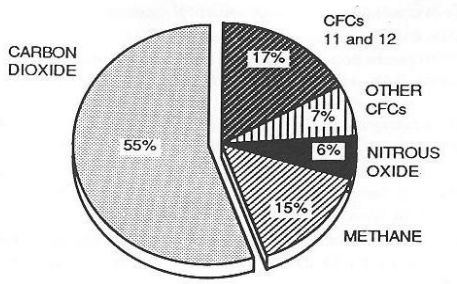

Figure 22: Pie chart showing the contribution from each of human –induced Greenhouse Gas changes to the change in radiative forcing from 1980 to 1990. (Source: IPCC Working Group I (1990)

• **Ozone** is a greenhouse gas that is continually produced and destroyed in the atmosphere by chemical reactions. In the troposphere, human activities have increased ozone through the release of gases such as carbon monoxide, hydrocarbons and nitrogen oxide, which chemically react to produce ozone. As mentioned above, halocarbons released by human activities destroy ozone in the stratosphere and have caused the ozone hole over Antarctica
Tropospheric ozone is produced by photochemical reactions in the atmosphere involving forerunner chemicals such as carbon monoxide, CH_4, volatile organic compounds and nitrogen oxides. These

chemicals are emitted by natural biological processes and by human activities including land use change and fuel combustion. Because tropospheric ozone is relatively short-lived, lasting for a few days to weeks in the atmosphere, its distributions are highly variable and tied to the abundance of its forerunner compounds, water vapor and sunlight. Tropospheric ozone concentrations are significantly higher in urban air, downwind of urban areas and in regions of biomass burning. The increase of 38% (20–50%) in tropospheric ozone since the pre-industrial era is human-caused. It is very likely that the increase in the combined radiative forcing from CO_2, CH_4 and N_2O was at least six times faster between 1960 and 1999 than over any 40-year period during the two millennia prior to the year 1800

- **Water vapor** is the most abundant and important greenhouse gas in the atmosphere however human activities have only a small direct influence on the amount of atmospheric water vapor. Indirectly, humans have the potential to affect water vapor substantially by changing climate. For example, a warmer atmosphere contains more water vapor. Human activities also influence water vapor through CH_4 emissions, because CH_4 undergoes chemical destruction in the stratosphere, producing a small amount of water vapor
- **Aerosols** are small particles present in the atmosphere (Hobbs. P. V.1988) with widely varying size, concentration and chemical composition. Some aerosols are emitted directly into the atmosphere while others are formed from emitted compounds. Aerosols contain both naturally occurring compounds and those emitted as a result of human activities. Fossil fuel and biomass burning have increased aerosols containing sulphur compounds, organic compounds and black carbon (soot). Human activities such as surface mining and industrial processes have increased dust in the atmosphere. Natural aerosols include mineral dust released from the surface, sea salt aerosols, biogenic emissions from the land and oceans and sulphate and dust aerosols produced by volcanic eruptions.
  Illustrates the influence of industrial emissions on atmospheric sulphate concentrations, which produce negative radiative forcing. Shown is the time history of the concentrations of sulphate, not in the atmosphere but in ice cores in Greenland (shown by lines; from which the episodic effects of volcanic eruptions have been removed). Such data indicate the local deposition of sulphate aerosols at the site, reflecting sulphur dioxide (SO_2) emissions at mid-latitudes in the Northern Hemisphere (Figure 23). This record, albeit more regional than that of the globally-mixed greenhouse gases, demonstrates the large growth in anthropogenic SO_2 emissions during the Industrial Era. The pluses denote the relevant regional estimated SO2 emissions (right-hand scale)

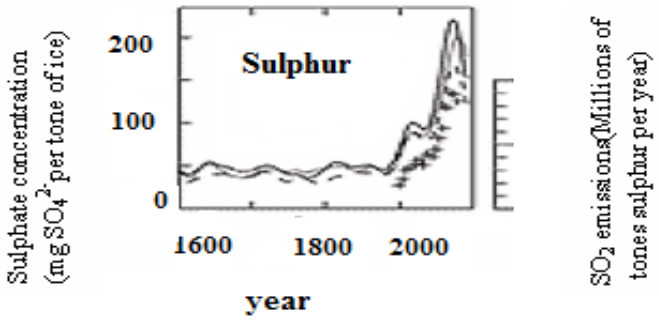

Figure 23: Sulphate aerosols deposited in Greenland ice (Source: IPCC 2001)

2.1.7.3 Radiative Forcing of Factors Affected by Human Activities

The contributions to radiative forcing (Houghton, J.T., et al. 1996) from some of the factors influenced by human activities are shown in Figure 24. The values reflect the total forcing relative to the start of the industrial era (about 1750). The forcings for all greenhouse gas increases due to human activities and are positive because each gas absorbs outgoing infrared radiation in the atmosphere. Among the greenhouse gases, CO_2 increases have caused the largest forcing over this period. Tropospheric ozone increases have also contributed to warming, while stratospheric ozone decreases have contributed to cooling.

Aerosol particles influence radiative forcing directly through reflection and absorption of solar and infrared radiation in the atmosphere. Some aerosols cause a positive forcing while others cause a negative forcing. The direct radiative forcing summed over all aerosol types is negative. Aerosols also cause a nega-

tive radiative forcing indirectly through the changes they cause in cloud properties.

The influence of a factor that can cause climate change, such as a greenhouse gas, is often evaluated in terms of its radiative forcing. Radiative forcing is a measure of how the energy balance of the Earth-atmosphere system is influenced when factors that affect climate are altered. The radiative balance controls the Earth's surface temperature. Radiative forcing is usually quantified as the 'rate of energy change per unit area of the globe as measured at the top of the atmosphere', and is expressed in units of 'Watts per square metre' (see Figure 24). When radiative forcing from a factor or a group of factors is evaluated as positive, the energy of the Earth-atmosphere system will ultimately increase, leading to a warming of the system. In contrast, for a negative radiative forcing, the energy will ultimately decrease, leading to a cooling of the system. Important challenges for climate scientists are to identify all the factors that affect climate and the mechanisms by which they exert a forcing, to quantify the radiative forcing of each factor and to evaluate the total radiative forcing from the group of factors.

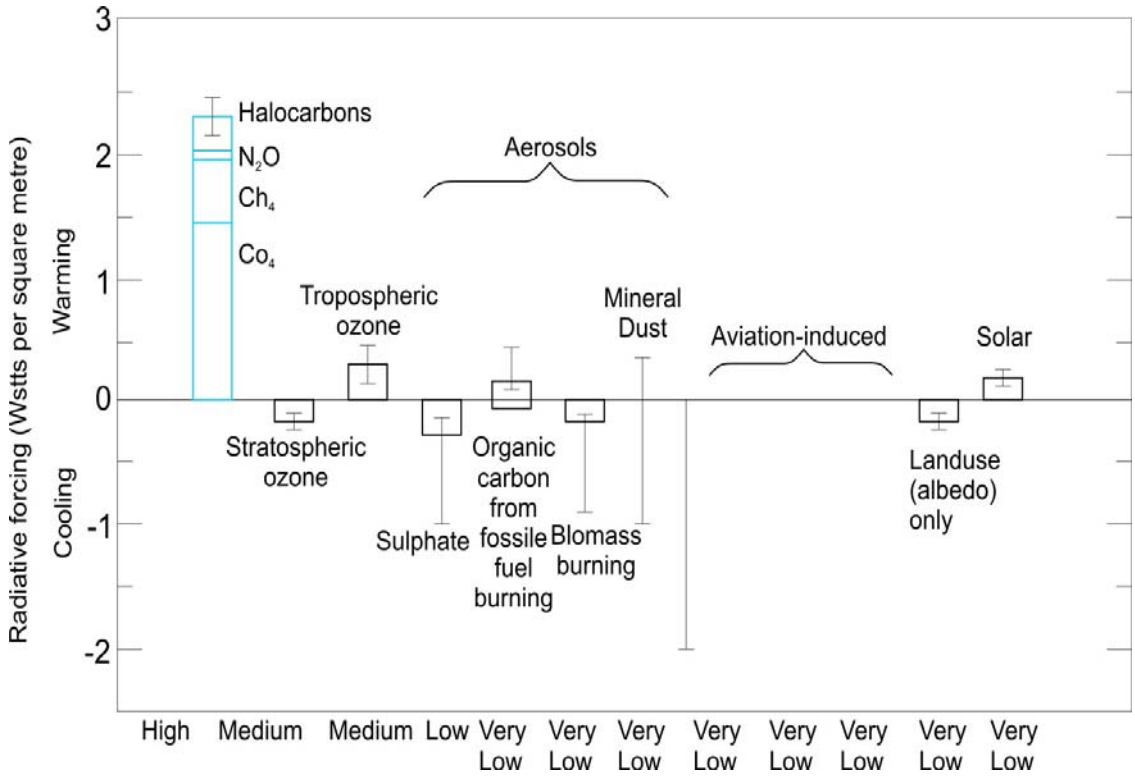

Figure 24: Summary of the principal components of the radiative forcing of climate change

All these radiative forcings result from one or more factors that affect climate and are associated with human activities or natural processes as discussed in the text. The values represent the forcings in 2005 relative to the start of the industrial era (about 1750). Human activities cause significant changes in long-lived gases, ozone, water vapor, surface albedo, aerosols and contrails. The only increase in natural forcing of any significance between 1750 and 2005 occurred in solar irradiance. Positive forcings lead to warming of climate and negative forcings lead to a cooling. The range of uncertainty for the respective radiative forcing are shown (Sources: IPCC, 2001).

2.1.8 Renewable Energy

Renewable energy sources are energy sources which are not expected to be depleted in a timeframe relevant to the human race, and which therefore contribute to the sustainability of all species. Renewable sources includes: solar, wind, biomass, wave, geothermal, tidal power and others. The International Energy Agency (IEA) has defined three generations of renewable energy technologies, reaching back more than 100 years:

First-generation technologies emerged from the industrial revolution at the end of the 19th century and include hydropower, biomass combustion, and geothermal power and heat. Some of these technologies are still in widespread use.

Second-generation technologies include solar heating and cooling, wind power, modern forms of bioenergy, and solar photovoltaic. These are now entering markets as a result of research, development and demonstration (RD&D) investments since the 1980s. The initial investment was prompted by energy security concerns linked to the oil crises of the 1970s but the continuing appeal of these renewable is due, at least in part, to environmental benefits. Many of the technologies reflect significant advancements in materials.

Third-generation technologies are still under development and include advanced biomass gasification, biorefinery technologies, concentrating solar thermal power, hot-dry-rock geothermal power, and ocean energy. Advances in nanotechnology may also play a major role.

There are many reasons for the growth of interest in renewable sources.

Renewable energy resources are more uniformly distributed geographically than are fossil fuels, providing indigenous energy resources for most fuel–poor nations. Some forms of renewable energy operate efficiently in small units and may be located close to consumers, reducing energy transmission costs. Because renewable energy sources have lesser environmental effects that conventional energy sources, especially in regard to the emission of toxic (air pollutant) and greenhouse gases (CO_2,NH_4,NO_x etc) to the atmosphere, they are expected to become an important source of energy in future years as environmental controls become more stringent.

In some form renewable energy(see Renewable energy alternatives for electricity generation, 2006) is available everywhere on Earth. Averaged over a year, the entire Earth ‘s surface (including the polar regions) intercepts some sunlight, making solar insulation universally available ;although low – latitude, dry (clear) climates have the most, whereas the polar regions have the least, solar flux at ground level. Solar insulation induces circulation in the Earth’s atmosphere, giving rise to wind and oceans waves, a long with precipitation into elevated drainage basins, providing secondary sources of solar energy. Biomass crops and forests grow in tropical and temperate lands having sufficient precipitation. Ocean tides are noticeable a long continental margins. Temperature gradients beneath the Earth‘s surface exist everywhere, providing the possibility of geothermal energy. But it is generally true that there is considerable geographic variability of each form of energy, so that some locations are more favorable for its development that others.

2.1.8.1 Solar Energy

Solar energy (REN21, 2008). (includes both direct radiation (i.e. harnessing energy from sunlight) and indirect forms of energy (such as biomass, wind, hydro, ocean thermal, ocean currents and wave energy) caused by the effects of the Sun on Earth. Most of these energy forms will be part of the energy mix when solar energy becomes the dominant traded-energy form. Some solar energy technologies are more advanced than others. The key to successful mass-utilization of solar energy is diversity. The solar energy mix will vary from region to region.

Photovoltaic, solar thermal energy (also called solar heat energy) and wind energy are presently the only solar energy technologies that can provide very large quantities of sustainable energy with high (more than 10 per cent) overall efficiency. These conversion technologies have small environmental impacts and insignificant military applications. In some countries biomass may also make a substantial contribution to energy supply, despite low conversion efficiency.

Solar energy options are:

2.1.8.1.1 Photovoltaics

Photovoltaics is the science of converting sunlight directly into electricity via solar cells without the use of moving parts. It is an elegant but expensive technology. It has found widespread use in niche markets such as consumer electronics, remote area power supplies and satellites. Large numbers of photovoltaic systems are being installed on house roofs in cities. The cost of photovoltaic systems is not a strong function of scale, which means that photovoltaic systems are often the most economical energy source for small applications. Over 90 per cent of the world photovoltaic market is serviced by crystalline silicon solar cells. This dominance is likely to continue for many years.

2.1.8.1.2 Solar Thermal Energy

Solar thermal energy can be harvested in many forms (see Renewables Global Status Report 2006 Update REN21, 2006), including high temperature steam, warm air and hot water. Most solar thermal electricity technologies use mirrors to concentrate sunlight onto a receiver. The resulting heat is ultimately used to generate steam, which passes through a turbine to produce electricity. Two non-concentrating exceptions are solar chimneys and solar ponds. Concentrator methods are equally applicable to concentrating photovoltaic systems. The usual ways of concentrating sunlight are point focus concentrators (dishes), line focus concentrators (troughs, both reflective and refractive) and central receivers (heliostats and power towers).

Solar thermal electricity is not yet a commercial proposition. The reason for this is that, unlike photovoltaic, there are strong economies of scale. This means that small systems that might be suitable for an individual household are far too expensive. This lack of a niche market, in contrast to photovoltaic, inhibits the development of solar thermal electricity in the short to medium term.

2.1.8.1.3 High Temperature Solar Heat

Concentrated solar energy can achieve the same temperatures as fossil and nuclear fuels, either directly (using mirrors) or through the use of chemicals (thermo chemicals or bio fuels) created using solar energy. One problem for high temperature solar heat is that heavy industry (e.g. the steel industry) is often located near coalfields, in regions that are relatively poorly endowed with solar energy. Solar heat can be used to extend fossil fuels. For example, if natural gas (CH_4) is heated using a dish concentrator in the presence of steam (H_2O) then hydrogen and carbon monoxide ($3H_2 + CO$) are produced. The energy content of the hydrogen and carbon monoxide is about 30 per cent greater than that of the methane, and so solar energy has been added to the original methane.

2.1.8.1.4 Low Temperature Solar Heat

Low temperature solar thermal technologies use the Sun to generate heat rather than electricity. Solar water heaters are perhaps the most well known type of solar thermal technology and are directly competitive with electricity or gas in most parts of the world. Solar concentrator water heaters have been combined with photovoltaic collectors to produce 60–70 per cent efficient hot water and electricity systems. Solar thermal technologies can also be used to heat buildings. Good building design, which allows the use of natural solar heat and light, together with good insulation, minimizes the requirement for space heating.

Solar energy collectors can be spread over a wide geographical area, unlike a nuclear power station, and terrorist strikes on a solar energy collector would not cause massive environmental problems. In addition, a renewable energy system is inherently robust because it comprises thousands of small collectors rather than a small number of large, and potentially vulnerable, generation units.

2.1.8.1.5 Other Forms Of Solar Energy

Indirect solar energy sources such as waves, ocean thermal gradients, ocean currents and hydro sources are geographically limited. Wave energy technology is still in the development phase, but could be important in the future in regions with large areas of shallow sea and frequent storms. Temperature differences between the deep and surface layers of the oceans can be used to create electrical energy, although there are severe technical problems. Hydro energy is usually associated with large environmental impacts arising fro the drowning of river valleys and the alteration of river hydrology. These energy forms could contribute modestly in particular regions to an environmentally responsible energy supply.

2.1.8.1.6 Solar Energy for Transport

Energy for transport is one of the most difficult markets for solar-derived energy to penetrate. Liquid fuels from biomass (e.g. ethanol) can power vehicles, but only at substantial environmental cost if used on a large scale. The private car in cities can be largely replaced by public transport, which is much more energy efficient than a car and can be powered by renewable electricity. Freight can be shifted to electrically powered trains. Lightweight electric cars are more efficient than current automobiles for city use. It is an open question as to whether significant private motor vehicle ownership can be afforded in an environmentally constrained world

2.1.8.2 Hydropower

Hydropower or hydraulic power is the energy of moving water. It may be captured for some useful purpose. A hydropower resource can be measured according to the amount of available power, or energy per unit time. In large reservoirs, the available power is generally only a function of the hydraulic head and rate of fluid flow. In a reservoir, the head is the height of water in the reservoir relative to its height after discharge. Each unit of water can do an amount of work equal to its weight times the head.
The amount of energy E released by lowering an object of mass m by a height h in a gravitational field is E= mgh where g is the acceleration due to gravity.
The energy available to hydroelectric dams is the energy that can be liberated by lowering water in a controlled way. In these situations, the power is related to the mass flow rate.
Substituting P for E/t and expressing m/t in terms of the volume of liquid moved per unit time (the rate of fluid flow) and the density of water, we arrive at the usual form of this expression:

$$P = \frac{E}{t} = \frac{mgh}{t} = \frac{\rho V g h}{t} = \rho \phi g h \text{ , where is } \phi = \frac{V}{t} = \frac{Sh}{t} = Sv \tag{28}$$

For P in Watts, ρ is measured in kg/m³, Φ is measured in m³/s, g is measured in m/s², V is measured in m^3 and h is measured in meters.
Some hydropower systems such as water wheels can draw power from the flow of a body of water without necessarily changing its height. In this case, the available power is the kinetic energy of the flowing water.

$$E_k = \frac{mv^2}{2} \text{, than } P = \frac{E_k}{t} = \frac{mv^2}{2t} = \frac{\rho V v^2}{2t} = \frac{1}{2}\rho \phi v^2 = \frac{1}{2}\rho S v^3 \tag{29}$$

where v is the velocity of the water, or with $\phi = Sv$ where S is the area through which the water passes, also Over-shot water wheels can efficiently capture both types of energy. The construction of the dam may provide benefits other than electric power, such as water for irrigation or flood control, that reduce the costs allocated to electricity production.

Small scale hydro or micro-hydro power with a capacity of 10 to 35 MW has been increasingly used as an alternative energy source, especially in remote areas where other power sources are not viable. Small scale hydro power systems can be installed in small rivers or streams with little or no discernible environmental effect on things such as fish migration. Most small scale hydro power systems make no use of a dam or major water diversion, but rather use water wheels. In poor areas, many remote communities have no electricity.

Micro hydro power, with a capacity of 100 kW or less, allows communities to generate electricity. This form of power is supported by various organizations.

Micro-hydro power can be used directly as "shaft power" for many industrial applications. Alternatively, the preferred option for domestic energy supply is to generate electricity with a generator or a reversed electric motor which, while less efficient, is likely to be available locally and cheaply.

2.1.8.2.1 Environmental Effects

Hydropower plants can have severe environmental effects. Where a reservoir is formed behind a dam, aquatic and terrestrial ecosystems are greatly altered. Downstream of the dam, the river in a flow is altered, interfering with ecosystems that have adjusted to the natural variable river flow pattern. The reservoir interrupts the natural siltation flow in the river and its contribution to alluvial deposits downstream. The flooding of land that previously served for agriculture and human habitation may be a significant social and economic loss. The construction of dams interferes with the migration of anadramous fish and adversely affects their populations, even where fish ladders are employed.

2.1.8.3 Biomass Energy

Biomass refers to combustible or fermentable biomaterials created via photosynthesis.
It can be derived from waste materials such as sugar cane bagasse, garbage, sawdust and sewerage or from energy crops such as trees or canola. Firewood is another common form of biomass energy. When biomass production for energy is combined with other useful purposes the economic viability of biomass energy can be substantially improved.

Another from biomass that can be converted to useful is animal waste. Digesters can generate methane from animal or human wastes; with the residue of this process being suitable for crop fertilizing. Organic matter in municipal waste landfills generates methane in an uncontrolled process that can supply low heating value gas.

Organic matter in terrestrial plants and soil is among other things, a temporary storage system for solar energy. The conversion of atmospheric CO_2 and H_2O to organic matter by photosynthetic reactions in plants stores the energy of visible light from the Sun in the form of chemical energy of the organic matter The latter may be utilized in the same manner as fossil fuels, releasing CO_2 back to the atmosphere. Thus no net emissions of CO_2 to the atmosphere result from this cycle. However, the efficiency of conversion of solar radiation to biomass energy is very low, less than 1%, with the terrestrial average energy conversion rate amounting to 0.5 W/m^2. The food energy stored in agricultural crops like grains is only a fraction of that in the entire crop mass, so that agricultural crop residues are potential sources of biomass energy. he energy required to collect, store and utilize this residue further reduces the amount of energy available from it to replace fossil fuels.

The overall photosynthetic process by which water and carbon dioxide are combined to form carbohydrate molecules in plants may be summarized as

$$nCO_2+mH_2O \rightarrow C_n(H_2O)_m+nO_2 \quad (30)$$

The first step of this overall process is the photosynthetic one, in which solar radiation provides the energy needed to start the processes that end in the producing of carbohydrates, such as sugar, starch, or cellulose. Subsequent steps dissipate some of that energy, storing the rest in chemical from. The process of conversion of solar energy into biomass is called primary production. All living systems depend ultimately upon this process to maintain their viability

The principal processes that utilize the energy content of primary biomass are as follows:

- Combustion
- Gasification

- Pyrolysis
- Fermentation
- Anaerobic digestion

Wood plants and grasses can be burned directly in furnaces, or boilers. Alternatively, biomass may be converted to a gaseous fuel composed of H_2 and CO in a thermal process that conserves most of its heating value, with the fuel being combustible in boilers and furnaces. Pyrolysis, the thermal decomposition of biomass, produces a combination of solid, liquid, and gaseous products that are combustible. Fermentation and distillation of carbohydrates produces ethanol (C_2H_5OH) a valuable liquid fuel that is commonly blended with gasoline for motor vehicle use.
Anaerobic digestion produces a gaseous mixture of CO_2 and CH_4.The gaseous fuels can be upgraded to a more desirable one, albeit at some loss of energy.
In the fermentation and distillation process that converts corn starch to ethanol, only 65% of the grain heating value is preserved in the ethanol output from process. In addition, fossil fuel is consumed in the production and harvesting of corn and the production of ethanol. As a consequence, use of ethanol as a vehicle fuel additive results in only a 50-60 % reduction in fossil fuel energy use and a 35-46% reduction in greenhouse gas emission, compared to the use of ordinary vehicle fuel. Thus the energy gain factor for corn –generated ethanol is 2-2.5.

2.1.8.3.2 Environmental Effect

The use of crops or their residues to supply fuel to replace fossil fuel creates environmental impacts similar to those associated with agriculture and silviculture: consumption of manufactured fertilizers, spreading of pesticides and herbicides, soil erosion, consumption of irrigation water, and interference with natural ecosystems. Air emissions from the combustion of biomass fuels are not always less that those from the fossil fuels they replace.

2.1.8.4 Geothermal Energy

Geothermal energy is heat energy that comes from the decay of radioactive elements within the Earth. This energy is what remains from the gravitational collapse of the interplanetary material from which the Earth was formed. The Earth‘s interior consists of a core of mostly molten material at a temperature of about 4000 ^{0}C, extending to a little more than half an Earth radius and surrounded by a mantle of deformable material. By drilling wells to depths of 5-10 km and pumping from them water or steam heated to 200 - 300 ^{o}C enough heat may be extracted to generate hundreds of megawatts of electrical power in a single geothermal plant. Heat associated with volcanic regions can be used to generate steam for district heating or to drive steam turbines to produce electricity.
Another form of geothermal energy is ‘hot dry rocks’, which refers to hot masses of slightly radioactive rock buried several kilometers below the surface of the Earth. Cold water forced down to this hot rock becomes steam that can be extracted from boreholes nearby. Geothermal energy is restricted to particular geographical locations. While it is sustainable in the sense that it can be harvested with limited environmental damage, the heat stored in a particular place can certainly be depleted.
One recent development that utilizes the heat storage capacity of an underground aquifier is called the geothermal heat pump. In this system, water from a well supplies heat to a heat pump that then releases a greater amount of heat to a building during cold weather. The heat pump produces much more heat per unit of electrical work required to run it than would be the case if the heat pump used cold winter ambient air as its heat source. In climates where air conditioning is needed in summertime, this same system can be reversed to deposit the heat rejecting it to the hot summer ambient air. This system is practical only for central air conditioning and heat pump systems and then involves the additional expense of well drilling. Depending upon the price of electricity, the savings in power may repay the additional investment.

2.1.8.4.1 Environmental Effects

Geothermal fluids contain dissolved gases, e.g. hydrogen sulfide, sulfur dioxide and radon, all of which are toxic to humans and must be safely removed from the condenser by steam ejectors, causing energy loss.

2.1.8.5 Wind Power

Wind energy Wind power is the conversion of wind energy into useful form, such as electricity, using wind turbines. In windmills, wind energy is directly used to crush grain or to pump water. At the end of 2007, worldwide capacity of wind-powered generators was 94.1 GW. Wind power is produced in large scale wind farms (Figure 25) connected to electrical grids, as well as in individual turbines for providing electricity to isolated locations. Wind energy is plentiful, renewable, widely distributed, clean, and reduces greenhouse gas emissions when it displaces fossil-fuel-derived electricity.

Figure 25: Wind Farms

Modern wind generators are very different from old-style water-pumping windmills. For one thing, they are huge. They have 40–70 m high tubular steel towers on a concrete foundation and have three blades, each 20–40 m long. They are computer-controlled and centrally monitored, with many safety features. They have capacities in the multi-megawatt range and will operate reliably for more than 20 years. Wind generator towers occupy very little land per machine. Many wind farms are located on cleared farming land. Provided that a wind farm is not located in an ecologically sensitive area, the only significant environmental impact of wind energy is visual.

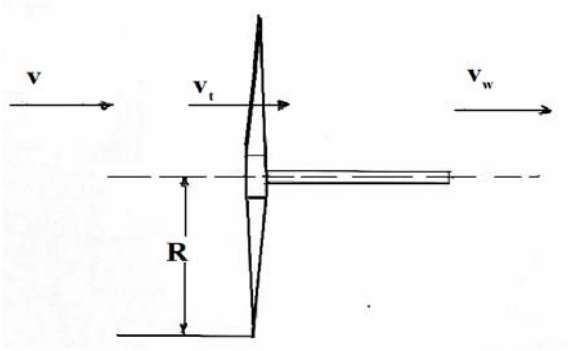

Figure 26: The flow of wind through a wind turbine whose blade radius is *R* is slowed at the turbine disk and is slowed even further in the wake region down stream of the turbine

The source of power from the wind is the flow of air through the wind turbine. If v is the wind speed, each unit mass of air possesses a kinetic energy of amount $mv^2/2$. If $S = \pi R^2$ in the area subtended by the rotating blades of length *R*, then mass flow rate of air through an area *S* of the undisturbed wind stream is ρvS, and the kinetic energy per unit mas,$v^2/2$,for a value of $\rho v^3 S/2$. In practice, the wind turbine power available from aerodynamically prefect design is less than this value because the action of the turbine modifies the surrounding wind flow, reducing the mass flow rate below the value of ρvS.
To illustrate this effect, Figure 26 shows the ideal wind flow past a turbine. Because the turbine extracts some of the kinetic energy of the wind flow, the wind speed is reduced in the vicinity of the turbine to a

value v_t at the turbine an even lower of v_w downstream of the turbine, called the wake region. The turbine power P is then the product of the mass flow rate through the turbine, $\rho\ v_t\ S$,and the reduction of kinetic energy of the wind,

$$m(v^2/2 - v_w^2/2), \quad \text{or } P = \frac{1}{2}\rho v_t (v^2 - v_w^2)S \tag{31}$$

Generally, tower height is proportional to turbine diameter, the turbine axis being about one to two diameters above ground.

Wind turbines need to be protected from damage by storm or hurricane level winds and, in northern climates, from icing conditions in winter months. Wind turbines are customarily installed at adjacent sites called “wind farms” an example of which is shown in Figure 26. Currently, wind turbines are manufactured in the power range of a few hundred kilowatts to several megawatts, so that hundreds of them must be deployed to equal the out put of a typical steam electric power plant.

2.1.8.5.1 Environmental Effect

There are several environmental drawbacks of wind energy systems. Wind turbines generate audible noise, somewhat akin to that of helicopters, but much less intense because of their much lower power levels. Nevertheless, wind turbines are unwelcome noisy neighbors in populated areas but have no adverse effect on livestock operations. They can however, kill migrating birds that attempt to fly through the turbine. To some observers they provide visual blight, especially if located in otherwise undeveloped natural areas.

2.1.9 Renewable Potentials in Kosovo

Kosovo has rivers with a hydropower potential (see: http://enrin.grida.no/htmls/kosovo/SoE/energy.htm) that could be considered for use in electric power production. West part of Kosovo has the hydropower potential of the Drini i Bardhë (White Drin) river, which represents more than the half hydropower potential of Kosovo. Usable hydropower potential of Kosovo is about 0.7 TWh/year. The most important hydropower plant that could be built in Kosovo, is the HPP of Zhur on the Drini i Bardhë flow with a potential of 0.377 TWh/year. Drini i Bardhë, Ibri, Morava, Lepenc and Llap river flows are characterized with an important potential for electric energy production.

Use of the solar energy is also possible in Kosovo (solar, thermal and photovoltaic) as well as the wind energy for which there are appropriate locations for building the wind farms, for example in the region of Shtime, where such a wind farm is foreseen to be built with foreign investments.

Kosovo has potentials for the use and production of bioenergy in its various forms (wood, biodisel, bioethanol, biogas production from farms, etc.)

The renewable energy of Kosovo (middle and small hydropower stations, solar, wind, etc.) are:

already existing: 2x17.5 MW; 5xHPP = 11.82 MW, and potential the following can be built:18 other small HPPs with the total power of 63.70 MW, (Table 3.), as well as 2 x middle HPPs with the total power of 292.8 MW, which in total amounts 403.32 MW.

Also, construction of a wind farm power station is planned in Shtime, with the installed power of 25 MW in 2012, and several other wind stations which will achieve an overall power up to 50 MW in 2025, whereas the solar energy in various modes (solar, thermal and photovoltaic) will achieve the power from 5 MW in 2012 to 50 MW in 2025.

Table 3: Renewable Potential of Kosovo

RENEWABLE POTENCIALS KOSOVO		
Hydropower Plant	Power (MW)	Energy(GWh)
Existing HPPs in the distribution network	11.82	38
New HPPs to be built	63.7	294
HPP Ujman	35	101
HPP Zhur	292.8	398
Total	403.32	831
Solar Energy[1]	Power MW	EnergyGWh
Solar	5	10
Photovoltaik	5	10
Termal	5	10
Biomas	35	70
Total	50	100
Wind Energy[2]	Power MW	EnergyGWh
Wind Farm Shtime	25	50
Other	25	50
Total	50	100
Total Renewable	503.2	1031

The total power from renewable sources in the year 2025 will be 503.32 MW, which will be 12.42% of the overall energy produced in that year. Possible identified potential for construction of 18 small hydropower plants (Source: MEM/2006) (see Table 4)

Table 4: New Hydropower Plant to be Built and/or Rehabilitated in Kosovo (Source: MEM/2006)

New HPPs to be built					
Name	Power (MW)	Energy (GWh)			
Name	3.9	17	10:HPP Dragash	2.2	10
1:HPP Kuqishte	6.2	27	11: HPP Orqush	5.6	25.6
2:HPP Drelaj	7.6	35	12: HPP Reqan	1.5	6.7
3:HPP Shtupeq	5.2	25	13: HPP Brezovice	2.1	10
4: HPP Belle	8.3	39	14: HPP Lepenc	3.5	16
5:HPP Deqan	3.1	14	15:HPP Bajske	0.3	1.4
6: HPP Lloqan	4	18	16: HPP Batare	1.1	5.8
7:HPP Mal	2	9	17: HPP Majance	0.6	2.9
8: HPP Erenik	1.9	9.7	18: HPP Mirusha	4.6	22
Total: New HPPs	Power(MW)		Energy (GWh)		
	63.7		294.1		
	Existing HPPs to be rehabalitated				
19:HPP Dikanc	1.9	10	22:HPP Prizren	0.33	1.4
20: HPP Radavc	0.35	1.8	23: HPP Shtime	0.14	0.6
21: HPP Burim	0.8	4.6			
Total: Existing HPPs	Power (MW)		Energy (GWh)		
	3.52		18.4		
Total: All HPPs	67.22		312.5		

2.1.10 Kyoto Protocol and Kosovo

The Kyoto Protocol (see The Kyoto protocol - A brief summary), is a protocol to the international Framework Convention on Climate Change with the objective of reducing Greenhouse gases that cause climate change. It was agreed on 11 December 1997 at the 3rd Conference of the Parties to the treaty when they met in Kyoto, and entered into force on 16 February 2005.
The Kyoto Protocol is an agreement made under the United Nations Framework Convention on Climate Change (UNFCCC). Countries that ratify this protocol commit to reduce their emissions of carbon dioxide and five other greenhouse gases, or engage in emissions trading if they maintain or increase emissions of these gases.
As of January 2008, and running through 2012, Annex I countries have to reduce their greenhouse gas emissions by a collective average of 5% below their 1990 levels (for many countries, such as the EU member states, this corresponds to some 15% below their expected greenhouse gas emissions in 2008). While the average emissions reduction is 5%, national limitations range up to 10% for Iceland; but since the EU's member states each have individual obligations, much larger increases (up to 27%) are allowed for some of the less developed EU countries (see below Increase in greenhouse gas emission since 1990). (Beltrami, E. 1998) Reduction limitations expire in 2013;
Kosovo has no obligations towards the Kyoto protocol (see https://www.ks-gov.net/mem). Ratifying the Energy Community Treaty, until 2015, it must fulfill its needs for energy with 10-12% from the renewable sources. Meanwhile, adhering in the European Union will oblige Kosovo to reduce the CO_2 level for 25-35%, increasing the level of exploring the renewable energy and applying new technologies for greenhouse gas reduction.

3 Materials and Methods

3.1 Zero Dimensional Greenhouse Effect and CO_2 Reduction-Dynamic Modeling

The radiation energy of the Sun constitutes the basic driving force for the atmospheric and oceanic general circulations. Thus, the most important external factor for the Earth's climate is the total incoming solar radiation. The incoming solar radiation is characterized by the solar constant, the obliquity, the eccentricity, and the longitude of perihelion for the Earth's orbit around the Sun.
The net flux of radiation at the Earth's surface results from a balance between the solar and terrestrial radiation fluxes:

$$\Phi_{rad}^{sfc} = \Phi_{sw} + \Phi_{LW} \tag{32}$$

The short-wave and long-wave radiation balance can be expressed by

$$\Phi_{SW} = \Phi_{SW}^{\downarrow} - \Phi_{SW}^{\uparrow} \tag{33}$$

and

$$\Phi_{LW} = \Phi_{SW}^{\downarrow} - \Phi_{SW}^{\uparrow} \tag{34}$$

Therefore, the overall radiation balance becomes

$$\Phi_{rad}^{sfc} = \Phi_{SW}^{\downarrow} - \Phi_{SW}^{\uparrow} + \Phi_{LW}^{\downarrow} + \Phi_{LW}^{\uparrow} \tag{35}$$

Where the downward and upward arrows denote the incoming and outgoing radiation components respectively.
The incident solar radiation $\Phi_{SW}^{\downarrow}$ is the sum of the direct and diffuse solar radiation. It has a pronounced diurnal and seasonal variation, and is also strongly affected by clouds. The outgoing short-wave solar radiation is the part reflected by the surface

$$\Phi_{SW}^{\downarrow} = a_{sfc}\Phi_{SW}^{\downarrow} \tag{36}$$

where a_{sfc} is the surface albedo so that the net short-wave radiation is:

$$\Phi_{SW} = \left(1 - a_{sfc}\right)\Phi_{SW}^{\downarrow} \tag{37}$$

The incoming long-wave radiation $\Phi_{LW}^{\downarrow}$ comes from the atmosphere and depends on the vertical temperature profile, the clouds and the vertical distribution of the absorbers. It does not show a significant diurnal variation. The outgoing long-wave radiation $\Phi_{LW}^{\downarrow}$ is given by the Stefan-Boltzmann law, assuming a given emissivity $\in$ for the Earth's surface. As expected, it follows the diurnal cycle in surface

temperature with a maximum value in the early afternoon and a minimum value in the early morning. The incoming and outgoing long-wave radiation components have the same order of magnitude so that the net long-wave radiation flux is small compared to a long-wave radiative cooling of the surface. The net radiation flux at the surface is then given;

$$\Phi_{rad}^{sfc} = \Phi_{SW}^{\downarrow}\left(1 - a_{sfc}\right) - \in \sigma T_{sfc}^{4} + \Phi_{LW}^{\downarrow} \tag{37}$$

This net radiation heats the surface.
The infrared emitted by the surface ;

$$\in \sigma T_{sfc}^{4} \tag{38}$$

is strongly absorbed by water vapor and carbon dioxide in the atmosphere. In turn, the atmosphere will re-emit the absorbed energy both upward and downward. The downward component will be absorbed by the Earth's surface and heat it. Thus the temperature of the Earth will be higher than it would be if the atmosphere were transparent for the long-wave radiation
The observed world-wide increase in the concentrations of CO_2 and other trace gases in the atmosphere increases the Earth surface temperature, and a smaller part is lost to the underlying layers or used to melt snow and ice. Thus, there are essentially four types of energy fluxes at the Earth's surface. They are the net radiation flux Φ_{rad} the (direct) sensible heat flux $\Phi_{SH}^{\uparrow}$, the (indirect) latent heat flux $\Phi_{SH}^{\uparrow}$, and the heat flux into the subsurface layers $\Phi_{G}^{\uparrow}$. Under steady conditions the balance equation for the energy is given by

$$\Phi_{rad}^{sfc} - \Phi_{SH}^{\uparrow} - \Phi_{LH}^{\uparrow} - \Phi_{G}^{\downarrow} - \Phi_{M} = 0 \tag{39}$$

Where Φ_M is the energy involved in melting snow and ice in freezing water.

3.1.1 Climate Model with No GHG in Atmosphere

Measurements of the planetary albedo combined with the known impinging solar radiation at the top of the atmosphere supply the necessary information on the first component of the radiation budget, the net solar input. The second component of the radiation budget involves measuring the long-wave, terrestrial radiation.
By and large, the Earth as whole is in radiative equilibrium averaged over a period of several years. In other words, as much energy must be leaving the system in the form of long-wave radiation as is entering in the form of short-wave radiation:

$$\Phi_{TA} = \int_{top}(1-a)\Phi_{SW}^{\downarrow}\,ds - \int_{top}\Phi_{LW}^{\uparrow}\,ds \approx 0 \tag{40}$$

Where Φ_{TA} net flux of radiation at the top of the atmosphere, $\Phi_{SW}^{\downarrow}$ incoming solar flux, and $\Phi_{LW}^{\uparrow}$ =Long wave flux to space. Since the average albedo of the Earth is on the order of 31%, an amount of solar radiation given by (see Figure 27).

$$\Phi_E = \Phi_S - a\Phi_S = (1-a)\phi_S = (\pi R^2 / 4\pi R^2)(1-a)S = (1-a)\frac{S}{4} \approx 235 Wm^{-2} \tag{41}$$

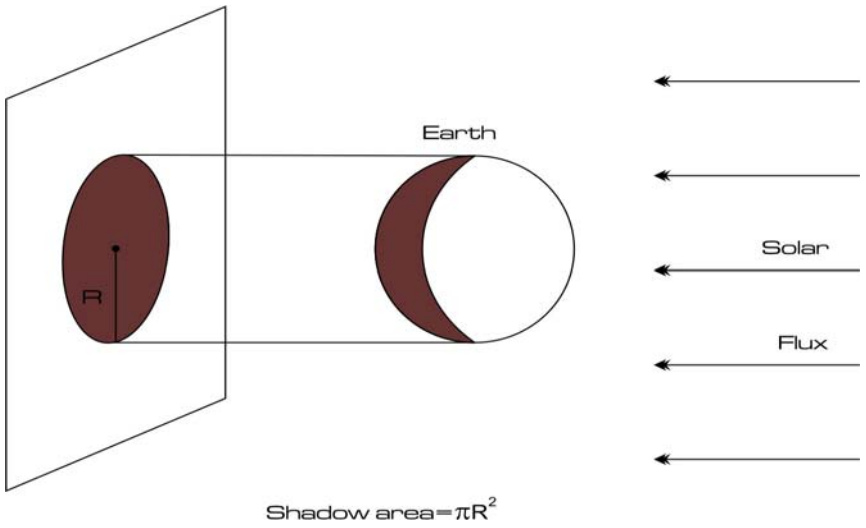

Figure 27: Diagram showing the shadow area of spherical planet.

that is absorbed in the atmosphere and oceans, and later re-emited as long-wave terrestrial radiation, where the solar constant S=1368 W/m^2.

We assuming that there is a balance between the amount of solar energy received and the amount of energy emitted by the Earth as a whole and that the Earth radiates according to the Stefan–Boltzmann law: $\left\langle \sigma T_E{}^4 \right\rangle = 235\ W/m^2$. The relationship between energy flux and surface temperature is given as: $\Phi_E = \sigma\, T_E{}^4$, where Φ_E = energy flux (W/m^2), σ is the Stefan-Boltzmann constant equal to 5.67 10^{-8} (W/m^2 /K^4), T= temperature in degrees Kelvin.
For the solar-Earth system described in Eq. 41, the amount of energy flux absorbed and radiated by the Earth (Φ_E) is equal to (1-a) Φ_s .Thus, the Earth's average surface temperature is calculated as:

$$T = (\frac{\Phi_E}{\sigma})^{\frac{1}{4}} = \left[\frac{(1-a)\Phi_s}{\sigma}\right]^{\frac{1}{4}} \qquad (42)$$

Note that temperature represents an average surface temperature - one that we expect if the solar energy flux were distributed equally over all parts of the globe. This, of course, is not the case, but it gives us a point of departure for studying the global warming phenomenon. By substituting values of a=0.313 and Φ_s =342W/m^2, we can calculate the value of the Earth's surface temperature to be approximately 254K (or -19˚C) (see: "no atmosphere climate model" (Figures 28, 29 and 30) (Robinson, 2001)). The temperature of -19^{o}C is achieved in 4 years if the albedo is 0.313, and if the albedo is 0.5 than during the same time interval the temperature becomes lower as can be seen from Fig 30.

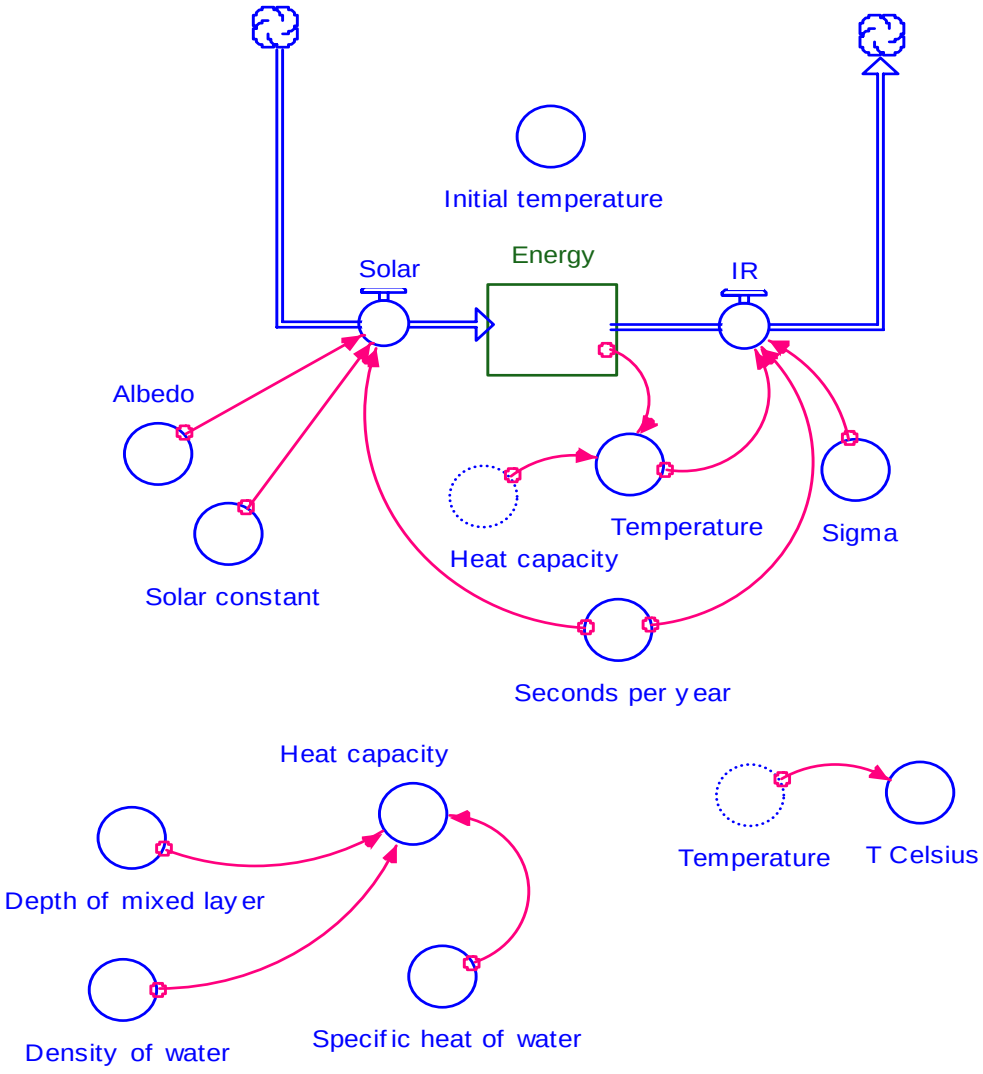

Figure 28: Climate model with no GHG in atmosphere.

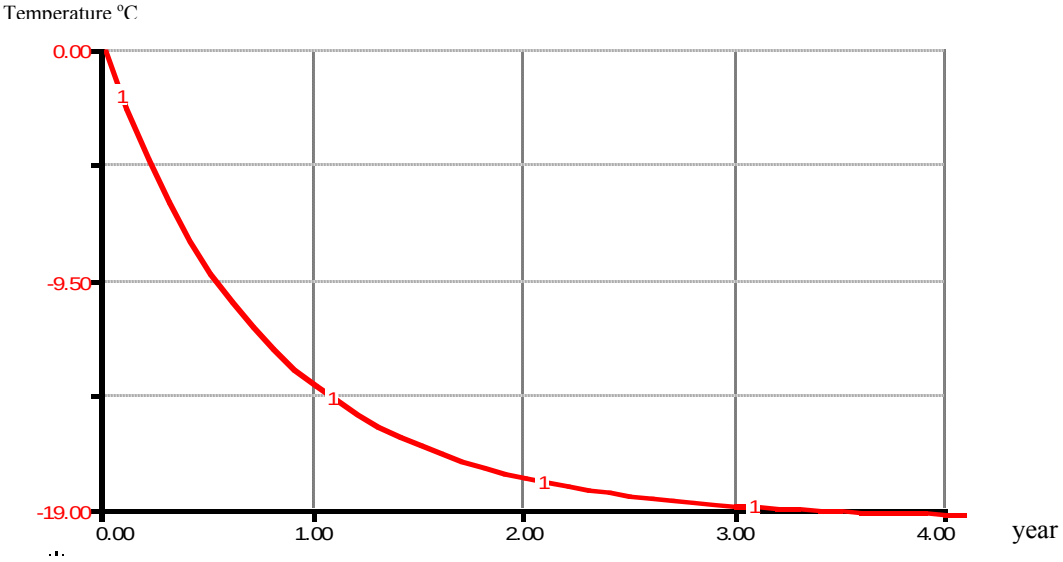

Figure 29: Temperature of the Earth surface in climate model with no GHG in atmosphere and with albedo a=0.313.

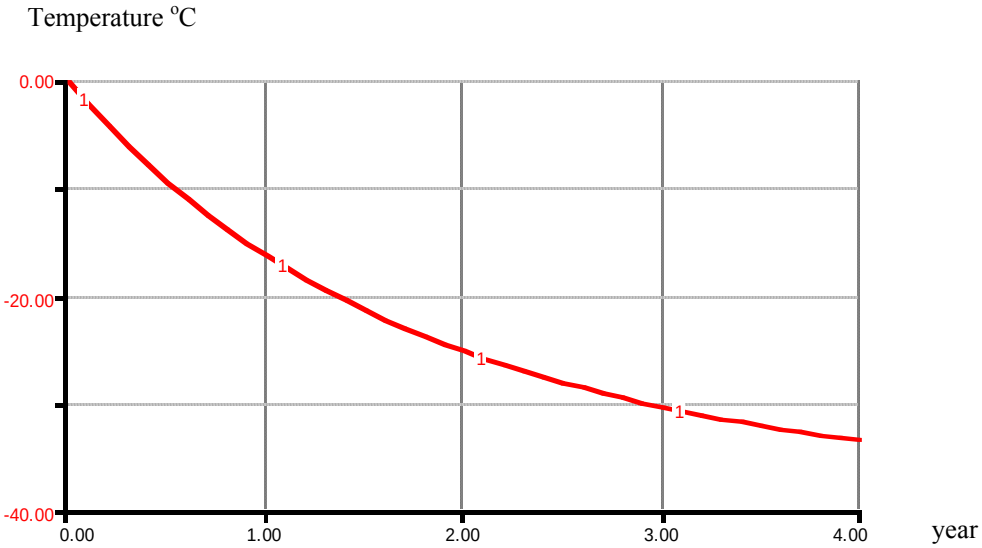

Figure 30: Temperature of the Earth surface in climate model with no GHG in atmosphere and with albedo $a = 0.5$.

3.1.2. Greenhouse Zero-Dimensional Model with CO_2 In Atmosphere - No Accumulation of CO_2

However, Eq. (37) shows that due to the existence of the atmosphere with gases that absorb and emit the long-wave radiation, the surface temperature of the Earth T_{sfc} is greater than the effective emission temperature T_e. Thus ;

$$T_{sfc} = T_e + \Delta T \tag{43}$$

Where ΔT represents the atmospheric greenhouse effect on the surface temperature. Since the mean surface temperature of the Earth is 288 K, the greenhouse effect due to the existence of the atmosphere on the surface temperature is $\Delta T = 34\ K$. The average surface temperature of the Earth, is not $-19^0 C$ (it is about $34^\circ C$ higher, or $+15^\circ C$), so we must revisit our assumptions to determine why our estimate is inaccurate. See Energy balance without accumulation GHG in atmosphere (Figure 31.) The albedo a = const, energy of radiation is constant $E=const.$, and therefore the temperature is constant and it amounts to $T = +15^\circ C$.(Figure 32). Using the albedo $a = 0.5$ we obtain the results in Fig 33. Note, that the effect of the larger albedo is to cause the time dependence of the temperature as seen in Fig 33.

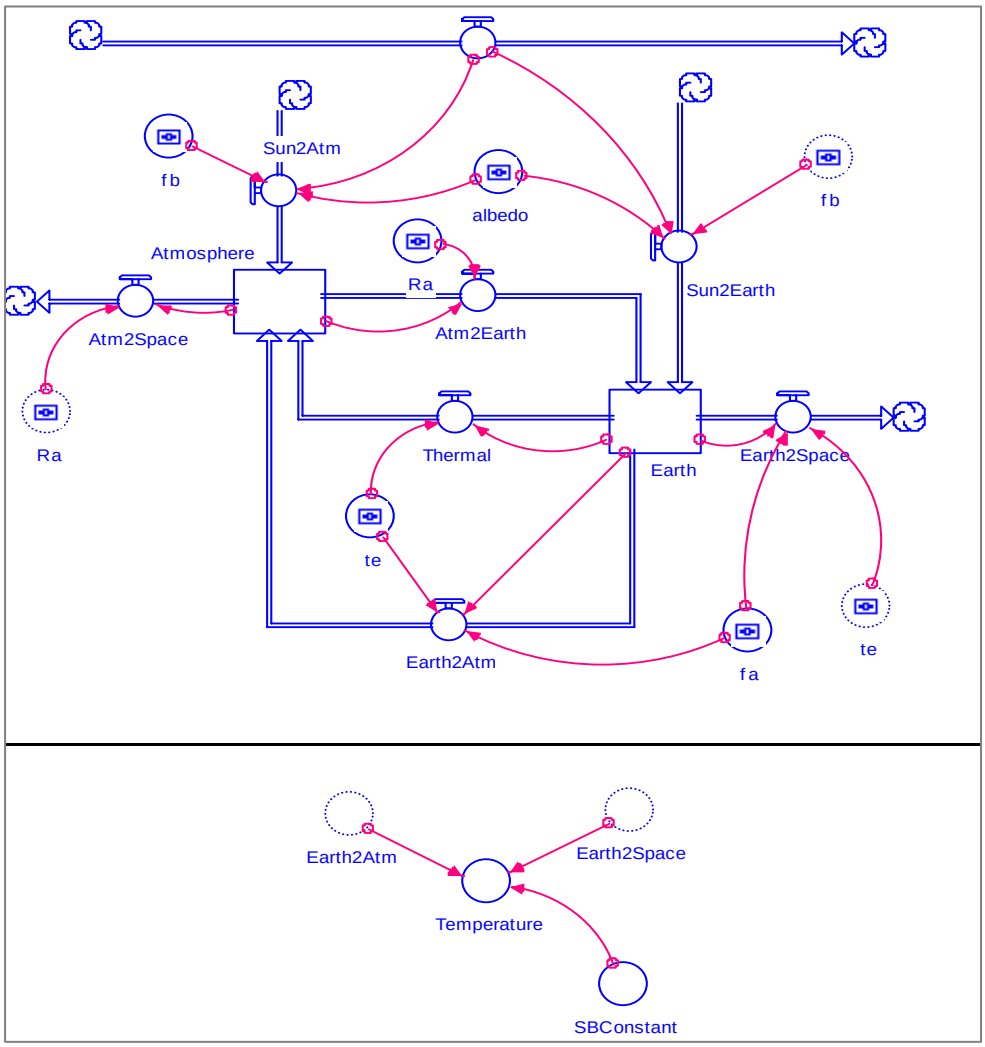

Figure 31: Greenhouse zero-dimensional model with $C0_2$ in atmosphere-no accumulation

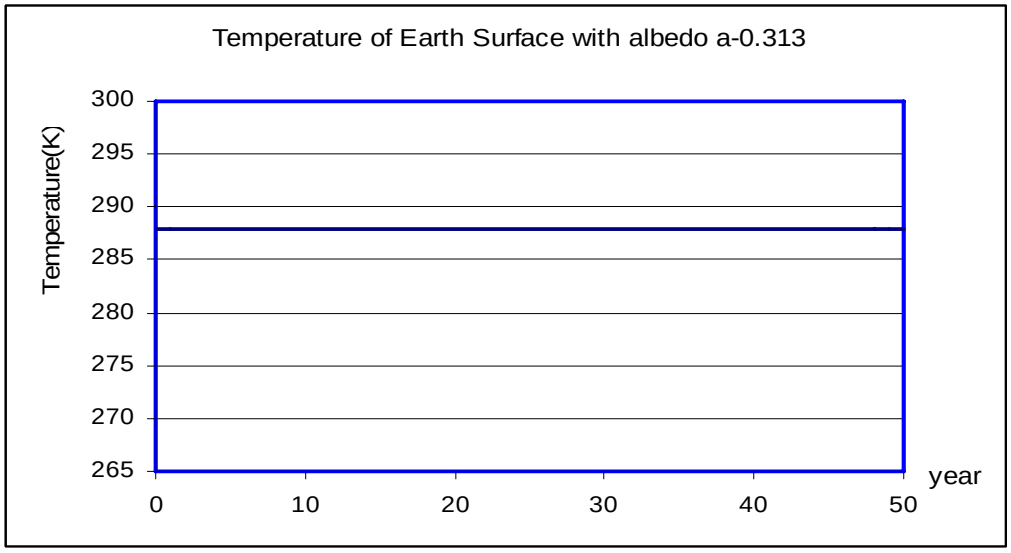

Figure 32: Temperature of the Earth surface in greenhouse zero-dimensional model with CO_2 in atmosphere-no accumulation with albedo *a=0.313*

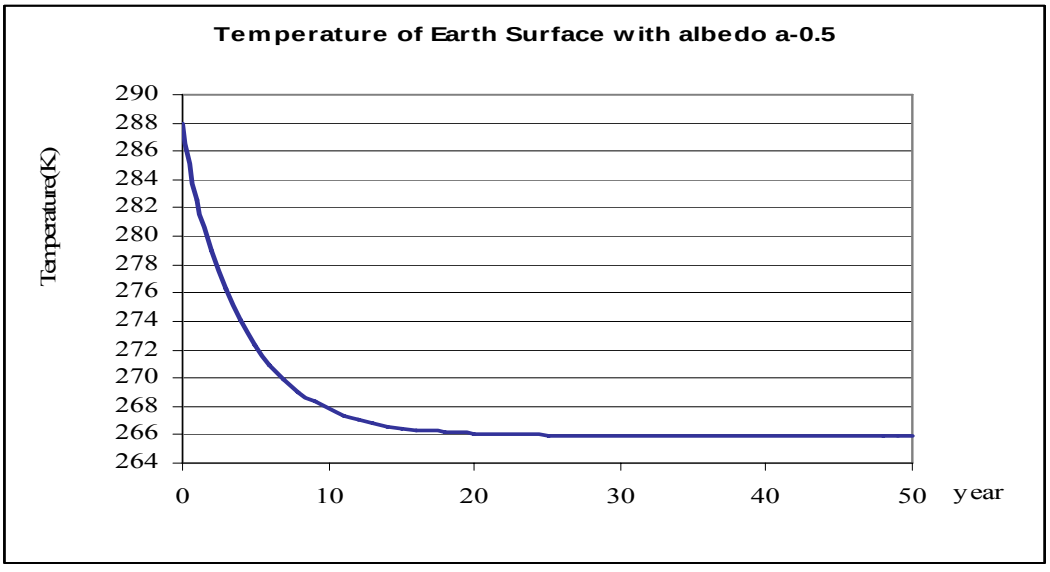

Figure 33: Temperature of the Earth surface in greenhouse zero-dimensional model with CO_2 in atmosphere-no accumulation with albedo *a=0.5*

3.2 Greenhouse Effect-Dynamic Modeling

The Sun powers Earth's climate, radiating energy at very short wavelengths, predominately in the visible or near-visible (e.g., ultraviolet) part of the spectrum (Figure 8). Roughly one-third of the solar energy that reaches the top of Earth's atmosphere is reflected directly back to space. The remaining two-thirds is absorbed by the surface and, to a lesser extent, by the atmosphere. To balance the absorbed incoming energy, the Earth must on average radiate the same amount of energy back to space. Because the Earth is much colder than the Sun, it radiates at much longer wavelengths, primarily in the infrared part of the spectrum (see Figure 8). Much of this thermal radiation emitted by the land and ocean is absorbed by the atmosphere, including clouds, and reradiated back to Earth. This is called the greenhouse effect (Deaton and Winebrake, 2000). The glass walls in a greenhouse (Philander, 1989) reduce airflow and increase the temperature of the air inside. Analogously, but through a different physical process, the Earth's greenhouse effect warms the surface of the planet. Without the natural greenhouse effect, (Kraljic, 1992) the average temperature at Earth's surface would be below the freezing point of water (-19^{o}C) (see climate model with no atmosphere, Figure 29.).
Thus, Earth's natural greenhouse effect makes life as we know it possible (T_e=15^{o}C, Figure 32). However, human activities, primarily the burning of fossil fuels and clearing of forests, have greatly intensified the natural greenhouse effect, causing global warming.

3.2.1 Physics of Greenhouse Effect

In 1824, Jean–Baptiste Fourier hypothesized that gases in the atmosphere act to trap heat within the Earth's biosphere. It was unknown how this happened until scientists started to investigate how gas molecules respond to interactions with energy. In 1859, John Tyndall identified through laboratory experiments the absorption of thermal radiation by complex molecules. He noted that changes in the amount of any of the radiatively active constituents of the atmosphere such as water (H_2O) or CO_2 could have produced changes of climate.
When molecules are struck by photons, those molecules absorb this energy and become excited. If the energy is in ultraviolet (UV) part of the electromagnetic spectrum (i.e., low wavelength, high frequency, high energy), then the energy may break the bonds of the molecule. If the energy is in the infrared (IR) part of the spectrum (i.e., high wavelength, low frequency, low energy), then it may set the molecule spinning or may cause the atoms in the molecule to vibrate (Figure 19).
Certain molecules, due to their composition and structure, will start vibrating when struck with IR radiation. These molecules absorb the incoming radiation, become excited, and then reradiate this energy (in all directions) as they move from this excited state back into a stable, or ground, state. Carbon dioxide (CO_2), water vapor (H_2O), methane gas (CH_4), nitrous oxide (N_2O) and chlorofluorocarbons (CFCs) are all molecules that behave in such a manner.
Thus, the gases mentioned earlier have the ability to absorb outgoing infrared radiation from the Earth and incoming radiation from the Sun, and to reradiate this energy in all directions. On average, half of the reradiated energy will be emitted up (i.e., toward space) and the other half will be emitted down (i.e., toward Earth),where it will be reabsorbed by the Earth and ultimately reradiated. Through this process, the amount of energy flux directed at the Earth is increased.
Earth now has two inputs: direct energy from the Sun and reradiated energy from atmospheric gases. Because Earth is in an energy balance, this also means that the amount of energy flux output from the Earth is increased. This increase in radiated energy increases the temperature of the Earth based on the black body radiation model discussed earlier.

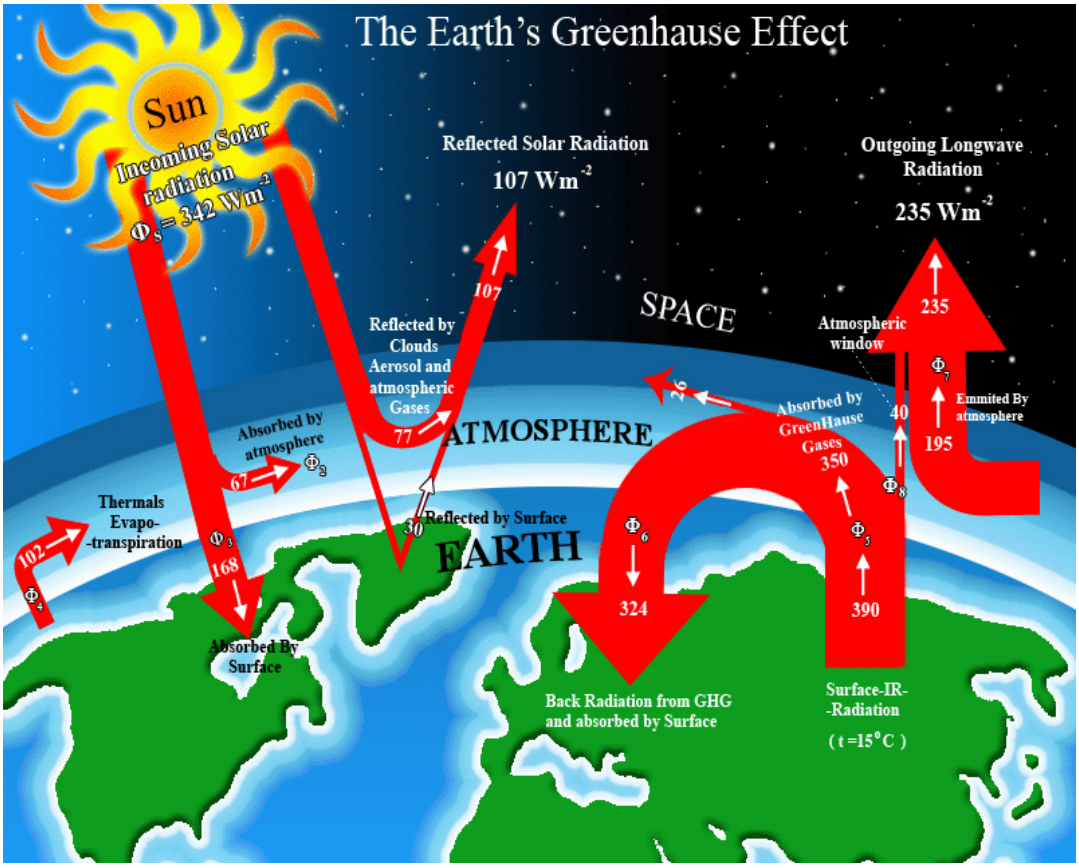

Figure 34: Schematic diagram of the Earth's greenhouse effect, with arrows proportional in size to the fluxes of energy by the particular process

Of incoming solar radiation *342 W/m*^{2}, about *107 W/m*^{2} is reflected back into space by clouds and the surface, about *67 W/m*^{2} is absorbed in the atmosphere, and about *168 W/m*^{2} is absorbed at the surface. Most of the infrared (heat) radiation emitted by the surface *390 W/m*^{2} is absorbed in the atmosphere *350 W/m*^{2} and the atmosphere in turn then emits about *324 W/m*^{2} of this amount back to the surface and 26 W/m^2 of the turbulent heat can be absorbed by water, ozone or oxygen. The extra energy at the surface *102 W/m*^{2} is used to evaporate water or heat the near surface atmosphere. In the atmosphere, the extra energy it receives from the Sun, from absorbed infrared radiation, from latent and turbulent heating released during precipitation, and from sensible heating, is emitted to space *235 W/m*^{2} to balance the net solar radiation absorbed by the surface and atmosphere

3.2.2 Mathematical Relationship for Sun-Atmosphere – Earth Energy Flow Diagram

To build a valid model of Earth's energy system, we must determine all the inflows and outflows of energy within the system. Figure 34 shows a diagram depicting the energy flows of this system.
Arrows represent each energy flow in Figure 34 and 35. These arrows are numbered from (Φ_1) through (Φ_8). In Table 6. each flow is identified according to its corresponding number, describes that flow, presents a mathematical relationship for that flow, and offers a current estimate of flow values (all "flows" here are in units of flux, or Watts per meter squared).
The system is depicted in Figures 34 and 35 and the relationships shown in Table 5. identify a system of equations that model the energy flows of the Sun-Earth-atmosphere system. We will now build a systems diagram similar to Figure 35 but which explicitly identifies each of the mathematical relationships within it.

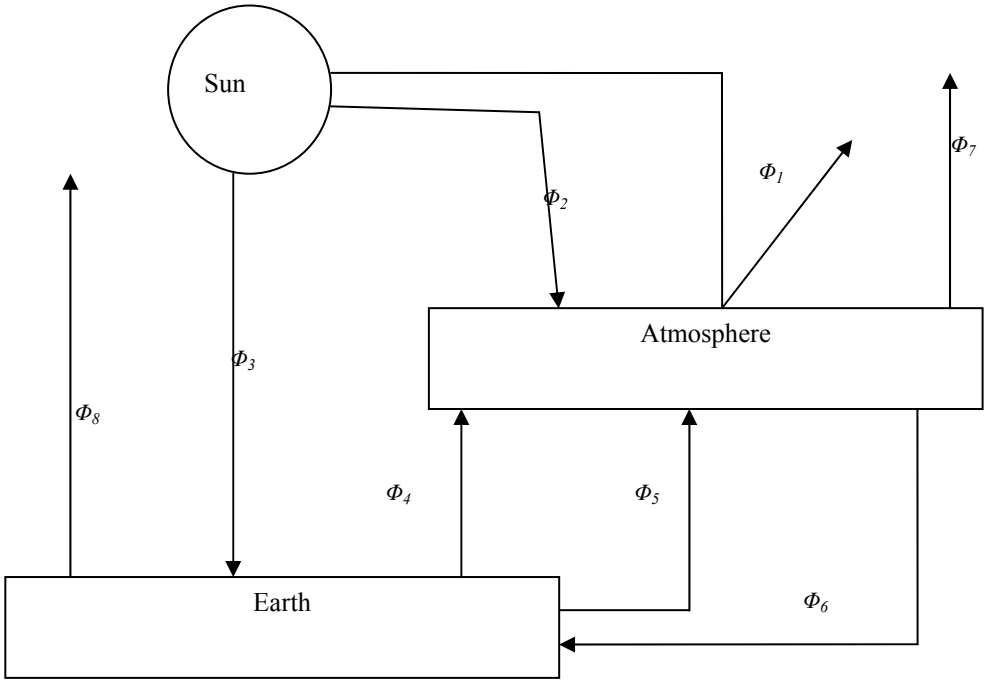

Figure 35: Sun-atmosphere –Earth energy flow diagram

Table 5. Description of energy flows for Figures 34 and 35.

Flows	Description	Mathematical equation	Flux(W/m^2)
Φ_1	Solar flux that is reflected off the atmosphere Earth and back into space	$\Phi_1 = a\,\Phi_s$	107
Φ_2	Solar flux that is absorbed in the atmosphere by atmospheric gases	$\Phi_2 = f_b\,(1-a)\,\Phi_s = f_b(\Phi_S - \Phi_1)$	67
Φ_3	Solar flux that is absorbed directly by the Earth's surface	$\Phi_3=(1-f_b)(1-a)\,\Phi_s = \Phi_S - \Phi_1 - \Phi_2$	168
Φ_4	Latent and thermal heat transfer from the Earth's surface to the atmosphere (nonradiative energy)	$\Phi_4=t_e\,\Phi_E$	102
Φ_5	Earth's radiated energy flux that is absorbed by atmospheric gases	$\Phi_5=f_a(1-t_e)\,\Phi_E = f_a(\Phi_E - \Phi_4)$	350
Φ_6	Atmospheric radiated energy flux that is radiated toward and absorbed by the Earth	$\Phi_6= R_a\,\Phi_A$	324
Φ_7	Atmospheric radiated energy flux that is radiated toward space	$\Phi_7= (1-Ra)\,\Phi_A = \Phi_A - \Phi_6$	195
Φ_8	Earth's radiated energy flux that is not absorbed by the atmosphere and goes directly to space	$\Phi_8= (1-f_a)(1-t_e)\,\Phi_E = \Phi_E - \Phi_4 - \Phi_5$	40

a = the albedo of the atmosphere-Earth system (a = 0,313)
f_b = the fraction of incoming solar energy absorbed by the atmosphere ;

t_e = the fraction of Earth's flux that is transferred to the atmosphere through latent and thermal processes;
f_a = the fraction of outgoing radiation from the Earth that is absorbed by the atmosphere;
R_a = the fraction of atmospheric radiation that is radiated toward and is absorbed by the Earth;
Φ_s = the total solar flux entering the Earth-atmosphere system;
Φ_E = the Earth energy flux radiated from the Earth;
Φ_A = the atmospheric energy flux radiated from the atmosphere.

The reservoirs would have units of energy per area (or Joules per meter squared) and can be considered energy densities. We are identifying two reservoir variables – one representing energy density for the Earth (*E),* the other representing energy density for the atmosphere (*A*).
We will next add solar energy flows (Φ_1, Φ_2 and Φ_3 listed in Table 5.)
These flows are shown in Figures 34 and 35.
First, we have the solar energy that is reflected off the Earth-atmosphere system, represented by the solar flux times the albedo of the Earth system, or a Φ_s.
Next, we have the solar energy that is not reflected, and is also absorbed by the atmosphere. This is equal to $f_b(1-a)\Phi s$,
Note that this accounts for the solar energy not fractional parameter f_b, that is less than 1 and represents the ability of atmospheric gases to absorb solar energy.
Because most atmospheric gases are good absorbers in the IR part of the spectrum and most of the incoming solar energy is in the visible-UV part of the spectrum, we expect f_b to be a small number.
Finally, we have the remainder of the solar energy that is absorbed by the Earth itself. This is represented as $(1- f_b)(1-a)\ \Phi s$,
We will consider next all of the energy that is reradiated from the Earth's surface..
This is described by flows Φ_4, Φ_5 and Φ_8 in Table 5. These flows are shown in Figures 34 and 35. First, we have a flow of thermal energy that is transported from the Earth's surface to the atmosphere via convection and evaporation-transpiration processes.
If we define E as the total energy reservoir of the Earth, then this thermal flow is represented as $t_e E$
where t_e represents the fraction of the Earth's thermal energy flux.
We have a flow of radiated energy from the Earth that is captured by atmospheric gases. This flow is identified as $\Phi_5=f_a(1-t_e)\ E$;
where f_a represent the fraction of the radiated energy that is absorbed. The value of f_a tends to be high because the atmosphere is a very good absorber of IR radiation.
Finally we have a flow of radiated energy that is not captured by the atmosphere, escaping instead into space through a radiation "window". This flow is represented by $\Phi_8= (1-f_a)(1-t_e)E$;
By denoting our flows using fractional values we have accounted for all the energy in the Earth's reservoir at each time unit.
Last, we need to consider energy radiated from the atmosphere.
The flows from the atmosphere are identified as flows Φ_6 and Φ_7 in table 5.
The atmosphere will radiate some of its energy back toward the Earth (this, in fact, is the cause of the greenhouse effect), and will radiate the remainder toward space**.**
We will define the amount of energy radiated back toward Earth as $\Phi_6=R_a\ A$;
where R_a represents the fraction of atmospheric radiation that is directed toward and is absorbed by the Earth.
The value $\Phi_7 = (1-Ra)\ A= \Phi_A- \Phi_6$ represents the atmospheric radiation directed into space.
In our account we have balanced all energy inputs and outputs of each of the reservoirs .

$$\sum_i \Phi_i = \sum_j \Phi_j \qquad (44)$$

For Earth reservoir we have:

$\Phi_8+\Phi_5+ \Phi_4= \Phi_3+ \Phi_6$ or 40+350+102=168+324 or 492=492 (45)

For atmospheric reservoir we have:

$\Phi_5 + \Phi_4 + \Phi_2 = \Phi_6 + \Phi_7$ or 350+102+67=324+195 or 519=519 (46)

In calculating surface temperatures, we are only concerned with the energy radiated from the Earth (and not energy transported by thermal processes). Greenhouse gases enter this system by directly affecting the way in which the atmosphere absorbs and radiates energy. These effects are mostly observed through the variables f_a and R_a

First, an increase in GHG in the atmosphere will have a direct effect in the ability of the atmosphere to absorb outgoing radiation from the Earth (i.e., an increase in f_a, see Figure 37.)This is what GHG do, as shown earlier in Figure 18. therefore, an increase in their concentrations will mean more molecules to intercept, absorb, and reradiate energy photons.

Second, an increase in GHG might also increase R_a (see Figure 36), the fraction of radiated atmospheric energy that is directed toward the Earth.

3.2.3 Dynamic Modeling of the Greenhouse Gases Effect

We will determine the impact of an increased level of carbon dioxide on average surface temperatures of the Earth. This increase in carbon dioxide is expected to affect two primary parameters in system directly.

First, it will affect f_a (the fraction of outgoing radiation from the Earth that is absorbed by the atmosphere, Figure 37), Second, it will affect R_a (the fraction of atmospheric radiation that is radiated toward and is absorbed by the Earth, Figure 36),

This model is written in STELLA software language and is presented in Figure 38.

Model also includes the values for each of parameters shown below. However, the parameters are modified in the model so that our time units are in years.

Φ_S=342 W/m^2,

A=518.15J/m^2.

E = 491.31 J/m^2.

f_a = 0.901,

f_b = 0.285,

R_a = 0.626,

a = 0.313,

t_e = 0.207.

We can add the CO_2 component to this model to address the impact of CO_2 increasing in Earth temperature. To do this, we might envision a stock of CO_2 (or other GHG) in atmosphere that changes over time. The reservoir would impact values of R_a and f_a which depends from CO_2 concentration in the atmosphere, and their dependence is not straightforward. However, we would expect that as CO_2 concentrations increase, our values for R_a and f_a would increase as well. This model includes a stock of CO_2 in the atmosphere in units of parts per million (ppm) and is initially set 380 ppm (present value in year 2007) The inflow is set as positive 1.3 ppm/year (i.e., an increase in CO_2 concentrations of 1.3 ppm annually).

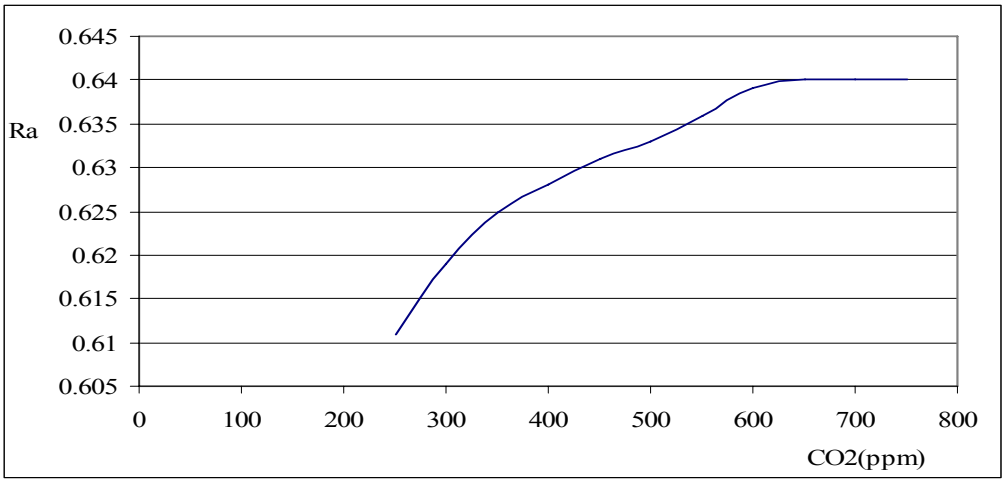

Figure 36: Functional dependence of R_a on CO_2 concentration in atmosphere

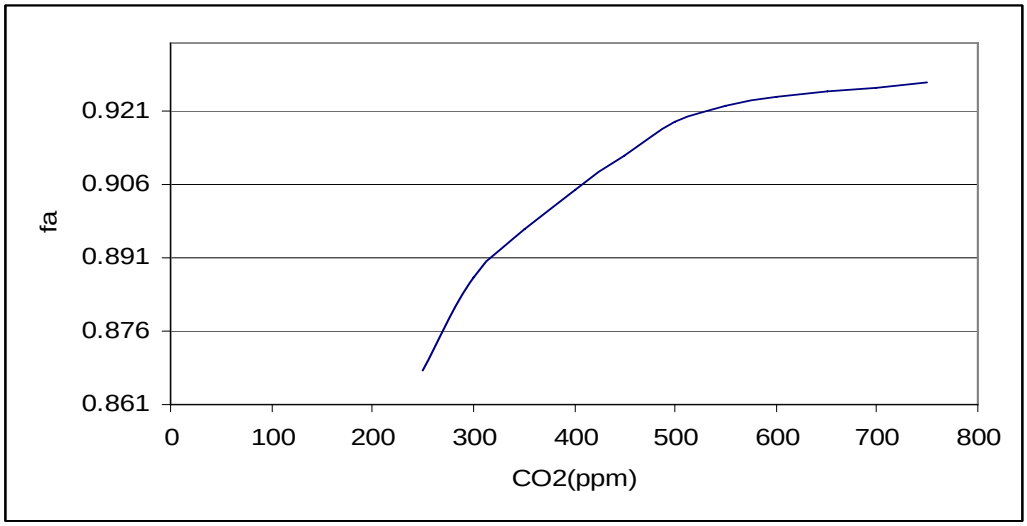

Figure 37: Functional dependence of f_a on CO_2 concentration in atmosphere

3.2.4 Greenhouse Zero-Dimensional Model with CO_2 Accumulation

Fig. 38 displays GHG model with accumulation, and the program follows:

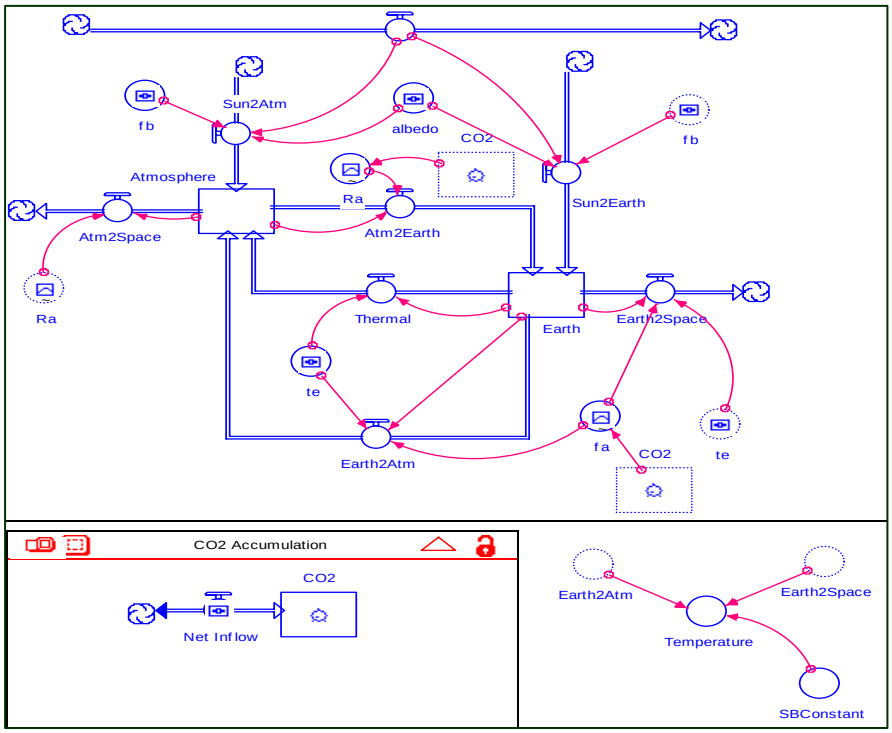

Figure 38: Greenhouse zero-dimensional model with CO_2 accumulation

Algorithm 1: Greenhouse Zero-Dimensional Model with CO_2 Accumulation
CO2 Accumulation
CO2(t) = CO2(t - dt) + (Net_Inflow) * dt
INIT CO2 = 375
INFLOWS:
Net_Inflow = 1.3
Energy Balance
Atmosphere(t) = Atmosphere(t - dt) + (Sun2Atm + Thermal + Earth2Atm - Atm2Earth - Atm2Space) * dt
INIT Atmosphere = 518.15*60*60*24*365
INFLOWS:
Sun2Atm = Solar_Flux*fb*(1-albedo)
Thermal = Earth*te
Earth2Atm = Earth*fa*(1-te)
OUTFLOWS:
Atm2Earth = Atmosphere*Ra
Atm2Space = Atmosphere*(1-Ra)
Earth(t) = Earth(t - dt) + (Sun2Earth + Atm2Earth - Earth2Space - Thermal - Earth2Atm) * dt
INIT Earth = 491.31*60*60*24*365
INFLOWS:
Sun2Earth = Solar_ Flux*(1-fb)*(1-albedo)
Atm2Earth = Atmosphere*Ra
OUTFLOWS:
Earth2Space = Earth*(1-fa)*(1-te)
Thermal = Earth*te
Earth2Atm = Earth*fa*(1-te)
UNATTACHED:

Solar_ Flux = 342*60*60*24*365
albedo =.313
fb =.285
te =.207
fa = GRAPH(CO2)
(250, 0.867), (300, 0.886), (350, 0.897), (400, 0.905), (450, 0.912), (500, 0.919), (550, 0.922), (600, 0.924), (650, 0.926), (700, 0.926), (750, 0.927)
Ra = GRAPH(CO2)
(250, 0.611), (300, 0.619), (350, 0.625), (400, 0.627), (450, 0.631), (500, 0.633), (550, 0.635), (600, 0.639), (650, 0.64), (700, 0.64), (750, 0.64)
Not in a sector
SBConstant = 60*60*24*365*5.67e-8
Temperature = ((Earth2Atm+Earth2Space)/SBConstant) ^.2

If CO_2 emitting in atmosphere is constant 1.3 ppm over a 50 year period, in the simulation the accumulation of CO_2 grew linearly (Figure 39) and the Earth's surface temperature will grow for 2 K until year 2050 (Figure 40) The stock (the accumulation of CO_2) doesn't remain constant 375pm like the emitting inflow 1.3ppm but accumulation grew linearly from 377.1 ppm in year 2005 to 440 ppm in the year 2055

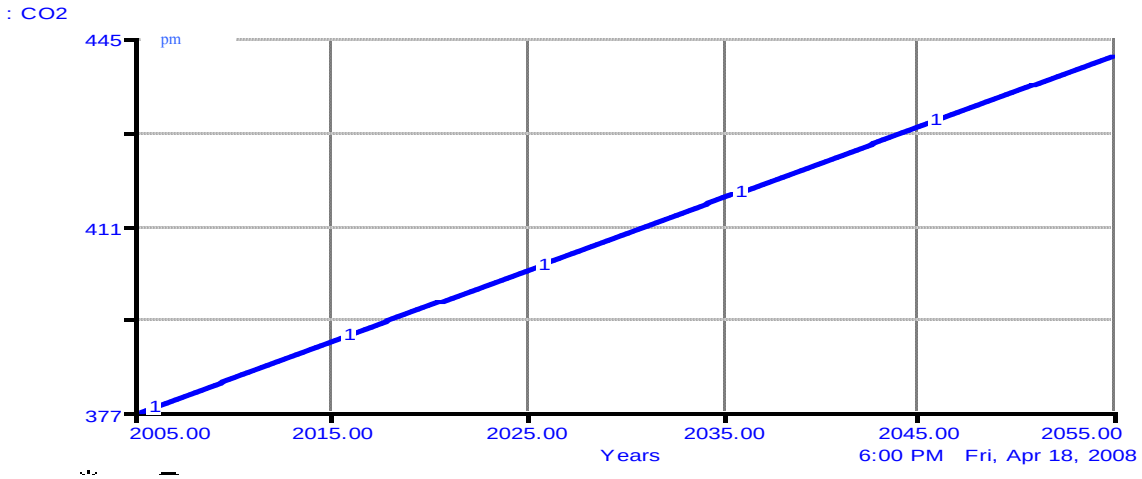

Figure 39: Carbon dioxide concentration linear growth rate during the next 50 years year period

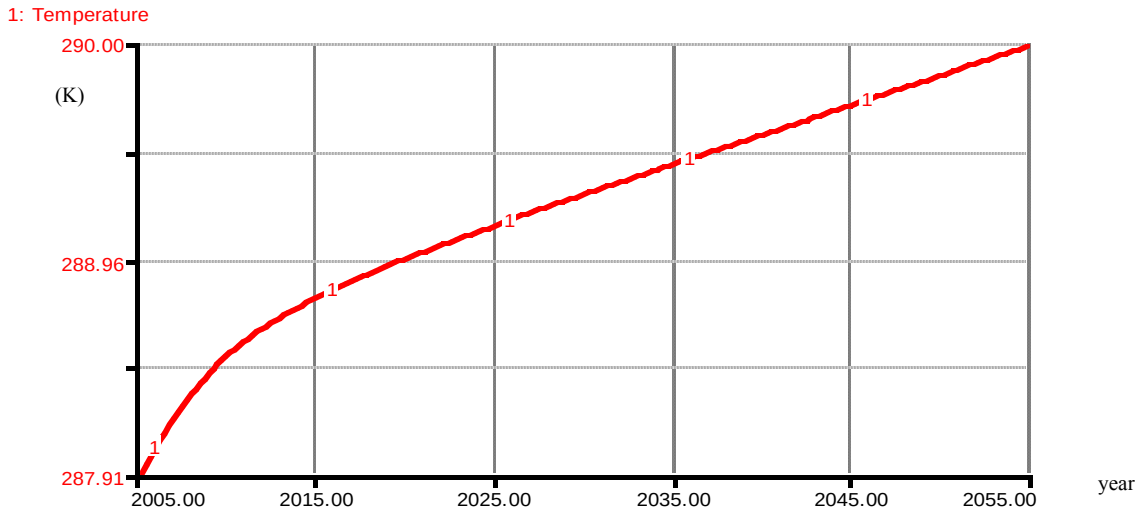

Figure 40: Temperature of the Earth surface in the model with CO_2 accumulation in atmosphere.

3.2.5 Greenhouse Zero-Dimensional Model With CO_2 Reduction In Emission Due To Renewable Energy Use And New Technologies

New technologies and renewable energy resources are added – see Fig 41. and the following computer program:

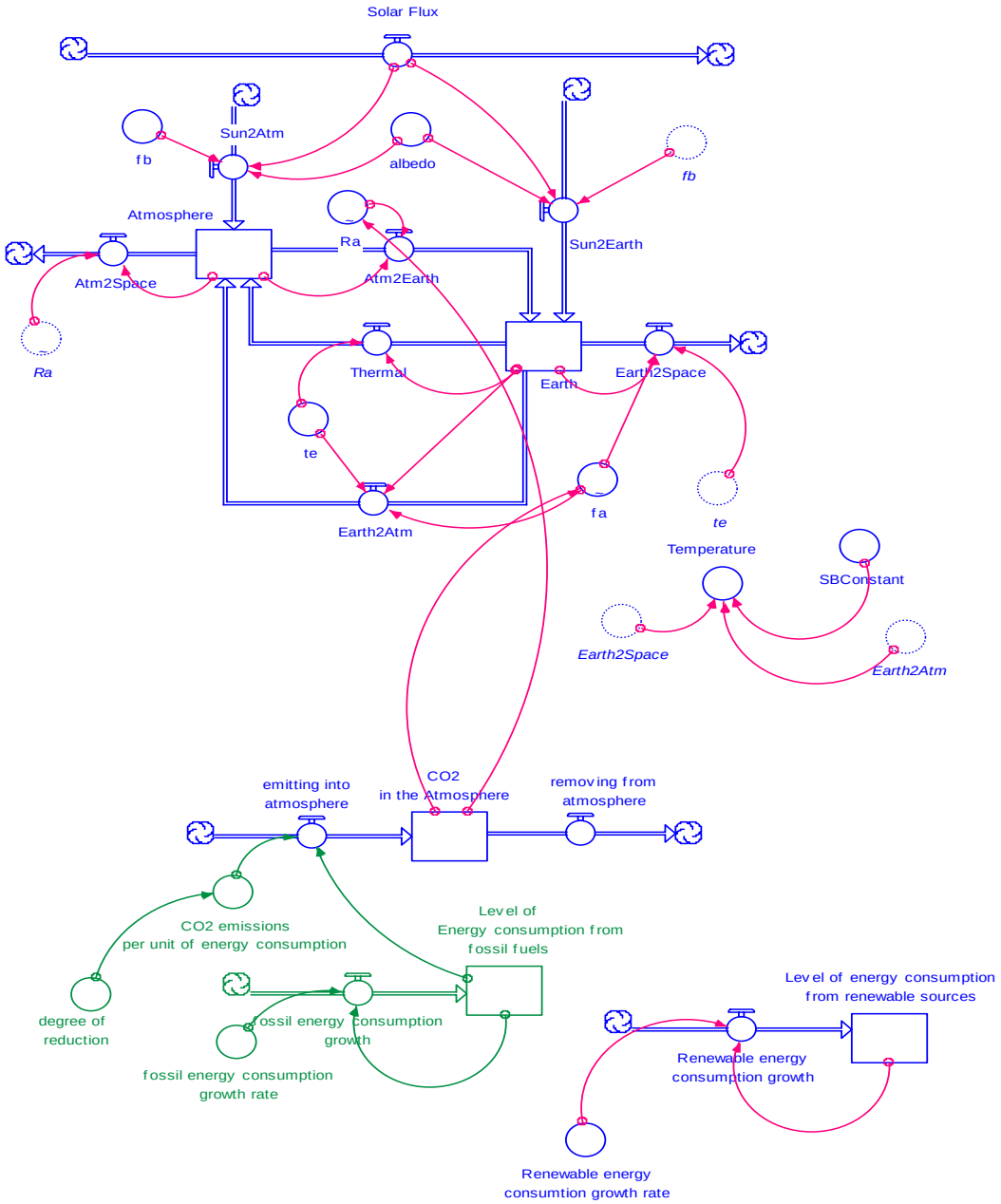

Figure 41: Greenhouse zero-dimensional model with CO_2 reduction in emission due to renewable energy use and new technology options.

Algorithm 2: Greenhouse Zero-Dimensional Model With CO_2 Reduction In Emission Due To Renewable Energy Use And New Technologies

```
CO2 ACUMULATION
CO2__in_the_Atmosphere(t) = CO2__in_the_Atmosphere(t - dt) + (emitting_into_atmosphere -
removing_from__atmosphere) * dt
INIT CO2__in_the_Atmosphere = 377.1
INFLOWS:
emitting_into_atmosphere =
Level_of__Energy_consumption_from__fossil_fuels*CO2_emissions_per_unit_of_energy_consumption
OUTFLOWS:
removing_from__atmosphere = 0.52-RAMP(0.12/50.0)
Level_of_energy_consumption_from_renewable_sources(t) =
Level_of_energy_consumption_from_renewable_sources(t - dt) +
(Renewable_energy_consumption_growth) * dt
INIT Level_of_energy_consumption_from_renewable_sources = 33
INFLOWS:
Renewable_energy_consumption_growth =
Level_of_energy_consumption_from_renewable_sources*Renewable_energy_consumtion_growth_rate
Level_of_Energy_consumption_from__fossil_fuels(t) = Level_of
Energy_consumption_from__fossil_fuels(t - dt) + (fossil_energy_consumption__growth) * dt
INIT Level_of_Energy_consumption_from__fossil_fuels = 400
INFLOWS:
fossil_energy_consumption__growth =
Level_of_Energy_consumption_from__fossil_fuels*fossil_energy_consumption___growth_rate
CO2_emissions_per_unit_of_energy_consumption =.00325-RAMP(degree_of___reduction*.00325/50, 0)
degree_of___reduction = 0.8
fossil_energy_consumption___growth_rate = 0.0254-RAMP(0.0254/50,0)
Renewable_energy_consumtion_growth_rate = 0.035+RAMP(0.035/50,0)
Energy Balance with CO2 Accumulation and with 80% degree of reduc
Atmosphere(t) = Atmosphere(t - dt) + (Sun2Atm + Thermal + Earth2Atm - Atm2Earth - Atm2Space) * dt
INIT Atmosphere = 518.15*60*60*24*365
INFLOWS:
Sun2Atm = Solar_Flux*fb*(1-albedo)
Thermal = Earth*te
Earth2Atm = Earth*fa*(1-te)
OUTFLOWS:
Atm2Earth = Atmosphere*Ra
Atm2Space = Atmosphere*(1-Ra)
Earth(t) = Earth(t - dt) + (Sun2Earth + Atm2Earth - Earth2Space - Thermal - Earth2Atm) * dt
INIT Earth = 491.31*60*60*24*365
INFLOWS:
Sun2Earth = Solar_Flux*(1-fb)*(1-albedo)
Atm2Earth = Atmosphere*Ra
OUTFLOWS:
Earth2Space = Earth*(1-fa)*(1-te)
Thermal = Earth*te
Earth2Atm = Earth*fa*(1-te)
UNATTACHED:
Solar_Flux = 342*60*60*24*365
albedo =.313
fb =.285
te =.207
Temperature = ((Earth2Atm+Earth2Space)/SBConstant)^.25
fa = GRAPH(CO2__in_the_Atmosphere)
(250, 0.867), (260, 0.87), (271, 0.874), (281, 0.878), (292, 0.882), (302, 0.886), (313, 0.888), (323, 0.89),
(333, 0.893), (344, 0.895), (354, 0.897), (365, 0.899), (375, 0.9), (385, 0.9), (396, 0.901), (406, 0.902),
(417, 0.903), (427, 0.905), (438, 0.906), (448, 0.908), (458, 0.909), (469, 0.912), (479, 0.914), (490, 0.916),
(500, 0.919)
Ra = GRAPH(CO2__in_the_Atmosphere)
```

(250, 0.611), (260, 0.613), (271, 0.614), (281, 0.616), (292, 0.617), (302, 0.619), (313, 0.62), (323, 0.621), (333, 0.623), (344, 0.624), (354, 0.625), (365, 0.625), (375, 0.626), (385, 0.626), (396, 0.627), (406, 0.627), (417, 0.628), (427, 0.628), (438, 0.629), (448, 0.629), (458, 0.63), (469, 0.63), (479, 0.631), (490, 0.631), (500, 0.633)
Not in a sector; SBConstant = 60*60*24*365*5.67e-8

3.2.6 Options for Reducing CO_2

In the model we made we study the effects due to the renewable energy use, new technology options for CO_2 reduction and policy initiatives.
The possible options for reducing CO_2 emissions include the following (Fay and Golomb, 2002):

- Demand-side conservation and efficiency improvements, including less space heating and better insulation, less air conditioning, fluorescent lighting, more energy-efficient appliances, process modification in industry, and, very importantly, more fuel-efficient automobiles. Such measures may even incur a negative cost(i.e., consumer savings by using less energy) or at least a rapid payback period for the investment in energy-saving devices.
- Supply-side efficiency measures. Here we mean primarily increasing the efficiency of coal fired power plants. Coal gasification combined –cycle power plants have a thermal efficiency in the 45-50% range, compared with single-cycle pulverized-coal plants in the 35-40% range. However, coal gasification power plants are more expensive than single-cycle plants.
- Capture of CO_2 from the flue gas of power plants and sequestration in terrestrial or deep ocean reservoirs. This is an expensive option, and it will be exercised only if governments mandate or subsidize it.
- Utilization of the captured CO_2.The utilization for enhanced oil and natural gas recovery is economically attractive: the utilization of CO_2 as a raw material for the production of some fuels and chemical requires extra energy input and does not appear to be economical.
- Shift to nonfossil energy sources. The choices here are agonizing, because the largest impact could be made by shifting to nuclear electricity and hydroelectricity, both presently very unpopular and fraught with environmental and health concerns. The shift to solar, wind, geothermal, and ocean energy are popular, but because of their limited availability and intermittency and because of their larger cost compared to fossil energy, a substantial shift to these energy sources can not be expected in the future.
- Greater use of biomass, especially wood. The use of biomass is reabsorbed in the growth of the next generation of vegetation.
- A forestation without using he trees for 100-200 years, during which period the CO_2 concentrations in the atmosphere will decline because of exhaustion of fossil fuel resources and shift to nonfossil energy sources
- Stopping slash and burning practices of forests, especially tropical forests, which are prodigious absorbents of CO_2, and the burning of which releases CO_2.

The total world energy consumption in quadrillions of BTU in 2005 is presented by the pie in Figure 42 and by the Fig. 43.

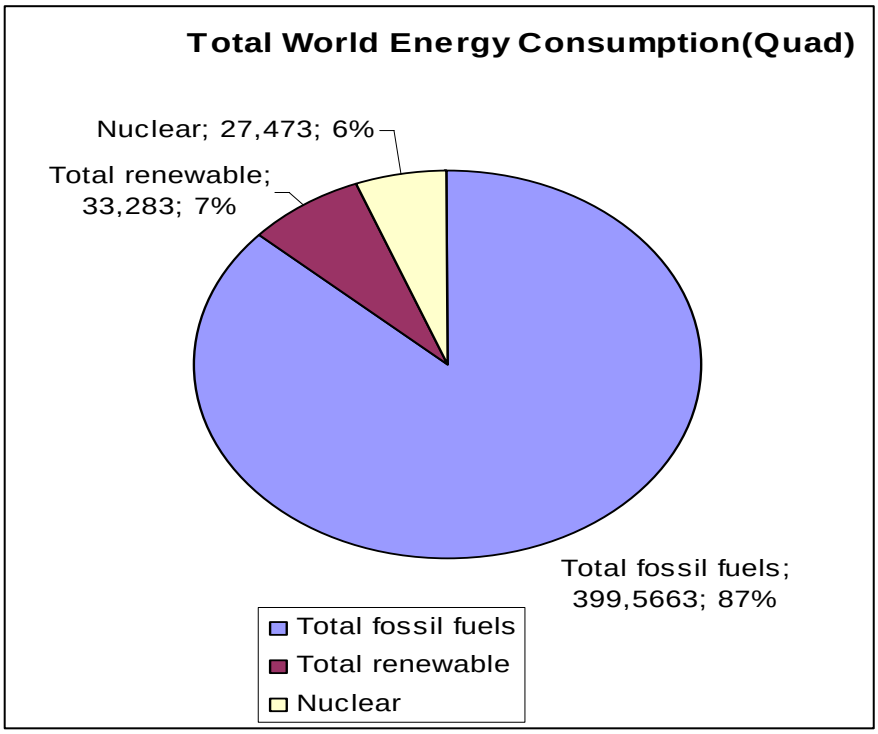

Figure 42: Total World Energy Consumption (Fossil, Renewable and Nuclear) in the year 2005 (Source: REN21)

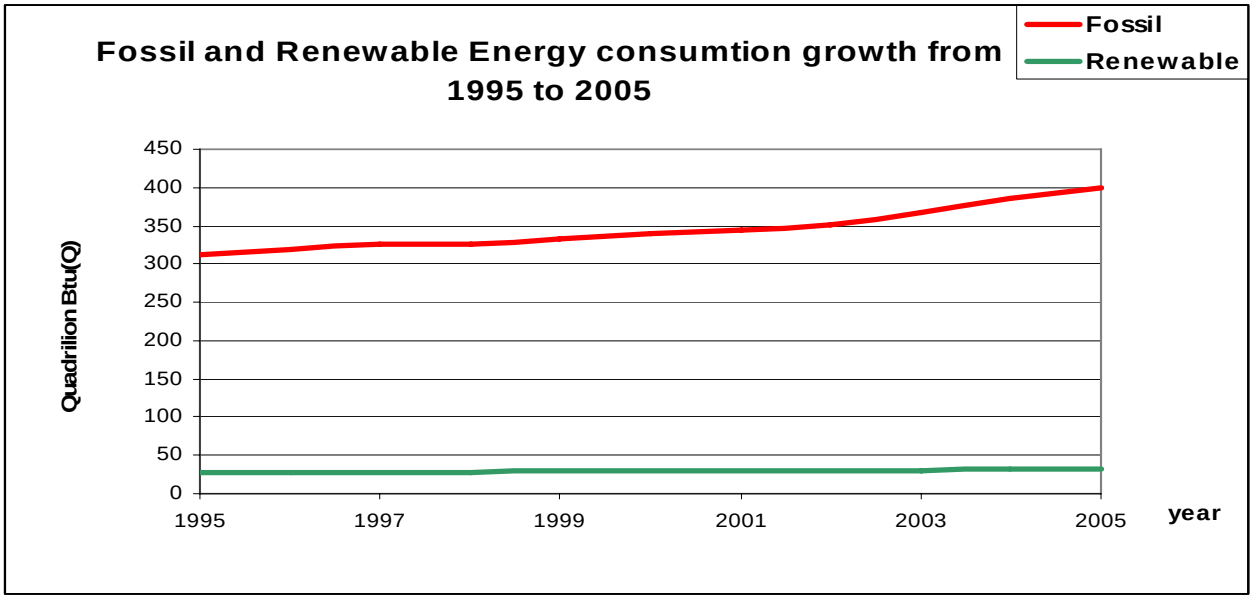

Figure 43: The World Energy Consumption growth (Fossil and Renewable) from year 1995 to 2005 (Source: REN21)

3.3 Modeling the Impacts of Renewable Energy and New Technologies on CO_2 Reduction in Kosovo

3.3.1 Modeling the Electrical Energy Demand–Supply and CO_2 Reduction

The model integrating the transport and the electricity is presented in Fig 44. and the following computer program:

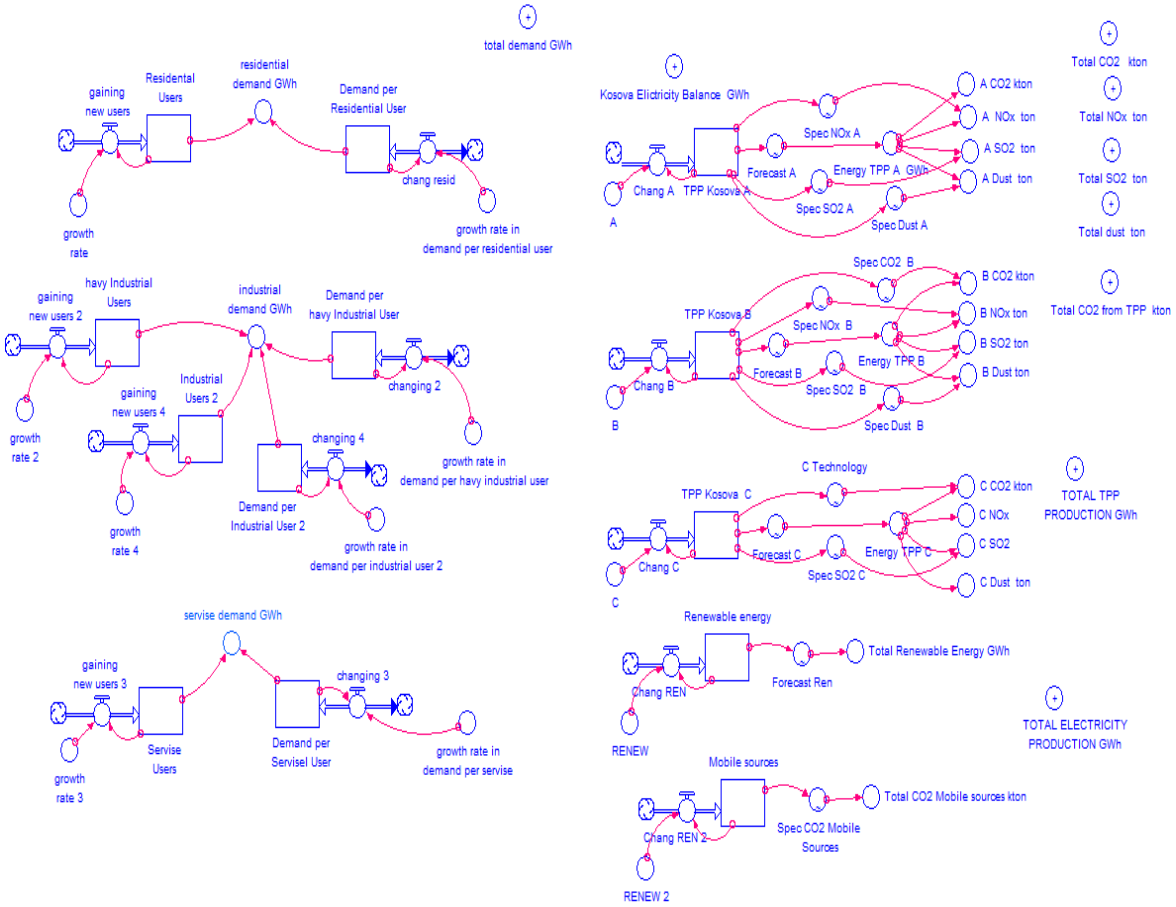

Figure 44: Model in CO_2 reduction emission due to renewable energy use in Kosovo

Algorithm 3: Modeling the Electrical Energy Demand–Supply and CO_2 Reduction

Demand_per_havy_Industrial_User(t) = Demand_per_havy_Industrial_User(t - dt) + (changing_2) * dt
INIT Demand_per_havy_Industrial_User = 0.03*365*24
INFLOWS:
changing_2 = Demand_per_havy_Industrial_User*growth_rate_in_demand_per_havy_industrial_user
Demand_per_Industrial_User_2(t) = Demand_per_Industrial_User_2(t - dt) + (changing_4) * dt
INIT Demand_per_Industrial_User_2 = 0.0002*24*365
INFLOWS:
changing_4 = Demand_per_Industrial_User_2*growth_rate_in_demand_per_industrial_user_2
Demand_per_Residential_User(t) = Demand_per_Residential_User(t - dt) + (chang_resid) * dt
INIT Demand_per_Residential_User = 0.0075
INFLOWS:

chang_resid = Demand_per_Residential_User*growth_rate_in_demand_per_residential_user
Demand_per_Servisel_User(t) = Demand_per_Servisel_User(t - dt) + (changing_3) * dt
INIT Demand_per_Servisel_User = 0.25
INFLOWS:
changing_3 = Demand_per_Servisel_User*growth_rate_in_demand_per_servise
havy_Industrial_Users(t) = havy_Industrial_Users(t - dt) + (gaining_new_users_2) * dt
INIT havy_Industrial_Users = 2
INFLOWS:
gaining_new_users_2 = havy_Industrial_Users*growth_rate_2
Industrial_Users_2(t) = Industrial_Users_2(t - dt) + (gaining_new_users_4) * dt
INIT Industrial_Users_2 = 200
INFLOWS:
gaining_new_users_4 = Industrial_Users_2*growth_rate_4
Mobile_sources(t) = Mobile_sources(t - dt) + (Chang_REN_2) * dt
INIT Mobile_sources = 300000
INFLOWS:
Chang_REN_2 = RENEW_2*Mobile_sources
Renewable_energy(t) = Renewable_energy(t - dt) + (Chang_REN) * dt
INIT Renewable_energy = 52
INFLOWS:
Chang_REN = RENEW*Renewable_energy
Residental_Users(t) = Residental_Users(t - dt) + (gaining_new_users) * dt
INIT Residental_Users = 352000
INFLOWS:
gaining_new_users = Residental_Users*growth_rate
Servise_Users(t) = Servise_Users(t - dt) + (gaining_new_users_3) * dt
INIT Servise_Users = 1000
INFLOWS:
gaining_new_users_3 = Servise_Users*growth_rate_3
TPP_Kosova_A(t) = TPP_Kosova_A(t - dt) + (Chang_A) * dt
INIT TPP_Kosova_A = 628
INFLOWS:
Chang_A = A*TPP_Kosova_A
TPP_Kosova_B(t) = TPP_Kosova_B(t - dt) + (Chang_B) * dt
INIT TPP_Kosova_B = 3000
INFLOWS:
Chang_B = B*TPP_Kosova_B
TPP_Kosova__C(t) = TPP_Kosova__C(t - dt) + (Chang_C) * dt
INIT TPP_Kosova__C = 4380
INFLOWS:
Chang_C = C*TPP_Kosova__C
A = 0.001
A_CO2_kton = Energy_TPP_A__GWh*1.5
A_Dust__ton = Energy_TPP_A__GWh*Spec_Dust_A
A_SO2__ton = Energy_TPP_A__GWh*Spec_SO2_A
A__NOx__ton = Energy_TPP_A__GWh*Spec_NOx_A
B = 0.001
B_CO2_kton = Energy_TPP_B*Spec_CO2__B
B_Dust_ton = Energy_TPP_B*Spec_Dust__B
B_NOx_ton = Energy_TPP_B*Spec_NOx__B
B_SO2_ton = Energy_TPP_B*Spec_SO2__B
C = 0.01
C_CO2_kton = Energy_TPP_C*C_Technology
C_Dust__ton = Energy_TPP_C*0
C_NOx = Energy_TPP_C*0.5
C_SO2 = Energy_TPP_C*Spec_SO2_C
Energy_TPP_A__GWh = Forecast_A
Energy_TPP_B = Forecast_B
Energy_TPP_C = Forecast_C
growth_rate = 0.037

growth_rate_2 = 0.027
growth_rate_3 = 0.05
growth_rate_4 = 0.04
growth_rate_in_demand_per_havy_industrial_user = 0.01
growth_rate_in_demand_per_industrial_user_2 = 0.025
growth_rate_in_demand_per_residential_user = -0.018
growth_rate_in_demand_per_servise = 0.025
industrial_demand_GWh =
(havy_Industrial_Users*Demand_per_havy_Industrial_User)+(Industrial_Users_2*Demand_per_Industrial
_User_2)
Kosova_Elictricity_Balance__GWh = TOTAL_ELECTRICITY__PRODUCTION_GWh -
total_demand_GWh
RENEW = 0.001
RENEW_2 = 0.001
residential_demand_GWh = Residental_Users*Demand_per_Residential_User
servise_demand_GWh = Servise_Users*Demand_per_Servisel_User
Total_CO2_from_TPP__kton = A_CO2_kton + B_CO2_kton + C_CO2_kton
Total_CO2_Mobile_sources_kton = Spec_CO2_Mobile__Sources*1000
Total_CO2___kton = A_CO2_kton + B_CO2_kton + C_CO2_kton + Total_CO2_Mobile_sources_kton
total_demand_GWh = industrial_demand_GWh + residential_demand_GWh + servise_demand_GWh
Total_dust__ton = A_Dust__ton + B_Dust_ton + C_Dust__ton
TOTAL_ELECTRICITY__PRODUCTION_GWh = Total_Renewable_Energy_GWh +
Energy_TPP_A__GWh + Energy_TPP_B + Energy_TPP_C
Total_NOx__ton = A__NOx__ton + B_NOx_ton + C_NOx
Total_Renewable_Energy_GWh = Forecast_Ren
Total_SO2__ton = A_SO2__ton + B_SO2_ton + C_SO2
TOTAL_TPP__PRODUCTION_GWh = Energy_TPP_A__GWh + Energy_TPP_B + Energy_TPP_C
C_Technology = GRAPH(TPP_Kosova__C)
(4380, 0.8), (4426, 0.8), (4472, 0.8), (4517, 0.8), (4563, 0.8), (4609, 0.8), (4655, 0.8), (4701, 0.8), (4747,
0.8), (4792, 0.8), (4838, 0.8), (4884, 0.8), (4930, 0.8), (4976, 0.8), (5021, 0.8), (5067, 0.8), (5113, 0.8),
(5159, 0.8), (5205, 0.8), (5251, 0.8), (5296, 0.8), (5342, 0.6), (5388, 0.6), (5434, 0.6), (5480, 0.6), (5525,
0.6), (5571, 0.6), (5617, 0.6)
Forecast_A = GRAPH(TPP_Kosova_A)
(628, 628), (628, 628), (628, 628), (629, 1138), (629, 1138), (629, 1138), (629, 1294), (629, 1294), (630,
1294), (630, 1536), (630, 1536), (630, 1536), (630, 904), (631, 904), (631, 904), (631, 860), (631, 860),
(632, 860), (632, 998), (632, 998), (632, 998), (632, 825), (633, 825), (633, 825), (633, 965), (633, 965),
(633, 965), (634, 999), (634, 999), (634, 999), (634, 1418), (634, 1420), (635, 1418), (635, 1760), (635,
1760), (635, 1760), (635, 1760), (636, 1760), (636, 1760), (636, 746), (636, 746), (636, 746), (637, 746),
(637, 746), (637, 746), (637, 746), (637, 746), (638, 746), (638, 746), (638, 746), (638, 746), (639, 0.00),
(639, 0.00), (639, 0.00), (639, 0.00), (639, 0.00), (640, 0.00), (640, 0.00), (640, 0.00), (640, 0.00), (640,
0.00), (641, 0.00), (641, 0.00), (641, 0.00), (641, 0.00), (641, 0.00), (642, 0.00), (642, 0.00), (642, 0.00),
(642, 0.00), (642, 0.00), (642, 0.00), (643, 0.00), (643, 0.00), (643, 0.00), (643, 0.00), (643, 0.00), (644, 0.00), (644,
0.00)
Forecast_B = GRAPH(TPP_Kosova_B)
(3000, 1334), (3001, 1334), (3002, 1334), (3003, 1485), (3004, 1485), (3005, 1485), (3006, 1855), (3007,
1855), (3008, 1855), (3009, 1781), (3010, 1781), (3011, 1781), (3012, 2089), (3013, 2089), (3014, 2089),
(3015, 2847), (3016, 2847), (3017, 2847), (3018, 3212), (3019, 3212), (3020, 3212), (3021, 3033), (3022,
3033), (3023, 3033), (3024, 3320), (3025, 3320), (3026, 3320), (3027, 3320), (3028, 3320), (3029, 3320),
(3030, 3320), (3031, 3320), (3032, 3320), (3033, 3320), (3034, 3320), (3035, 3320), (3035, 3320), (3036,
3320), (3037, 3320), (3038, 3068), (3039, 3068), (3040, 3068), (3041, 3068), (3042, 3068), (3043, 3068),
(3044, 3068), (3045, 3068), (3046, 3068), (3047, 3068), (3048, 3068), (3049, 3068), (3050, 3068), (3051,
3068), (3052, 3068), (3053, 3068), (3054, 3068), (3055, 3068), (3056, 3068), (3057, 3068), (3058, 3068),
(3059, 1368), (3060, 1368), (3061, 1368), (3062, 1368), (3063, 1368), (3064, 1368), (3065, 1368), (3066,
1368), (3067, 1368), (3068, 1368), (3069, 1368), (3070, 1368), (3071, 1368), (3072, 1368), (3073, 1368),
(3074, 1368), (3075, 1368), (3076, 1368)
Forecast_C = GRAPH(TPP_Kosova__C)
(4380, 0.00), (4396, 0.00), (4412, 0.00), (4428, 0.00), (4444, 0.00), (4460, 0.00), (4476, 0.00), (4492, 0.00),
(4509, 0.00), (4525, 0.00), (4541, 0.00), (4557, 0.00), (4573, 0.00), (4589, 0.00), (4605, 0.00), (4621, 0.00),
(4637, 0.00), (4653, 0.00), (4669, 0.00), (4685, 0.00), (4701, 0.00), (4717, 0.00), (4733, 0.00), (4750, 0.00),
(4766, 0.00), (4782, 0.00), (4798, 0.00), (4814, 0.00), (4830, 0.00), (4846, 0.00), (4862, 0.00), (4878, 0.00),

(4894, 0.00), (4910, 0.00), (4926, 0.00), (4942, 0.00), (4958, 3000), (4974, 3000), (4990, 3000), (5007, 3000), (5023, 3000), (5039, 3000), (5055, 3000), (5071, 3000), (5087, 3000), (5103, 3000), (5119, 3000), (5135, 3000), (5151, 3000), (5167, 3000), (5183, 3000), (5199, 3000), (5215, 3000), (5231, 3000), (5248, 3000), (5264, 3000), (5280, 3000), (5296, 3000), (5312, 3000), (5328, 3000), (5344, 5900), (5360, 5900), (5376, 5900), (5392, 5900), (5408, 5900), (5424, 5900), (5440, 5900), (5456, 5900), (5472, 5900), (5489, 5900), (5505, 5900), (5521, 5900), (5537, 5900), (5553, 5900), (5569, 5900), (5585, 5900), (5601, 5900), (5617, 5900)
Forecast_Ren = GRAPH(Renewable_energy)
(52.0, 52.0), (52.0, 52.0), (52.0, 52.0), (52.1, 68.0), (52.1, 68.0), (52.1, 68.0), (52.1, 84.0), (52.1, 84.0), (52.1, 84.0), (52.2, 92.0), (52.2, 92.0), (52.2, 92.0), (52.2, 86.0), (52.2, 86.0), (52.2, 86.0), (52.3, 78.0), (52.3, 78.0), (52.3, 78.0), (52.3, 63.0), (52.3, 63.0), (52.3, 63.0), (52.4, 70.0), (52.4, 70.0), (52.4, 70.0), (52.4, 107), (52.4, 107), (52.4, 107), (52.5, 118), (52.5, 118), (52.5, 118), (52.5, 116), (52.5, 116), (52.5, 116), (52.6, 107), (52.6, 107), (52.6, 107), (52.6, 107), (52.6, 107), (52.7, 107), (52.7, 747), (52.7, 747), (52.7, 747), (52.7, 757), (52.7, 757), (52.8, 757), (52.8, 762), (52.8, 762), (52.8, 762), (52.8, 772), (52.8, 772), (52.9, 772), (52.9, 892), (52.9, 892), (52.9, 892), (52.9, 897), (52.9, 897), (53.0, 897), (53.0, 902), (53.0, 902), (53.0, 902), (53.0, 1037), (53.0, 1037), (53.1, 1037), (53.1, 1037), (53.1, 1037), (53.1, 1037), (53.1, 1037), (53.1, 1037), (53.2, 1037), (53.2, 1037), (53.2, 1037), (53.2, 1037), (53.2, 1031), (53.3, 1031), (53.3, 1031), (53.3, 1031), (53.3, 1031), (53.3, 1031)
Spec_CO2_Mobile__Sources = GRAPH(Mobile_sources)
(300000, 0.64), (300304, 0.7), (300607, 0.74), (300911, 0.78), (301215, 0.8), (301518, 0.82), (301822, 0.85), (302125, 0.88), (302429, 0.91), (302733, 0.94), (303036, 0.97), (303340, 1.01), (303644, 1.05), (303947, 1.05), (304251, 1.05), (304554, 1.01), (304858, 0.99), (305162, 0.97), (305465, 0.95), (305769, 0.93), (306073, 0.91), (306376, 0.87), (306680, 0.83), (306983, 0.79), (307287, 0.75), (307591, 0.7)
Spec_CO2__B = GRAPH(TPP_Kosova_B)
(3000, 1.40), (3003, 1.40), (3006, 1.40), (3009, 1.40), (3012, 1.40), (3015, 1.40), (3018, 1.40), (3021, 1.40), (3024, 1.40), (3027, 1.40), (3030, 1.40), (3033, 1.40), (3036, 1.40), (3039, 1.40), (3043, 1.40), (3046, 1.40), (3049, 1.40), (3052, 1.40), (3055, 1.40), (3058, 1.40), (3061, 1.12), (3064, 1.12), (3067, 1.12), (3070, 1.12), (3073, 1.12), (3076, 1.12)
Spec_Dust_A = GRAPH(TPP_Kosova_A)
(628, 3.40), (629, 3.40), (629, 3.40), (630, 2.00), (631, 2.00), (631, 1.20), (632, 1.00), (632, 1.00), (633, 1.00), (634, 1.00), (634, 1.00), (635, 1.00), (636, 1.00), (636, 1.00), (637, 1.00), (638, 1.00), (638, 1.00), (639, 1.00), (639, 1.00), (640, 1.00), (641, 1.00), (641, 1.00), (642, 1.00), (643, 1.00), (643, 1.00), (644, 1.00)
Spec_Dust__B = GRAPH(TPP_Kosova_B)
(3000, 1.40), (3003, 1.40), (3006, 1.40), (3009, 1.00), (3012, 1.00), (3015, 1.00), (3018, 0.5), (3021, 0.5), (3024, 0.5), (3027, 0.5), (3030, 0.5), (3033, 0.5), (3036, 0.5), (3039, 0.5), (3043, 0.5), (3046, 0.4), (3049, 0.3), (3052, 0.3), (3055, 0.3), (3058, 0.3), (3061, 0.3), (3064, 0.3), (3067, 0.3), (3070, 0.1), (3073, 0.1), (3076, 0.1)
Spec_NOx_A = GRAPH(TPP_Kosova_A)
(628, 4.00), (629, 4.00), (629, 4.00), (630, 4.00), (631, 4.00), (631, 4.00), (632, 4.00), (632, 4.00), (633, 4.00), (634, 3.80), (634, 3.80), (635, 3.80), (636, 3.80), (636, 3.80), (637, 3.80), (638, 3.80), (638, 3.80), (639, 0.00), (639, 0.00), (640, 0.00), (641, 0.00), (641, 0.00), (642, 0.00), (643, 0.00), (643, 0.00), (644, 0.00)
Spec_NOx__B = GRAPH(TPP_Kosova_B)
(3000, 3.80), (3003, 3.80), (3006, 3.80), (3009, 3.80), (3012, 3.80), (3015, 3.80), (3018, 3.80), (3021, 3.80), (3024, 3.80), (3027, 3.50), (3030, 3.50), (3033, 3.50), (3036, 3.50), (3039, 1.70), (3043, 1.70), (3046, 1.70), (3049, 1.70), (3052, 1.70), (3055, 1.70), (3058, 1.70), (3061, 1.70), (3064, 1.70), (3067, 1.70), (3070, 1.70), (3073, 1.70), (3076, 1.70)
Spec_SO2_A = GRAPH(TPP_Kosova_A)
(628, 3.20), (629, 3.20), (629, 3.20), (630, 3.20), (631, 3.20), (631, 3.20), (632, 3.20), (632, 3.20), (633, 3.20), (634, 3.20), (634, 3.20), (635, 3.20), (636, 3.20), (636, 3.10), (637, 3.10), (638, 3.10), (638, 3.10), (639, 3.10), (639, 3.10), (640, 3.10), (641, 3.10), (641, 3.10), (642, 3.10), (643, 3.10), (643, 3.10), (644, 3.10)
Spec_SO2_C = GRAPH(TPP_Kosova__C)
(4380, 0.00), (4429, 0.00), (4479, 0.00), (4528, 0.00), (4578, 0.00), (4627, 0.00), (4677, 0.00), (4726, 0.00), (4776, 0.00), (4825, 0.00), (4875, 0.00), (4924, 0.00), (4974, 0.00), (5023, 0.00), (5073, 0.00), (5122, 0.00), (5172, 0.00), (5221, 0.5), (5271, 0.5), (5320, 0.5), (5370, 0.5), (5419, 0.25), (5469, 0.25), (5518, 0.25), (5568, 0.25), (5617, 0.25)

Spec_SO2__B = GRAPH(TPP_Kosova_B)(3000, 3.10), (3003, 3.10), (3006, 3.10), (3009, 3.10), (3012, 3.10), (3015, 3.10), (3018, 3.10), (3021, 3.10), (3024, 3.10), (3027, 3.10), (3030, 3.10), (3033, 3.10), (3036,

3.10), (3039, 1.00), (3043, 1.00), (3046, 1.00), (3049, 1.00), (3052, 0.5), (3055, 0.5), (3058, 0.5), (3061, 0.5), (3064, 0.5), (3067, 0.5), (3070, 0.5), (3073, 0.5), (3076, 0.5)

3.3.2 Modeling the Dynamic Mobile Source Emission Systems and CO2 Reduction with Renewable Energy Use and New Technology

One of the primary sources of CO_2 in Kosovo (except TPP) are light-and heavy-duty vehicles (i.e., mobile sources as: cars, buses, tractors, vans, trailers, etc.).

Automobiles, vans, trucks, tractors and buses population in Kosovo have topped approximately 215,000 vehicles registered in 2003 (source: Statistic Office of Kosovo) that is 172% increasing rate from the pre-conflict (before March 1999) number of vehicles 125000 (provided by the Motor Vehicle Registration Authority - MVRA of Kosovo).

Each traveling an average of 16000 km/year, at an average fuel economy of 12 l/100 km, this transportation represents the consumption of about 0.5 million tons oil/year.

The total emission for CO_2 emitted from the total number of vehicles is

$$E^{v}_{CO_2}(t) = \sum_{j=1}^{2} \sum_{k=1}^{5} (1 + p_j(t))(1 - r_k) \cdot V_{jk}(t-1) \cdot VKMT_{jk}(t) \cdot EF^{v}_{CO_{2\,jk}}(t) \quad (47)$$

where j = 1, 2 indicates two types of vehicles: light vehicles and heavy vehicles, t = 2001, 2002,..., 2025 year; t = 2000 is the initial year with initial value in the year 2000.
k = 1, 2,.., 5 represents cohort (the family of vehicles with the same age).
Increase rate per year while in the cohort, $(1 + p_j(t))$, does not depend on the age of the automobile, and scrappage rate r_k (fraction of vehicles scrapped while in the cohort) does not depend on time
For our calculation of emission CO_2 from all kinds of transportation means, light and heavy, we start from the following initial conditions: We have divided the vehicles in five groups according to the age: 0-2 years, 3-5 years, 6-8 years, 9-11 years and >11 years. Assuming that 90% of vehicles in the year 2000 have been older than 10 years, and the rest newer than 10 years, we have obtained the initial number represented in Table 6. following the groups listed above

Table 6. Number of vehicles by cohort in the year 2000 (initial value) and scrapped rates.

Age	Light vehicles	Heavy Vehicles	Total Vehicles	Scrap rates	
0-2 year	1500	607	15607	r_1	0.1
3-5 year	7500	2000	9500	r_2	0.15
6-8 year	15000	3000	18000	r_3	0.2
9-11 year	40000	9000	49000	r_4	0.25
>11 year	75000	14500	89500	r_5	0.4
Total	139000	29107	168107		

For the initial values of emissions factor for CO_2, we have obtained the values represented in Table 7., based on the length of service of the vehicles. In Table 6. scrappage rate is also represented, based on the age, and this factor remains constant over the years till to the year 2025.
http://www.eia.doe.gov/oiaf/1605/transport.html

Table 7: Emission factors for CO_2 (g/km)of Light (LV) and Heavy Vehicles (HV)

Emission factors for CO2 (g/km) of light(LV) and heavy (HV) vehicles initial value		
Age		$EF^{v}_{CO_2\,jk}$
	LV	HV
0-2year	138	270
3-5year	161	290
6-8year	184	324
9-11year	208	351
>11year	231	378

The factors of emission (Figure 45), and the average value of kilometers traveled per year (Figure 46) change, starting from the year 2015, due to the Policy and Technology Options for Reducing Mobile Emissions that have to be applied in Kosovo in order to comply with the European Union emission standards http://enrin.grida.no/htmls/kosovo/SoE/energy.htm

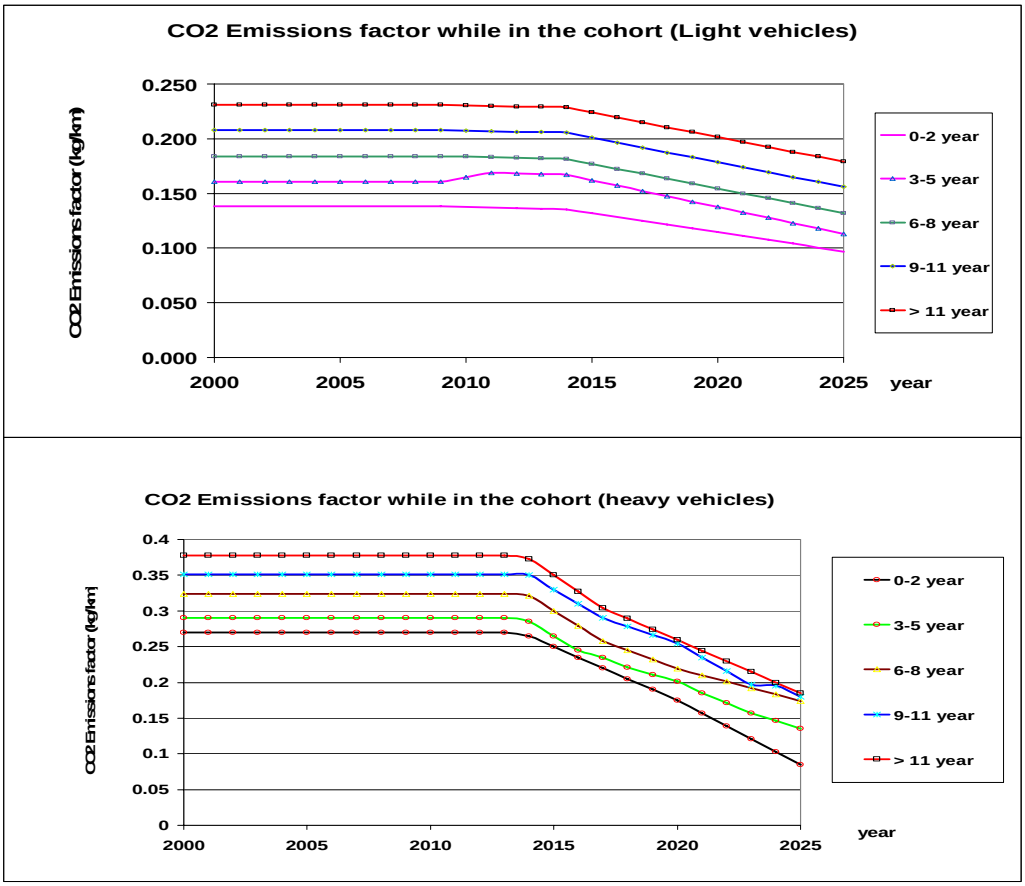

Figure 45: Time dependence change of CO_2 emission factors while in cohort (Light and Heavy Vehicles)

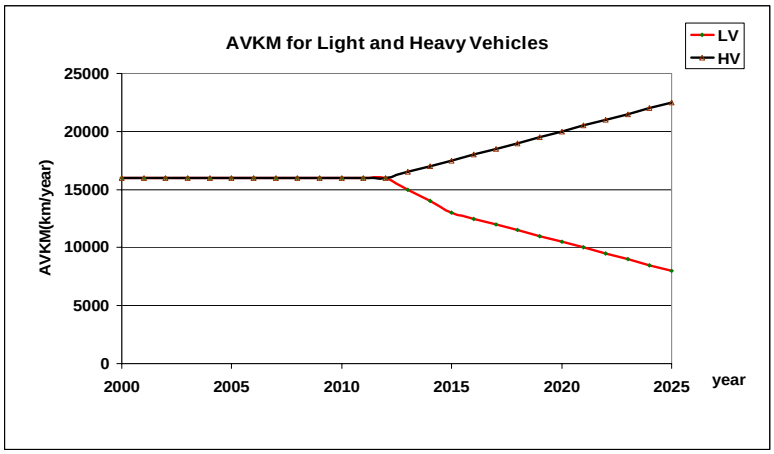

Figure 46: Time dependence change of Average Kilometers Traveled (AVKM)

3.3.1 Options for Reducing CO_2 from Mobile Source

There are a variety of policy and technology options that may be employed to reduce CO_2 emissions from mobile sources. Policies that encourage people to drive less or to use public transportation or carpools have been widely instituted throughout many industrialized countries (Hobbs, P.V.1995) Such policies will be applied also in Kosovo, particularly after 2015. Some of them are:

- High-occupancy vehicle lanes - this option reduces the number of vehicles on the road by providing an incentive (faster transit time) to people who carpool.
- Vehicle scrappage programs and incentives - this option reduces the number of older model year vehicles on the road, because these vehicles are thought to be largest emitters of urban pollutants (This program has partially commenced in Kosovo in 2005)
- Rebates for mass-transit usage - this option offer an economic incentive for people who use mass transit.
- Corporate Average Fuel Economy (CAFE) standards - this option forces manufacturers to improve average energy efficiency in vehicles (km/l) so that less fuel is burned for a given travel distance (which means less CO_2 emission).
- Tolls on certain roadways - this option create a disincentive for driving a personal vehicle on roadways with tolls.

Technology Options

Technologies that increase vehicle efficiencies, decrease CO_2 emissions factor or reduce the need to drive altogether have been used worldwide (Klaassen et al.2002) (Franchi, 2005) to reduce mobile source emissions. Such technologies are expected to be applied in Kosovo after 2015, among others:

- High-efficiency Vehicles
- Alternative transportation fuels (e.g., natural gas, ethanol, methanol, propane, hydrogen, electric vehicles)
- Improved catalytic converters
- New forms of efficient mass-transit
- Nanotechnologies

3.4 Impacts of Renewable Energy on the Greenhouse Gas Reduction and Air Pollutions from Mobile Sources in Kosovo-Dynamic Modeling

3.4.1 Mobile Source Air Pollution and GHG in Kosovo

3.4.1.1 Modeling the Dynamic Mobile Source Emission Systems

We develop a model in which we identify technology and policy options for reducing mobile source GHG and air pollution, and explain how these options might affect the different variables of a mobile source emission model. The equation we use to calculate emission in this model (Bunce, 1994) (see:http://www.eia.doe.gov/oiaf/1605/transport.html) is:

$$E_i(t) = \sum_j \sum_k V_{jk}(t).VKMT_{jk}(t).EF_{ijk}(t)) \quad (48)$$

where V_{jk} is the total number of vehicles of type j and cohort type k on the road during a certain year (vehicles), $VKMT_{jk}$ is the average annual kilometers traveled for vehicles of type j and cohort type k (km/vehicle/year), EF_{ijk} is the average emission of pollutant i for vehicle type j and cohort type k (gr/km) - vehicle emission factor, E_i is the total annual emission of pollutant i (t/year).
Each cohort has its own individual scrappage rate (r_k). These rates represent the fraction of vehicles scrapped over the transit time for each conveyor.
Larger and older vehicles usually have higher emission values than do newer and lighter vehicles. Larger vehicles have lower efficiencies (defined in kilometers per liter), so they need to consume more fuel per km driven. Thus, their emissions per km tend to be higher. Vehicle age is an important factor, because as a vehicle gets older and accumulates kilometers, engine wear, and loss of efficiency in catalytic converters lead to higher emissions.
The total number of vehicles we have determined from the ESTAP forecast (Energy Sector Technical Assistance Project). According to ESTAP, a dependence between the number of vehicles per household and GNP per capita, could be established by the equation

$$y = 0.3526 \ln x - 2.095 \quad (49)$$

Where x is GNP per capita and y is the number of vehicles per household

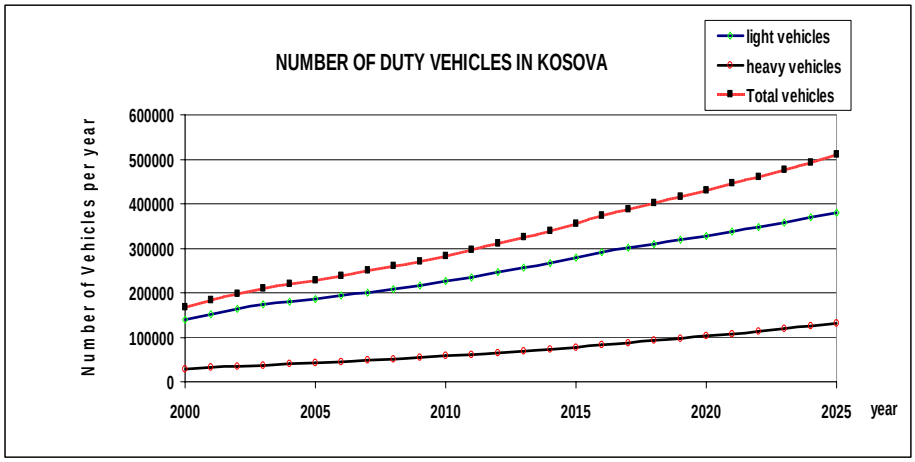

Figure 47: Increase in number of vehicles

Based on the established correlation, the following rough estimate of the future number of vehicles in Kosovo depending on the forecast GNP per capita and population (number of household) growth can be made [ESTAP], see Figure 47. Figure 47 shows estimated increase of the total number of vehicles over the next 18 years. It should be noted that the estimated number of vehicles in 2003 is very close to the data provided by the Motor Vehicle

Registration Authority (MVRA) of Kosovo estimates.215,000 of vehicles in 2003. Between the total number of vehicles per year $V_j(t)$ and percentage increasing per year $q_j(t)$ we can establish the equation

$$V_j(t) = (1 + q_j(t))\, V_j(t - 1) \tag{50}$$

We can calculate the values of $q_j(t)$ from the ESTAP's data represented in Figure 47. Calculated values for $q_j(t)$ are listed in Table 8.

We have established a correlation between the total number of vehicles per year $V_j(t)$, increase rate per year while in the cohort $(1 + p_j(t))$, and scrappage rate r_k (fraction of vehicles scrapped while in the cohort):

$$V_j(t) = \sum_{k=1}^{5} V_{jk}(t) = \sum_{k=1}^{5} (1 + p_j(t)) \cdot (1 - r_k) \cdot V_{jk}(t - 1) \tag{51}$$

where $k = 1, 2, ..., 5$ represents cohort.

The factor $1 + p_j(t)$ does not depend on the age of the automobile, whereas the scrap factor r_k does not depend on time.

From Eqs. (50) and (51) we can calculate the increasing factor of imported vehicles while in the cohort $1 + p_j(t)$. These results are shown in the Table 8.

Table 8: Percentage increasing per year $q(t)$ and increasing rate per year while in the cohort $(1+p_j(t))$.

year	2000	2001	2002	2003	2004	2005	2006	2007	2008
$q_1(t)$	0%	9.4%	7.2%	6.7%	3.4%	3.3%	3.8%	4.1%	4%
$q_2(t)$	0%	10%	8%	7%	7%	7%	7%	7%	6%
$1+p_1(t)$	1	1.6	1.55	1.51	1.44	1.41	1.40	1.38	1.36
$1+p_2(t)$	1	1.59	1.54	1.49	1.47	1.44	1.42	1.40	1.37
year	2009	2010	2011	2012	2013	2014	2015	2016	2017
$q_1(t)$	3.8%	4.1%	4.0%	4.7%	4.1%	4.3%	4.5%	3.0%	3.0%
$q_1(t)$	6%	6%	6%	6%	6%	6%	6%	6%	6%
$1+p_1(t)$	1.34	1.33	1.32	1.32	1.3	1.3	129	128	1.26
$1+p_2(t)$	1.35	1.34	1.33	1.32	1.31	1.30	1.29	1.28	1.28
year	2018	2019	2020	2021	2022	2023	2024	2025	
$q_1(t)$	3%	3%	3%	3%	3%	3%	3%	3%	
$q_1(t)$	6%	6%	5%	5%	5%	5%	5%	5%	
$1+p_1(t)$	1.25	1.25	1.24	1.24	1.23	1.23	1.22	1.22	
$1+p_2(t)$	1.27	1.26	125	124	1.24	1.23	1.23	1.23	

The total emission for pollutant i emitted from the total number of vehicles is

$$E_i(t) = \sum_{j=1}^{2} \sum_{k=1}^{5} (1 + p_j(t))(1 - r_k) \cdot V_{jk}(t-1) \cdot VKMT_{jk}(t) \cdot EF_{ijk}(t) \qquad (52)$$

where j = 1, 2 indicates two types of vehicles: light vehicles and heavy vehicles, i indicates CO_2, CO, NO_x, SO_2 and dust, t = 2001, 2002,..., 2025 year; t = 2000 is the initial year with initial value in the year 2000.

For our calculation of overall emission of air pollutants and GHG: CO, NO_x, SO_2, dust and CO_2 from all kinds of transportation means, light and heavy, we start from the following initial conditions: we have divided the vehicles in five groups according to the age: 0-2 years, 3-5 years, 6-8 years, 9-11 years and >11 years. Assuming that 90% of vehicles in the year 2000 have been older than 10 years, and the rest newer than 10 years, we have obtained the initial number represented in Table 9 following the groups listed above

Table 9: Number of vehicles by cohort in the year 2000 (initial value) and scrapped rates.

age	Light vehicles	Heavy Vehicles	Total Vehicles	Scrap rates	
0-2 year	1500	607	15607	r_1	0.1
3-5 year	7500	2000	9500	r_2	0.15
6-8 year	15000	3000	18000	r_3	0.2
9-11 year	40000	9000	49000	r_4	0.25
>11 year	75000	14500	89500	r_5	0.4
Total	139000	29107	168107		

For the initial values of the emission factors for CO, NOx, SO2, NHx, dust and CO_2, we have obtained the values http://www.ec.europa.eu/environment/ipcc/index.htm
and http://enrin.grida.no/htmls/kosovo/SoE/energy.htm represented in Table 10, based on the length of service of the vehicles. In Table 9. scrappage rate is represented, based on the age, and this factor remains constant over the years till to the year 2025.

Table 10: Emission factors for Air Pollution and GHG (gr/km)of Light (LV) and Heavy Vehicles (HV).

Emission factors for CO, NOx, SO_2, NHx, dust and CO2 (gr/km) of light(LV) and heavy (HV) vehicles initial value												
	EF_{CO}		EF_{NOx}		EF_{SO2}		EF_{NHx}		EF_{Dust}		EF_{CO2}	
Age	LV	HV	LV	HV	LV	HV	LV	HV	LV	HV	LV	HV
0-2year	1.88	4.6	0.5	0.5	0.5	1.3	0.3	0.36	0.3	0.75	138	270
3-5year	2.13	5.9	0.6	0.7	0.6	1.58	0.4	0.4	0.4	0.87	161	290
6-8year	2.38	6.1	0.7	0.85	0.7	1.7	0.5	0.7	0.41	0.9	184	324
9-11year	2.63	6.6	0.8	1.05	0.8	1.9	0.6	0.83	0.43	1.1	208	351
>11year	3.28	7.5	1	1.13	0.9	2.2	0.7	0.9	0.5	1.2	231	378

3.5 Dynamic Modeling the Electricity Demand-Supply, GHG and Air Pollution Reduction with Renewable Energy in Kosovo

3.5.1 Kosovo Electricity Demand Forecast

3.5.1.1 Historical Demand

The evolution of electrical energy consumption in Kosovo is closely linked to political events and to the resulting economic changes. The curves in Figure 48 show that from 1980 to 1988, electricity consumption increased at a very high rate of 9.1% per annum. This was the period of a high economical development in Kosovo, afterwards followed by a stagnation period until 1992 coinciding with the crisis and the political disintegration of former Yugoslavia. From 1993 to 1997 electric consumption started to increase again especially due to the growth of households and the services sector, while the industrial sector was declining. In 1998 and 1999 the political tensions followed by the conflict, caused a drop in electricity consumption, which evened out in 2000 recording values similar to those in 1998. After the year 2000, electric consumption restarted to increase, exceeding in the year 2002 the historical maximum and reaching in 2006, 4261 GWh. For several years the electricity sector in Kosovo is confronted with supply problems. Lack of electricity production, very height consumption of electricity for heating, billing deficiency and non-paid bills are main factors for supply problems.

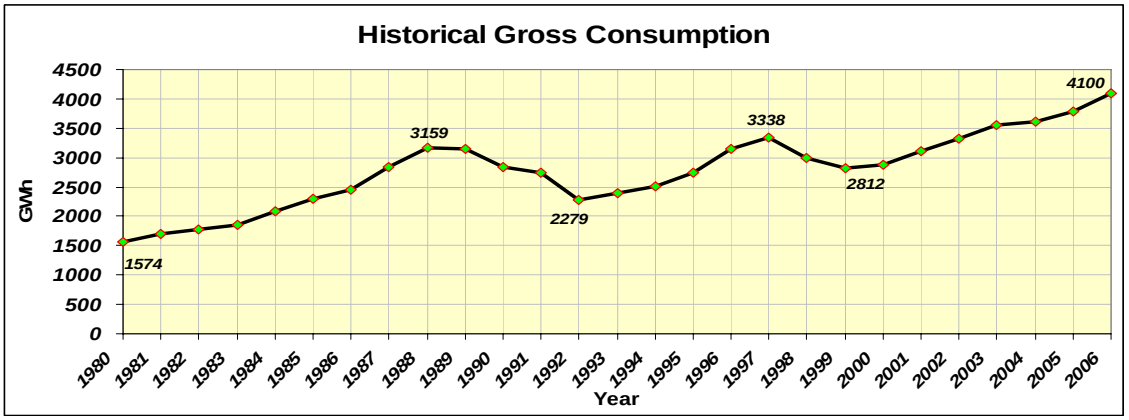

Figure 48: Historical Gross consumption of electricity for time period 1980-2006 (Source:KOST)

3.5.1.2 Electricity Demand Forecast Model

For developing the electricity demand forecast model for Kosovo we used the *"STELLA"* software.
The most important source we use for demand forecast are historical data from KOSTT (TSO of Kosovo)

and KEK.
For the yearly demand forecast a distinction is made between:

- Residential demand
- Heavy industrial and light industrial demand, and
- Service demand

Most important factors for electricity demand forecast for Kosovo taken in consideration are:

- Economic growth forecast
- Population growth forecast
- Energy price forecast, and
- Billing forecast.

3.5.1.3 Model configuration

We have considered the year 2000 as the initial condition for demand forecast model of Kosovo.
Figure 49 shows the configuration model of demand forecast of Kosovo using STELLA software.

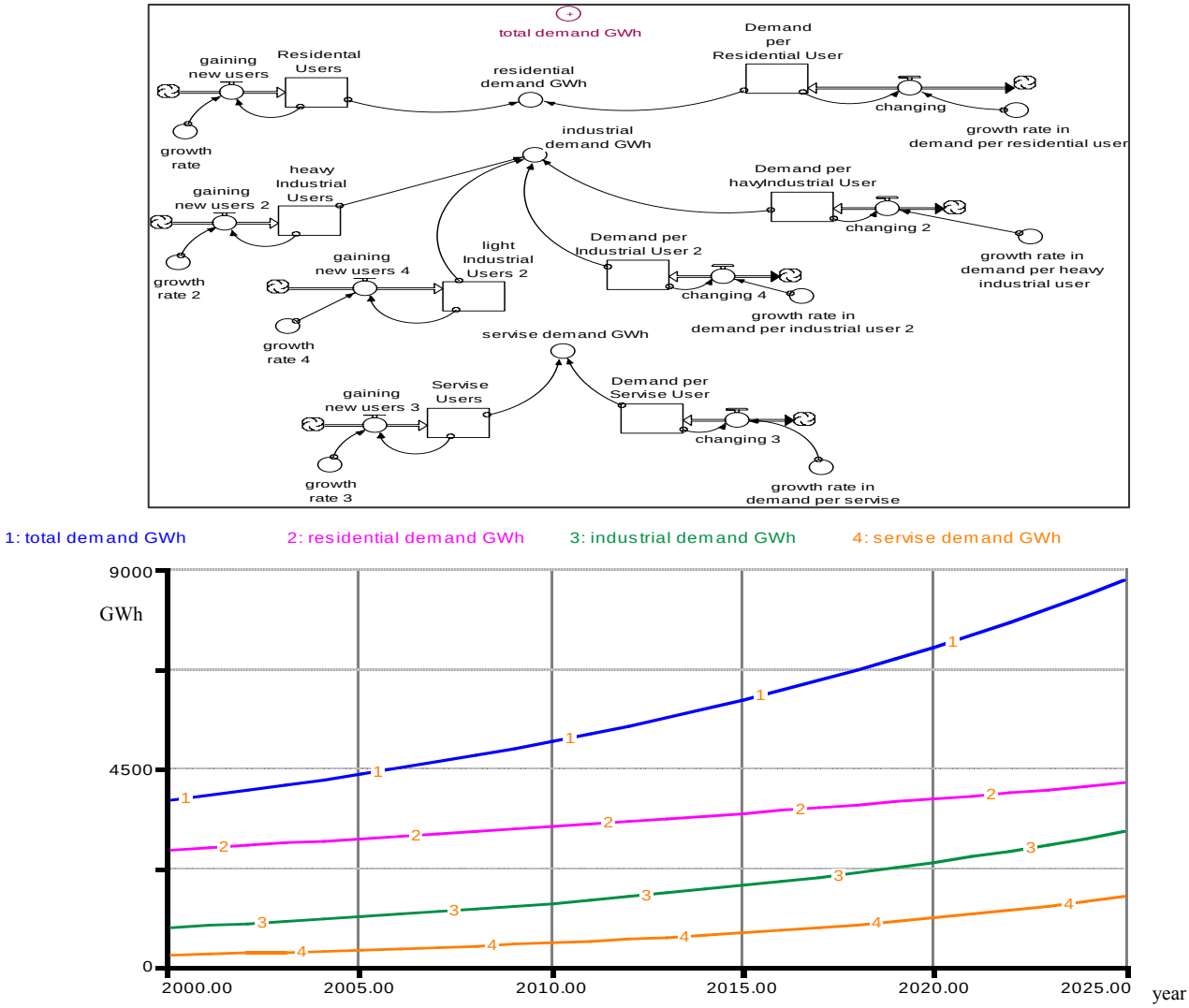

Figure 49: Electricity demand forecast model

3.5.1.4 Simulation results

In Figure 49 we can see the simulation results:

- **Residential demand**. The main factor for the increase of residential will be the population growth and economic development. But, in the course of population growth and economic development, the consumption per residential unit will decrease, and according to the model, an annual decrease of 1.5% is forecast. This will make possible an affordable and normal increase of residential demand. The factors that affect the reduction of consumption per residential unit are: regular and steady billing of the electric power consumption, billing prices, construction of building with proper and qualitative insulation, etc.
- **Industrial demand.** The highest impact on the increase of general demand for energy will have the industrial, light and heavy sectors. Capital investments from the foreign investors will be the crucial factors in the development of the industrial sector. Until the year 2015 three major units of heavy industry is expected to operate in Kosovo: Ferronickel Foundry, Mine and Foundry Complex of Trepcha and the Cement Factory Sharr-Cement. A significant increase of demand for electric power in the heavy industry sector is expected in the mine and ore-dressing sector (metals, coal, etc.). A significant increase is expected also in the light industry sector which will evolve in parallel with the development of heavy industry. In this development the foreign investments in the nutrition industry, metal processing industry, etc, will influence as well. This increase in demand for energy in the industrial sector after 2000 is related to the increase in economic growth after a period of stagnation from the year 1993 to 1999. Therefore, it is reasonable to expect further increase in the industrial development in Kosovo in the near future. It is also expected that during the assession process to EU Kosovo will start developing knowledge-based economy and society, new environmentaly friendly technologies etc. (see: Lojze Sočan, 2008).
- **Service demand.** In the service sector an increase in demand is expected for electric power, which in percentage is expected to be less than in the industrial sector, but greater than in the residential sector.

4 Results

4.1 Greenhouse Zero-Dimensional Model with CO_2 Reduction in Emission Due to Renewable Energy Use and New Technologies-Results

Our results are shown in Figures 50-57 for greenhouse zero-dimensional model with CO_2 reduction in emission due to renewable energy use and new technologies:

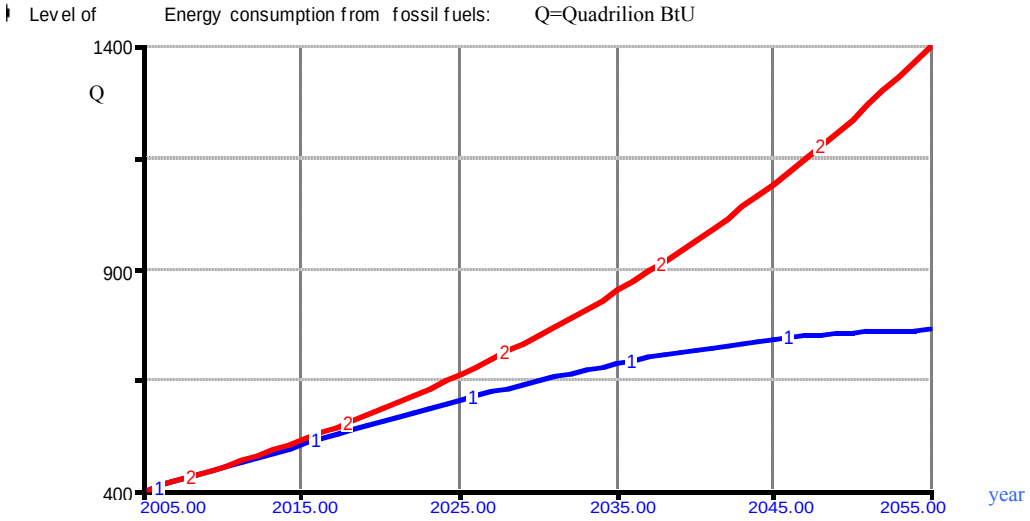

Figure 50: Level of Total Energy Consumption from Fossil Fuels. The curve (2) shows the increasing fossil energy consumption growth at the present rate of about 2.54%, and curve (1) shows the desirable consumption growth for fossil fuels during the next 50 years due to including renewables and new technologies.

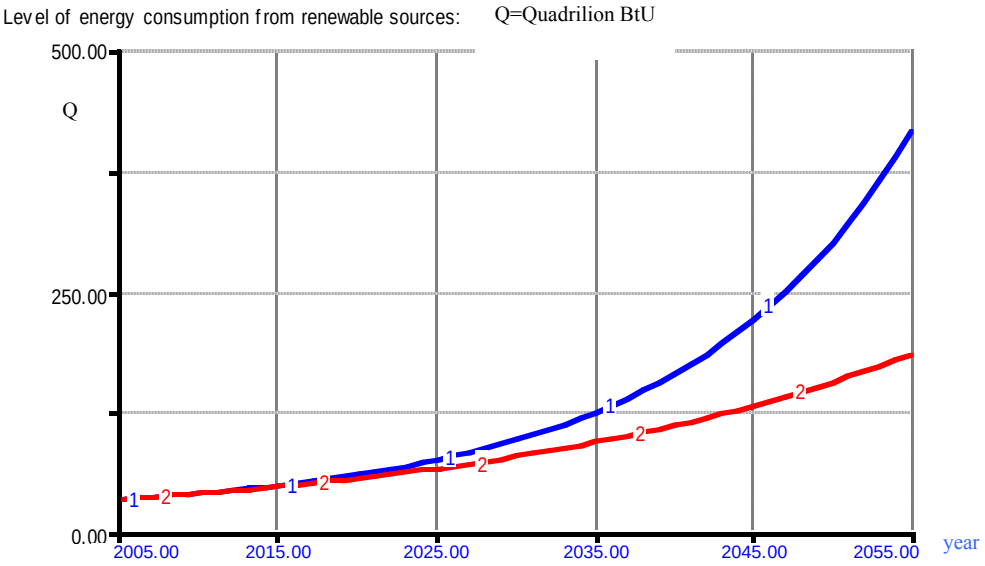

Figure 51: Total level of renewable energy consumption forecast (Q), during the next 50 year. Curve (1) shows the desired increasing renewable energy consumption and (2) shows the present growth rate of 3.5% per year for renewable energy

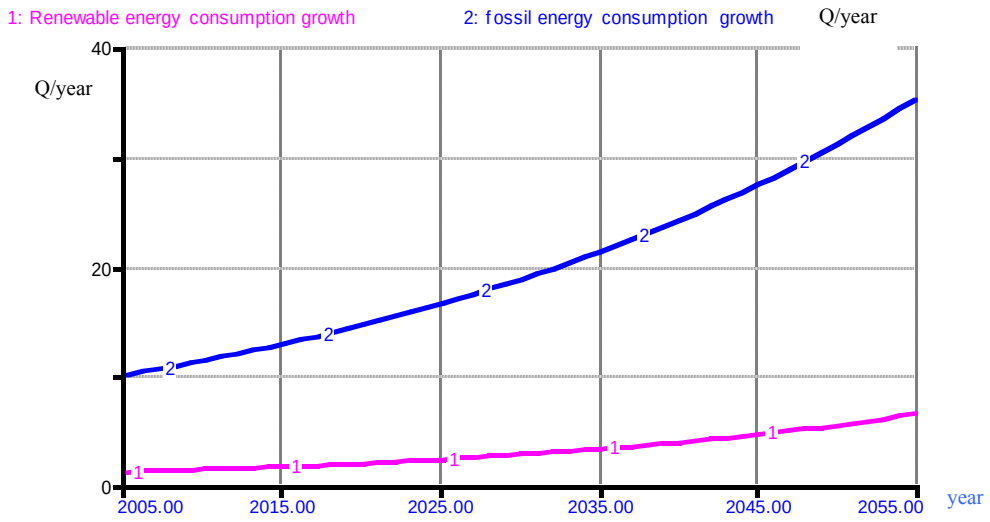

Figure 52: Renewable and fossil energy consumption growth (Q/year) during the next 50 years

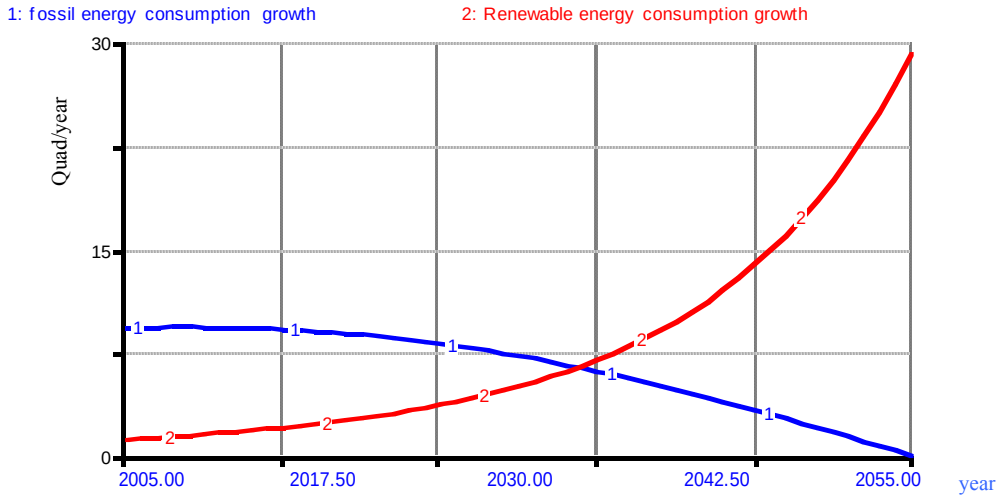

Figure 53: Decrease the global fossil consumption growth and increase the global renewable consumption growth forecast (Q /year) during the next 50 year

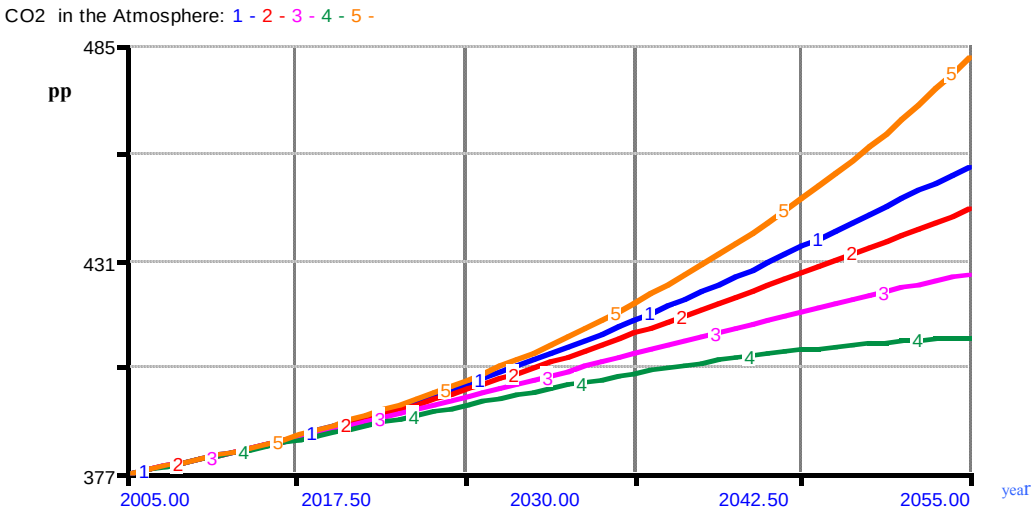

Figure 54: CO_2 accumulation per year in ppm/year in the model with 0%(1), 20%(2), 50%(3) and 80%(4) reduction rate in CO_2 emissions per unit of energy and 0% reduction rate with increase the global fossil consumption growth (5) during next 50 year.

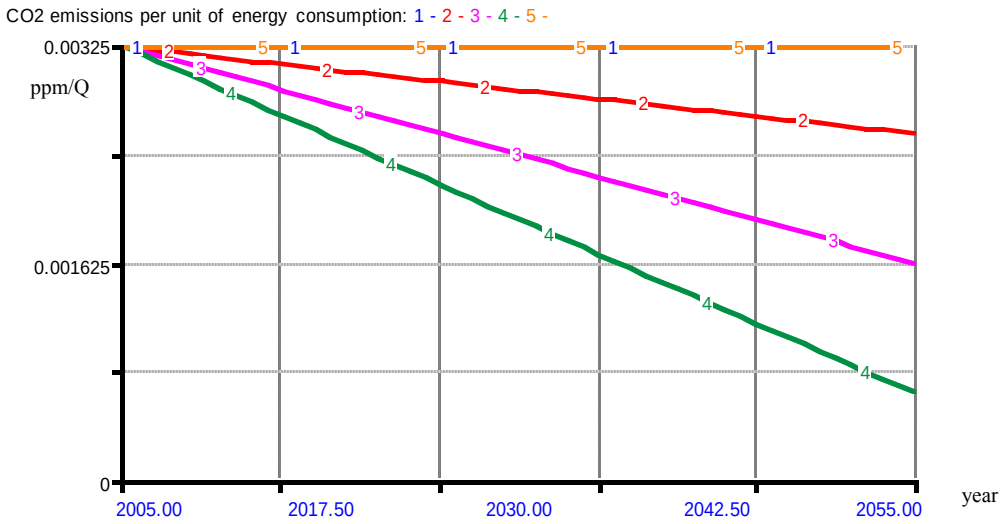

Figure 55: CO_2 Emissions per unit of fossil energy consumption (ppm/Quad) in the model with 0% (1), 20% (2), 50% (3) and 80% (4) degree of reduction rate in emissions during next 50 year and (5) with 0% reduction rate with increase the global fossil consumption growth

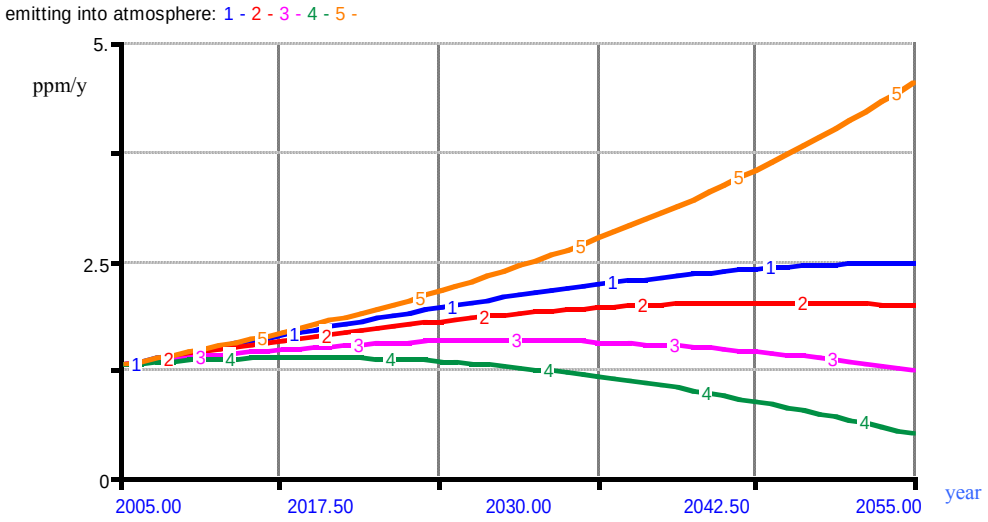

Figure 56: CO_2 Emissions per total of fossil energy consumption per year (ppm/year) in the model with 0% (1), 20% (2),50% (3) and 80% (4) degree of CO_2 reduction rate year and (5) with 0% reduction rate with increase the global fossil consumption growth during next 50 years

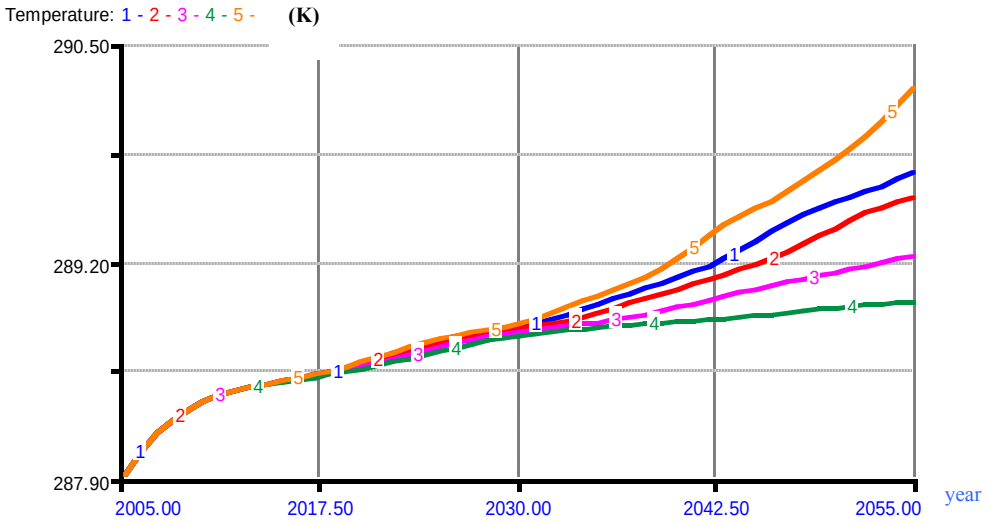

Figure 57: Temperature of the Earth surface in the model with 0% (1), 20% (2),50% (3)and 80% (4) degree of reduction rate in CO_2 emission and (5) with 0% reduction rate with increase the global fossil consumption growth during next 50 years

4.2 Modeling the Electrical Energy Demand–Supply and CO_2 Reduction-Results

We describe 2 scenarios with dominant Electricity production from fossil fuels in Kosovo

Scenario1.
In Kosovo the electric power is produced 95-97% from the lignite power plants: Units $A_j = \{A_1,A_2,A_3,A_4,A_5\}$ and $B_j = \{B_1,B_2\}$. The beginning of construction of the unit $C_j = \{C_1,C_2,C3\}$is planned for the year 2012. The rest of only 3-5% of electric power is produced from the renewable resources we will designate by R_j. Therefore, $U_j = A_j + B_j + C_j + R_j$, and substituting in Eq. (5), we have

$$EP = \sum_j (\mathrm{Aj} + \mathrm{Bj} + \mathrm{Cj} + \mathrm{Rj}) \cdot EP_j \tag{53}$$

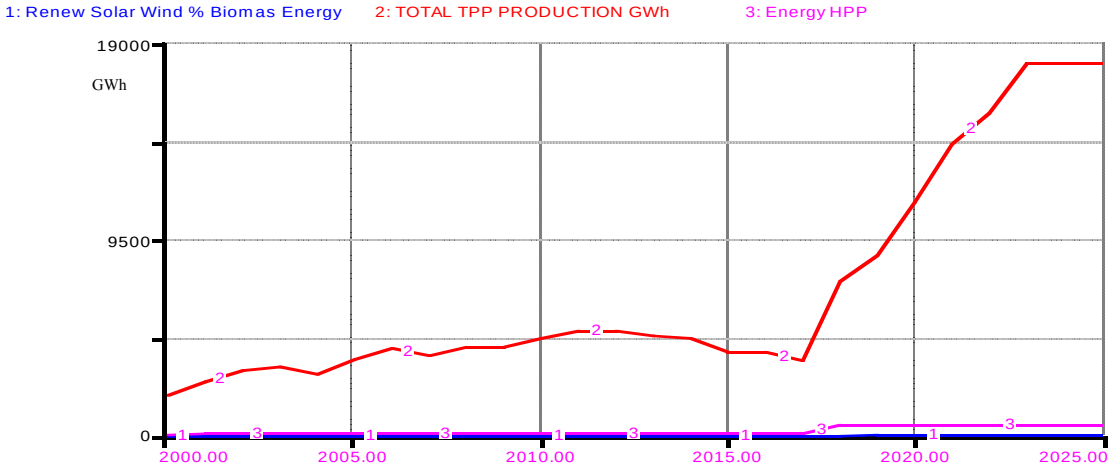

Figure 58: Energy production with dominant 95-97% fossil fuels (coal) and 3-5% renewable(Solar, wind Biomass and HPP)

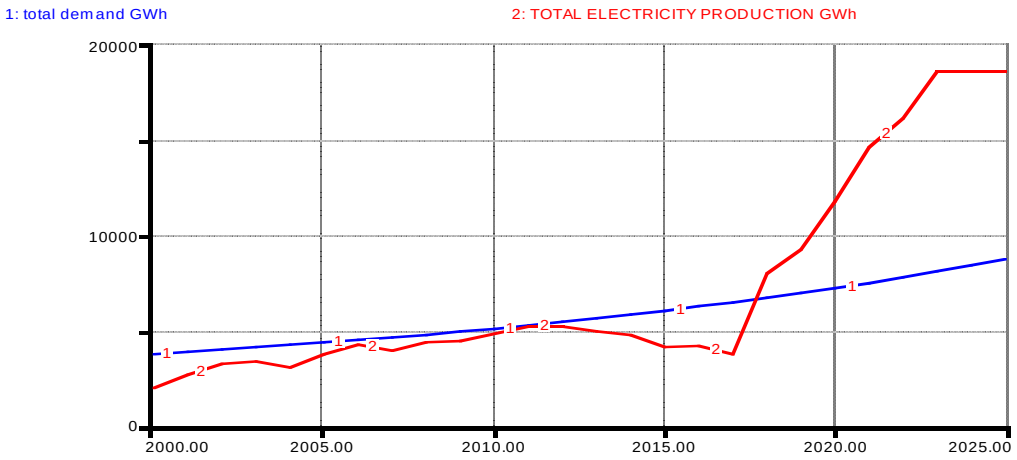

Figure 59: Total Electricity Energy Demand –Supply with Dominant Nonrenewable Sources

In Figure 58. the scenario of the total annual energy production from the all production units U_j is shown. According to this scenario, the electric power production is dominated with 95% by the energy produced from lignite. From Figure 58 we see that until the year 2017 (when the A unit is expected to finish with production) the Energy Demand –Supply are balanced, whereas from the year 2017 we will witness a great increase in production which will continue until the year 2025, when the C_1, C_2 and C_3 units are expected to

start production, and a further increase in production. According to this scenario, the renewable energy participates with 2.6%-3% of the total energy production for the time period 2000-2017, with an increase of 3%-5% for the time period 2017-2025. This participation of the renewable energy in the total electric power production does not satisfy the Energy Power Community Treaty (EPCT) demands, a member of which is Kosovo as well. This treaty forecasts that until the year 2015 the total needs for energy must be ensured up to 10-12% from the renewable resources.
As a result of the energy production from lignite we have the emission of gases that cause the greenhouse effect, such as CO_2. Emission is calculated by the formula

$$E_{CO_2}^{TPP} = \sum_j (\mathrm{Aj} + \mathrm{Bj} + \mathrm{Cj} + \mathrm{Rj}) \cdot EP_j \cdot EF_{CO_{2j}}^{TPP} \tag{54}$$

Where $E_{CO_2}^{TPP}$ is the total annual emission of CO_2, $EF_{CO_{2j}}^{TPP}$ is the emission factor for CO_2 from production unit j (t/MWh) and EP_j is the energy production from unit j. in Eq. (10) we regard the fact that the emission from the unit R_j is zero, $E_{Rj} = 0$.
For the initial values of the emission factors we have taken the values listed in the Table 11

Table 11: CO_2 Emissions factor for TPP

CO_2 Emission factor (t/MWh)			
EF_A	EF_B	EF_C	EF_R
1.5	1.4	0.8	0

These values will change with the establishment of the EU standards for emission as well as with the advance in new technologies for sequestration of CO_2 (Fay, James A and Golomb. 2002) and the increase of the coefficient of the exploitation of lignite. Using these initial values for emission and the values that are expected in the future, along with the results shown in Figure 58, from the Eq. (54) for the emission of CO_2 per year (Mt/year) we obtain the results shown in Figure 60.
From Figure 60 we see that according to the scenario 1, we have an increase in emission of CO_2 until the year 2010, and thereafter a decrease in emission until the year 2017. In course of this period the unit *A* will fall out of use. In the year 2017 the TPP C_1, C_2 and C_3 will start with production, with a power capacity of 2100 MW and as a result we have an increase of the CO_2 output.

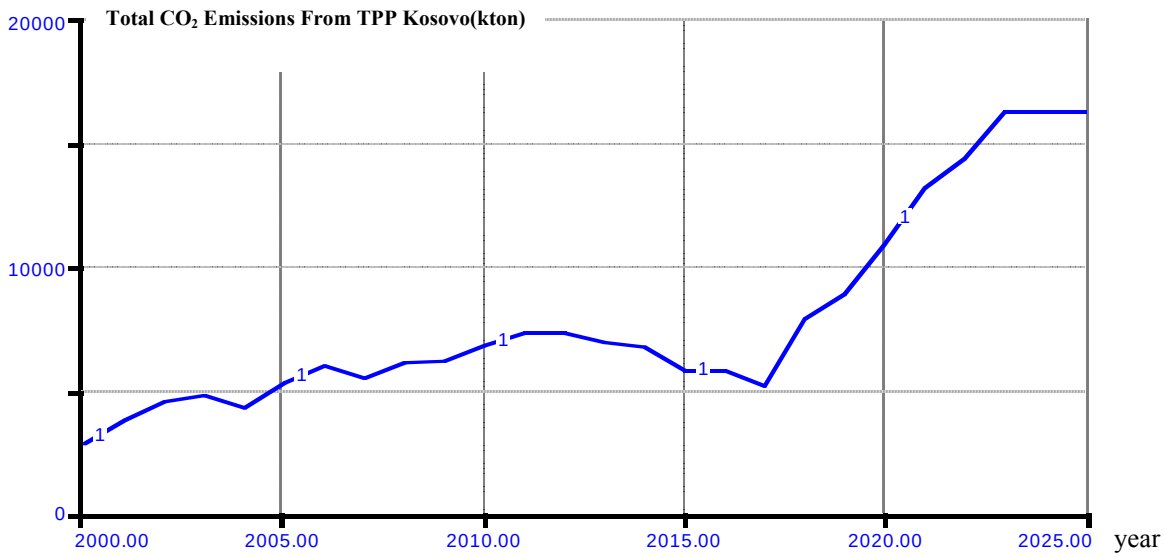

Figure 60: Total CO_2 Emission From TPP Kosovo (kton) from 2000-2025 (Scenario with 95-97% nonrenewable sources)

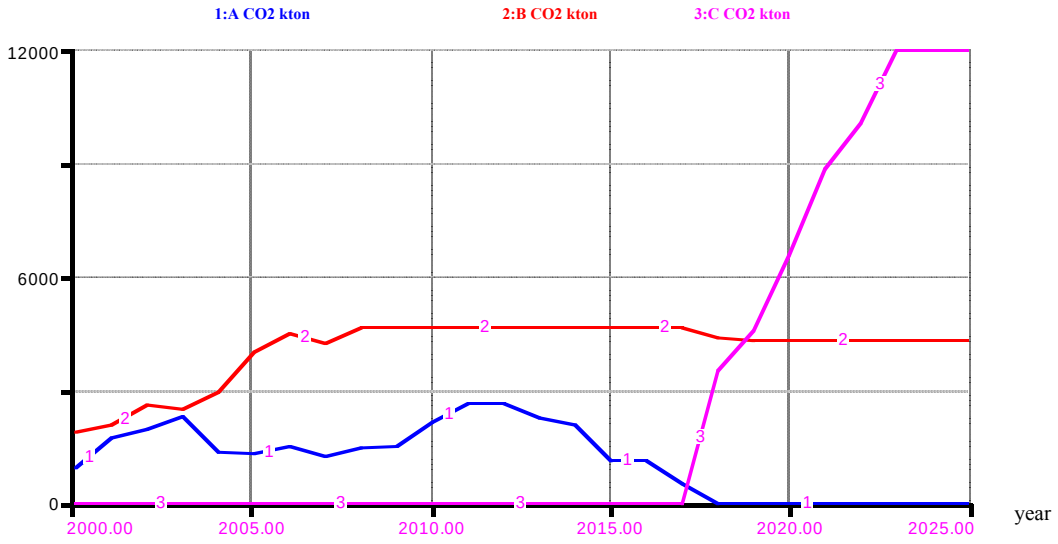

Figure 61: Total CO_2 Emission from TPP (Unit A, B and C)

Scenario 2.

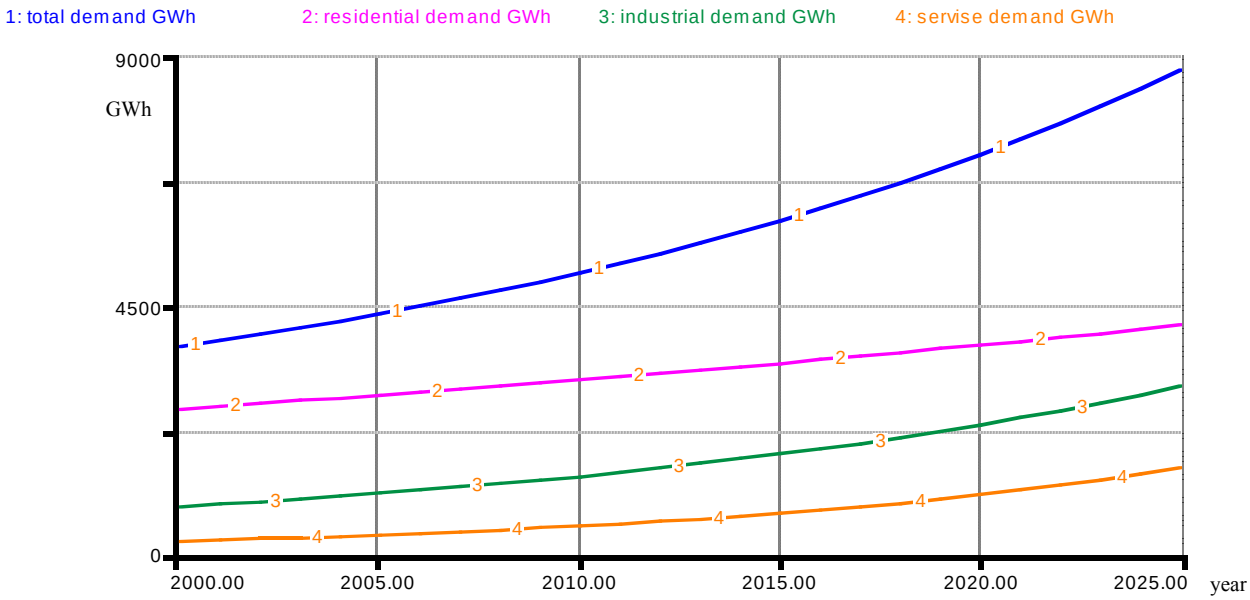

Figure 62: Total Electricity Demand for Kosova

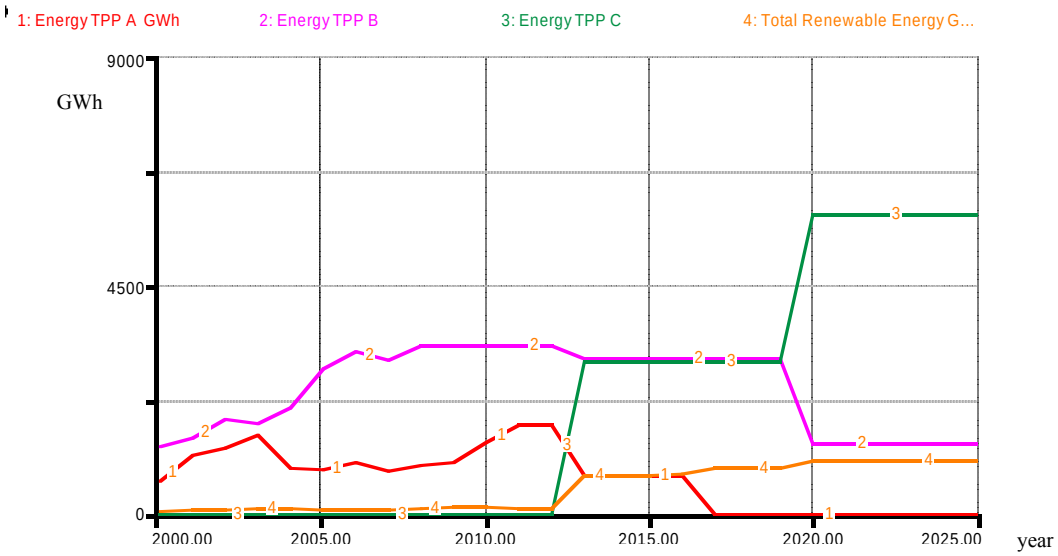

Figure 63: Total Energy Production from TPP (Unit A,B and C) and Renewable Sources

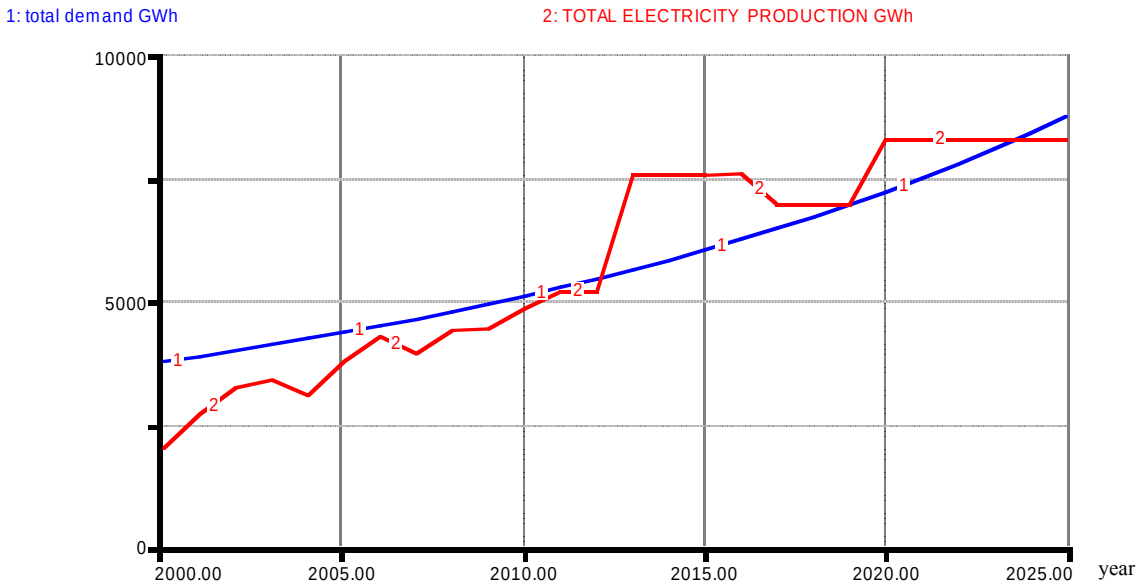

Figure 64: Total Electricity Production(line 3) from Renewable Sources(line 2) and Fossil fuels

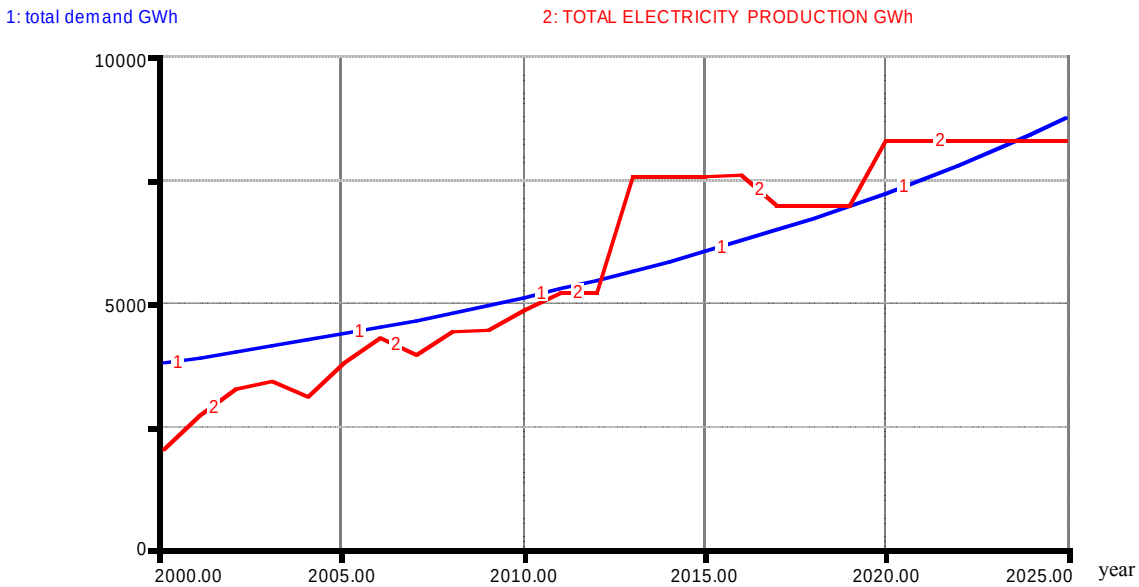

Figure 65: Electricity Demand-Supply for Kosovo from year 2000 to 2025

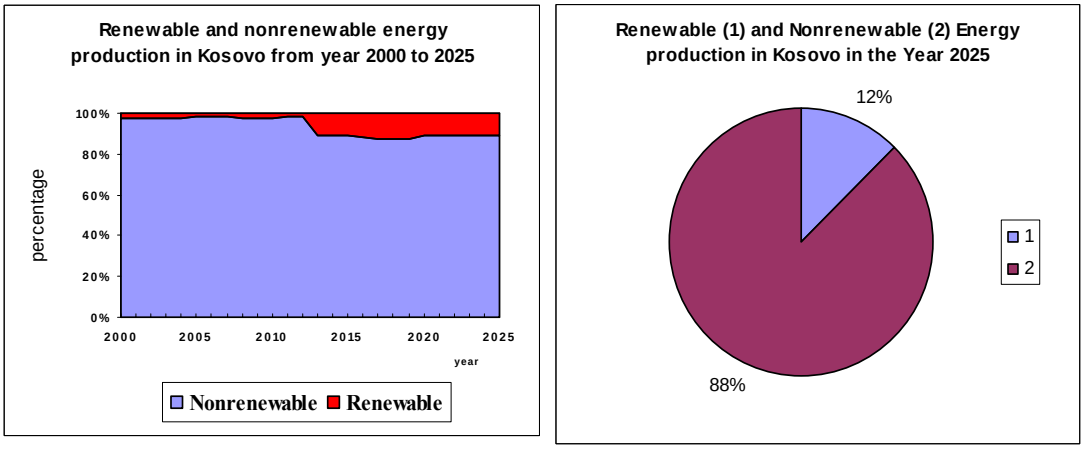

Figure 66: Participation of renewable energy in total energy production in Kosovo from year 2000 to 20025 (a) and in year 2025 (b)

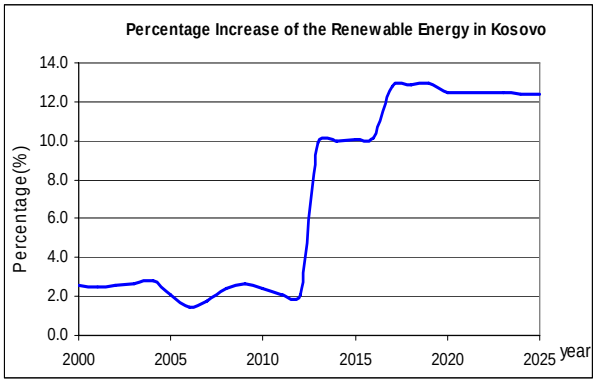

Figure 67: Percentage increase of Renewable energy in Kosovo from year 2000 to 2025

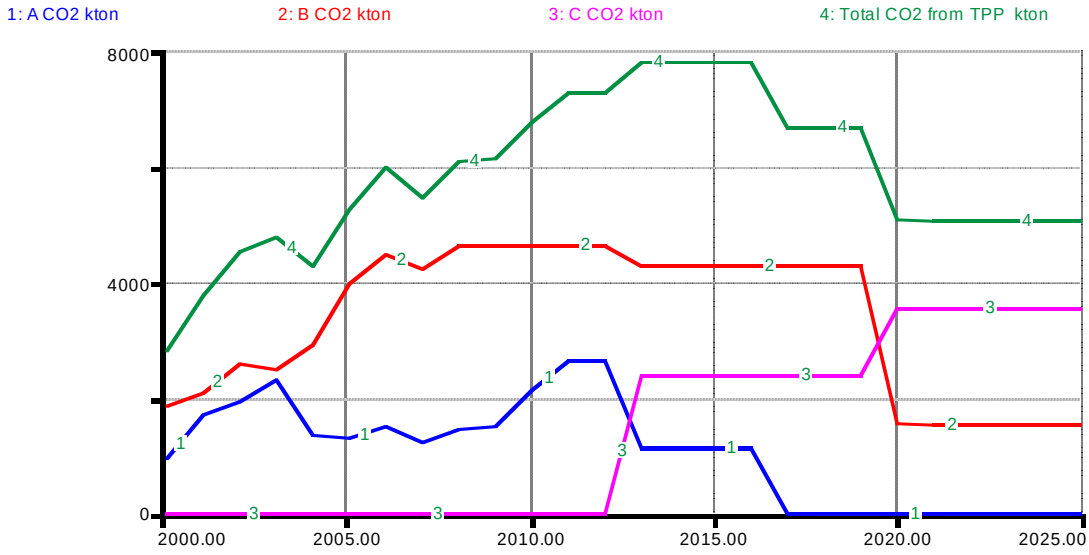

Figure 68: Emissions From Kosovo TPP (Scenario2)

The renewable energy potentials (middle and small hydro power stations, solar, wind, etc.) are: presently existing: 2x17,5 MW; 5xHPP = 11.82 MW, and to be built: 18 other small HPPs with the power of 63,70 MW, as well as 2 x middle HPPs with the power of 292.8 MW, which in total amounts 403.32 MW see Table 3. Also construction of a wind farm power station is planned in Shtime, with the installed power of 25 MW in 2012, and several other wind stations which will achieve an overall power up to 75 MW in 2025, whereas the solar energy in various modes (solar, thermal, biomass and photovoltaic) will achieve the power from 5 MW in 2012 to 25 MW in 2025. The total power from renewable the year 2025 will be 503.32MW, which is 12,3% of the overall energy produced in that year.

4.3 Modeling the Dynamic Mobile Source Emission Systems and CO2 Reduction with Renewable Energy Use and New Technology-Results

Effects of policy and technology options after 2015 can be seen in Figure 69.

Substituting data from Table 8 in the Eq.(52) and after the application of Policy and Technology Options for Reducing Transport Emissions for the total emission of CO_2 (M*t*/year), we obtain results presented in Figure 69.

From the Figure 69 we see that implementing the emission reduction policies and introducing new technologies in transportation, after the year 2015, a continual reduction in air pollution will take place, whereas the CO_2 output to the year 2025 will be reduced by 25% in comparison with the emission values of the year 2007 and will be approximately the same as the values of the year 2001

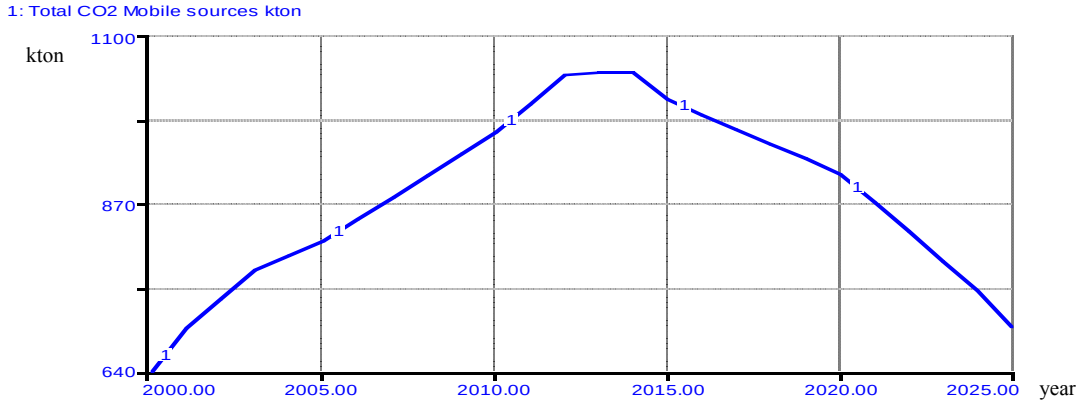

Figure 69: Total emission of CO_2 from Mobile Sources Kosova until year 2025

4.4 Total CO2 Reduction in Kosovo

Implementing the emission reduction policies and introducing new technologies in transportation and in electrical power production in Kosovo for total CO_2 emission we have from Eq.(47) and Eq.(54)

$$E^{T}_{CO_2} = E^{v}_{CO_2} + E^{TPP}_{CO_2} \tag{55}$$

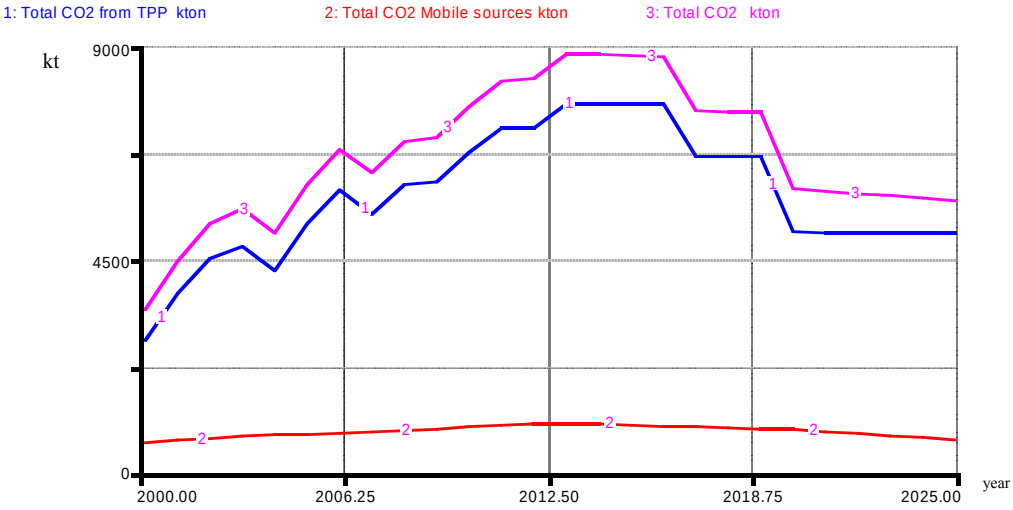

Figure 70: Total CO_2 Emissions from TPP Kosovo and from Mobile sources until year 2025

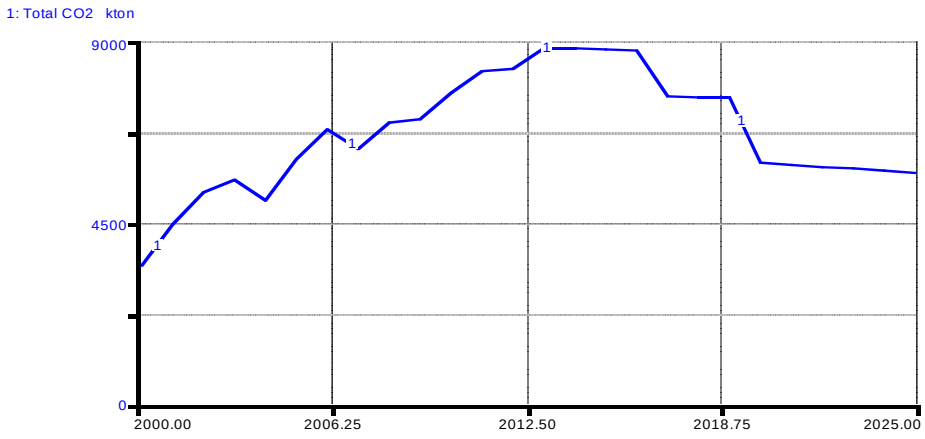

Figure 71: Total CO_2 emission in Kosovo due to use of renewable energy until the year 2025

(4.75 Mt CO_2 in comparison with 5.99 Mt in year 2006) the emission of CO_2 will be reduced for about 20% in comparison with that of the year 2006

4.5 Impacts of Renewable Energy on the Greenhouse Gas Reduction and Air Pollutions from Mobile Sources in Kosovo-Dynamic Modeling-Results

The factors of emission (Figures 72 and 74), and the average value of kilometers traveled per year (Figure 46), change starting from the year 2015, due to the Policy and Technology Options for Reducing Mobile Emissions that have to be applied in Kosovo in order to comply with the European Union emission standards http://www.ec.europa.eu/environment/ipcc/index.htm and http://enrin.grida.no/htmls/kosovo/SoE/energy

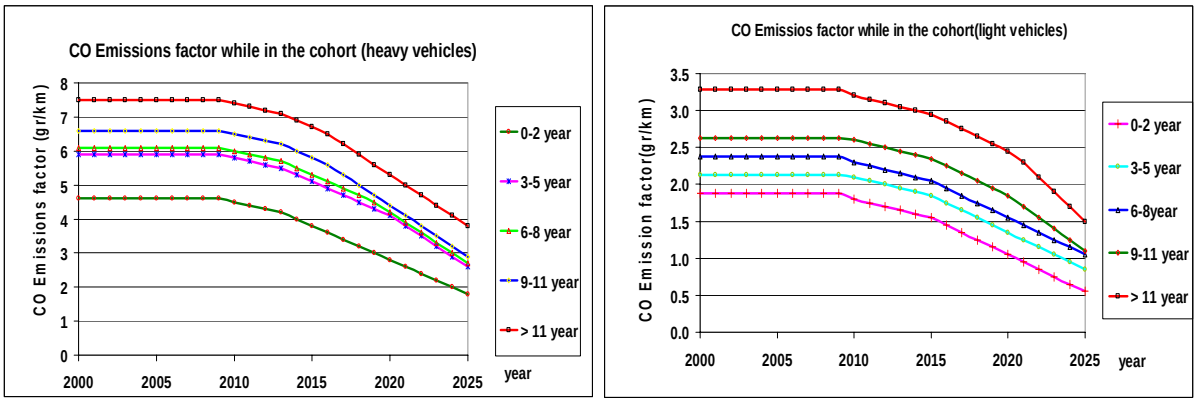

Figure 72: Time dependence change of CO emission factors while in cohort (Light and Heavy Vehicles)

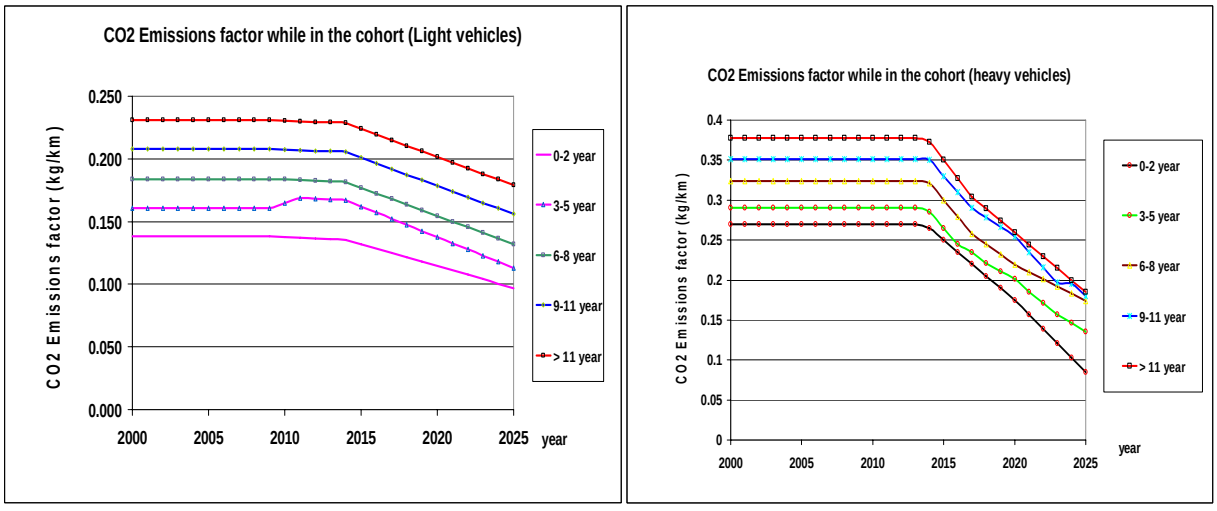

Figure 73: Time dependence change of CO_2 emission factors while in cohort (Light and Heavy Vehicles)

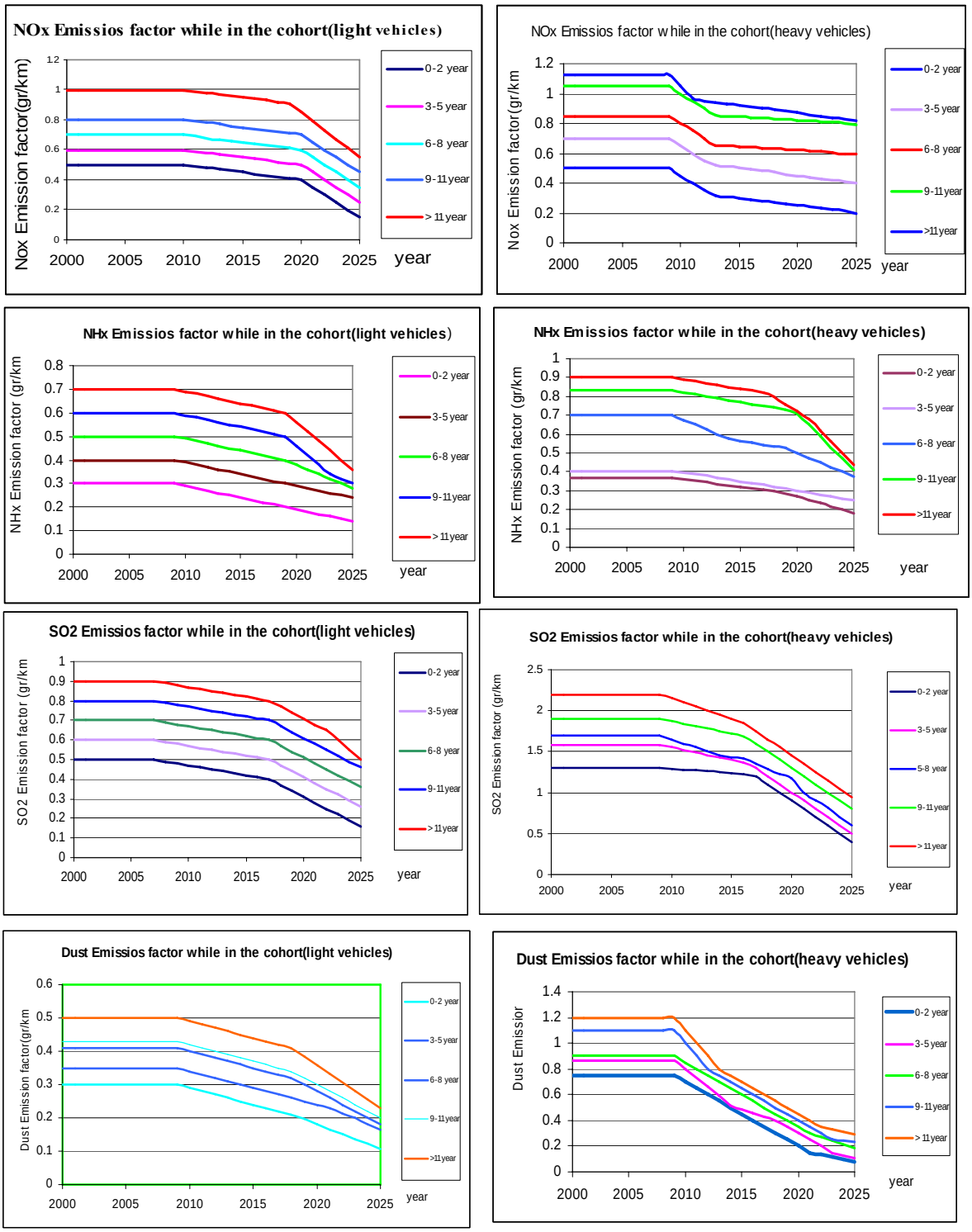

Figure 74: Emissions factor while in cohort (light and heavy vehicles) for NO_x,SO_2,NH_x and Dust

Effects of policy and technology options after 2015 can be seen in Figures 69 -74.
Substituting these data in the Eq.(68), and after the application of Policy and Technology Options for Reducing Transport Emissions for the total emission of CO, NO_x, SO_2, NH_x, dust (t/year) and CO_2 (M*t*/year), we obtain results presented in Figure 75 and Table 12.

Table 12: Total emissions (CO2, CO, NOx,SO2 and dust) from mobile sources air pollution in Kosova (light and heavy vehicles).

Total emissions (CO2, CO, NOx,SO2 and dust) from mobile sources air pollution in Kosova (light and heavy vehicles)						
year	**CO(t/year)**	**NOx(t/year**	**NHx(t/year)**	**SO2(t/year)**	**Dust(t/year)**	**CO2(Mt/year)**
2000	9703	2445	1777	2773	2359	0.6428
2001	10448	2623	1908	2993	1670	0.6953
2002	11029	2757	2007	3166	1770	0.7372
2003	11567	2879	2096	3327	1865	0.7766
2004	11886	2933	2135	3424	1925	0.7994
2005	12217	2985	2172	3522	1986	0.8225
2006	12605	3052	2218	3636	2056	0.8493
2007	13054	3132	2272	3765	2135	0.8798
2008	13474	3207	2321	3852	2210	0.9085
2009	13913	3284	2370	3939	2287	0.9379
2010	14152	3327	2381	4008	2268	0.9728
2011	14369	3329	2387	4076	2243	1.0093
2012	14649	3346	2405	4162	2223	1.0481
2013	14519	3211	2315	4129	2119	1.0488
2014	14288	3110	2227	4102	2008	1.0469
2015	14053	3009	2146	4081	1928	1.0102
2016	13892	2992	2120	4143	1887	0.9945
2017	13584	2941	2073	4116	1823	0.9729
2018	13263	2890	2028	3957	1752	0.9523
2019	12926	2838	1983	3783	1646	0.9322
2020	12466	2775	1889	3571	1526	0.9063
2021	11875	2576	1788	3340	1399	0.8704
2022	11251	2382	1691	3088	1314	0.8325
2023	10591	2192	1597	2813	1228	0.7906
2024	9889	2008	1513	2512	1141	0.7511
2025	9143	1830	1429	2184	1053	0.7037

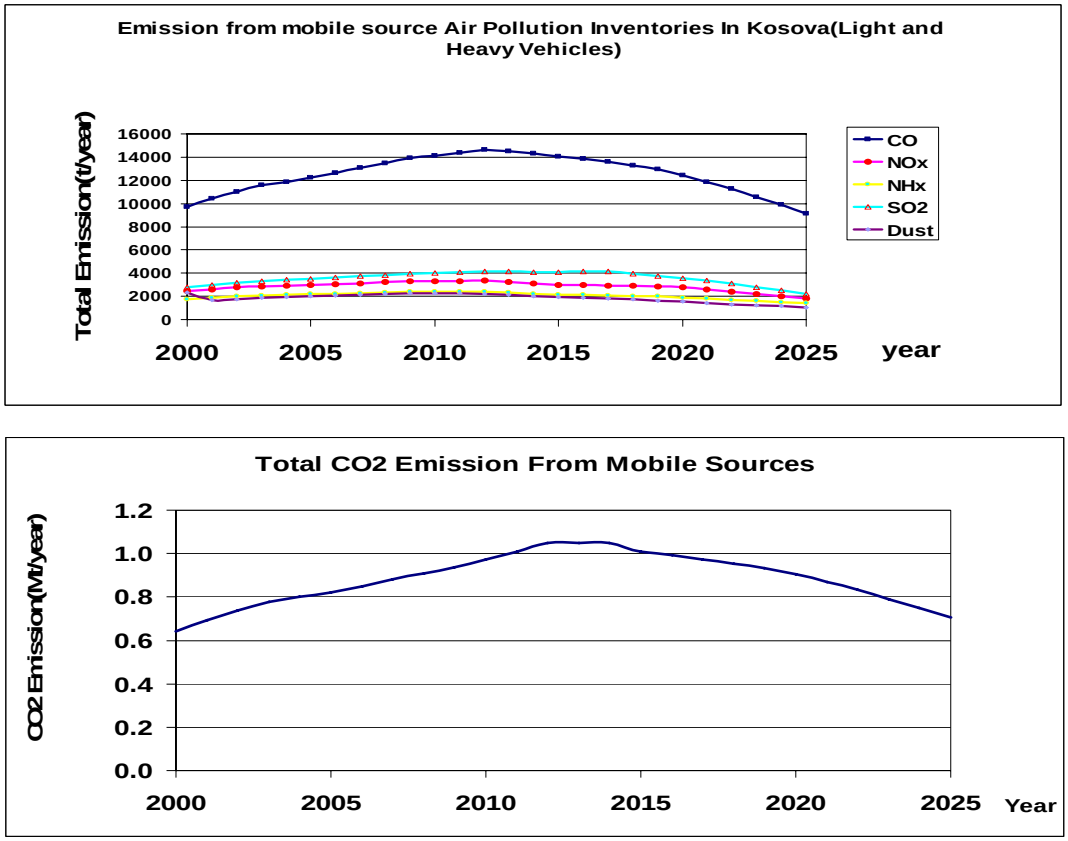

Figure 75: Total emission of air pollution (CO, NOx, NHx, SO2, dust) and GHG (CO_2) From Mobile Sources

Results of Dynamic Modeling the Electricity Demand-Supply, GHG and Air Pollution Reduction with Renewable Energy in Kosovo

The total annual electric power (GWh/year) we can calculate by the expression

$$EP = \sum_j U_j \cdot EP_j \tag{56}$$

where U_j is the j unit that produces electric power in scope of the electric power system of Kosovo, EP_j is the total annual electric power produced by the unit U_j (GWh/year).

Scenario1.
In Kosovo the electric power is produced 97% from the lignite power plants: Units $A_j = \{A_1,A_2,A_3,A_4,A_5\}$ and $B_j = \{B_1,B_2\}$. The beginning of construction of the unit $C_j = \{C_1,C_2,C3\}$is planned for the year 2008. The rest of only 3% of electric power is produced from the renewable resources we will designate by R_j. Therefore, $U_j = A_j + B_j + C_j + R_j$, and substituting in Eq. (11), we have

$$EP = \sum_j (\mathrm{Aj} + \mathrm{Bj} + \mathrm{Cj} + \mathrm{Rj}) \cdot EP_j \tag{57}$$

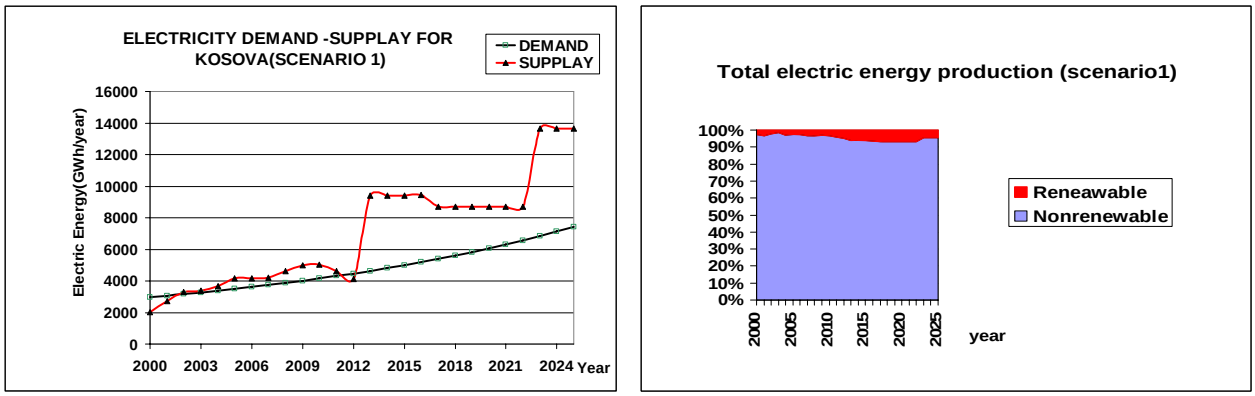

Figure 76: No sustainable Demand-supply electricity energy in Kosovo (Scenario1)

As a result of the energy production from lignite we have the emission of gases that cause the greenhouse effect, such as CO_2 and air pollutants SO_2, NO_x and dust. Emission is calculated by the formula:

$$E_i = \sum_j (\mathrm{Aj} + \mathrm{Bj} + \mathrm{Cj} + \mathrm{Rj}) \cdot EP_j \cdot EF_{ij} \tag{58}$$

where E_i is the total annual emission of pollutant i (t/year); i - CO_2, SO_2, NO_x and dust, EF_{ij} is the emission factor pollutant i from production unit j (t/MWh). In Eq. (57) we regard the fact that the emission from the unit R_j is zero, $E_{Rj} = 0$.
For the initial values of the emission factors we have taken the values listed in the Table 13.

Table 13: Emissions factor for TPP

CO_2 Emission factor(t/MWh)				NO_x Emission factor (kg/MWh)				SO2 Emission factor (kg/MWh)				Dust Emission factor (kg/MWh)			
EF_A	EF_B	EF_C	EF_R	EF_A	EF_B	EF_C	EF_R	EF_A	EF_B	EF_C	EF_R	EF_A	EF_B	EF_C	EF_R
1.5	1.4	0.8	0	4	3.8	1.2	0	3.1	2.8	0.2	0	3	1.4	0	0

In Figure 77 results from the Eq. (58) for the emission of CO_2 per year (Mt/year) and SO_2, NO_x and dust (t/year) are presented. These values will change with the establishment of the EU standards for emission of air pollutants (SO_2,NO_x and dust) as well as with the advance in new technologies for sequestration of CO_2 (Berkowitz, N.1994) and the increase of the coefficient of the exploitation of lignite.

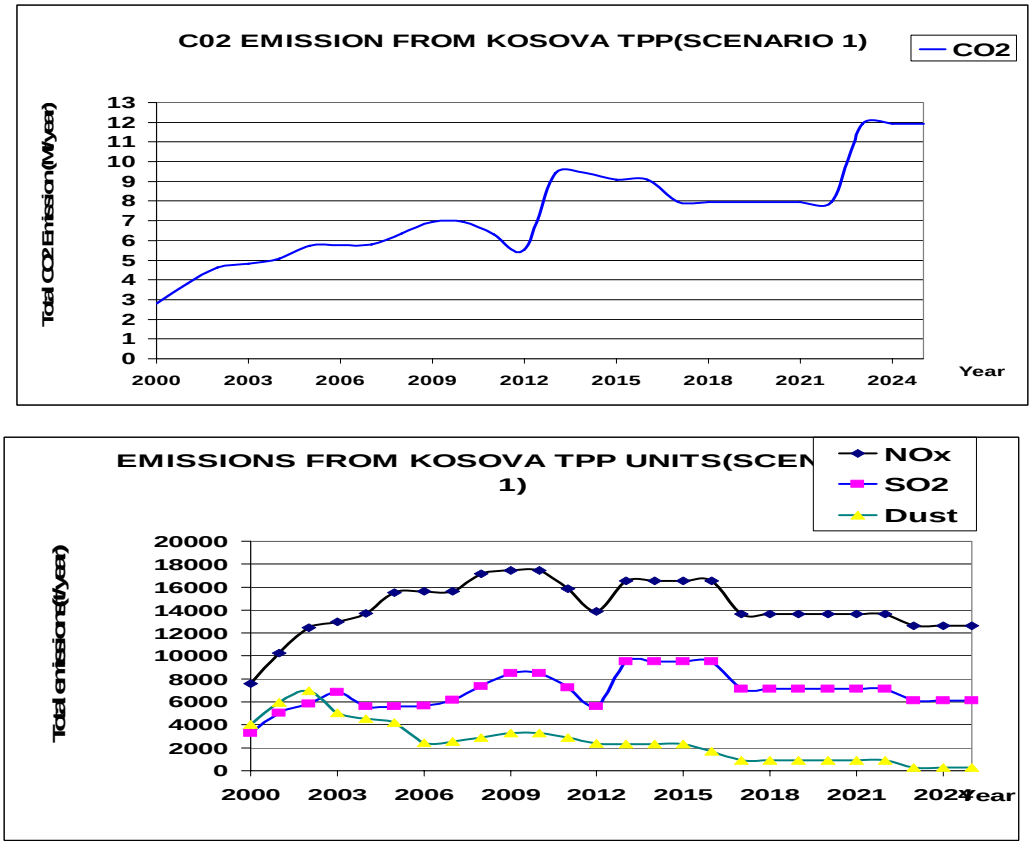

Figure 77: Emissions From Kosovo TPP (Scenario1)

From the Fig. 77 we see that according to the scenario 1, we have an increase in emission of CO_2 until the year 2010, and thereafter a decrease in emission until the year 2013. In course of this period two blocks of the unit *A* will fall out of use. In the year 2013 the TPP C_1 will start with production, with a power capacity of 700 MW and as a result we have an increase of the CO_2 output. Another decrease in emission is expected in the year 2017, when the unit A will completely fall out of use, and this level of emission will retain until the year 2022 when with the renewed increase of the CO_2 output. After the reconstruction of the units A and B which has been undertaken in 2002 and 2004, the emission of dust will continually decrease even after the construction of the new power plant C, due to the advanced technology, and a slight gradual decrease will be observed for the NO_x and SO_2 outputs as well, due to the standards that Kosovo must meet before a EU membership. This gradual decrease will take place from the year 2014, when hopefully Kosovo will become an EU member.

Scenario 2. In Figure 78 the electric power production from the lignite and renewable energy is shown. According to this scenario, the renewable energy from the year 2012 to the year 2025 will consist in 20% of the total energy production in Kosovo. With this percentage of the renewable energy, Kosovo as e signatory of the Community of Energy Treaty will accomplish the requirements of this treaty which demands that the energy needs should be fulfilled up to 10-12% from the renewable resources, until the year 2015.
The renewable energy potentials (middle and small hydro power stations, solar, wind, etc.) are: currently existing: 2x17,5 MW; 5xHPP = 11.82 MW, and to be built 18 other small HPPs with the power of 63,70 MW, as well as 2 x middle HPPs with the power of 292.8 MW, which in total amounts 403.32 MW see Table. Also construction of a wind farm power station is planned in Shtime, with the installed power of 25 MW in 2012, and several other wind stations which will achieve an overall power up to 75 MW in 2025, whereas the solar energy in various modes (solar, thermal, biomass and photovoltaic) will achieve the power from 5 MW in 2012 to 25 MW in 2025. The total power from renewable the year 2025 will be 503.32MW, which is 12,3% of the overall energy produced in that year

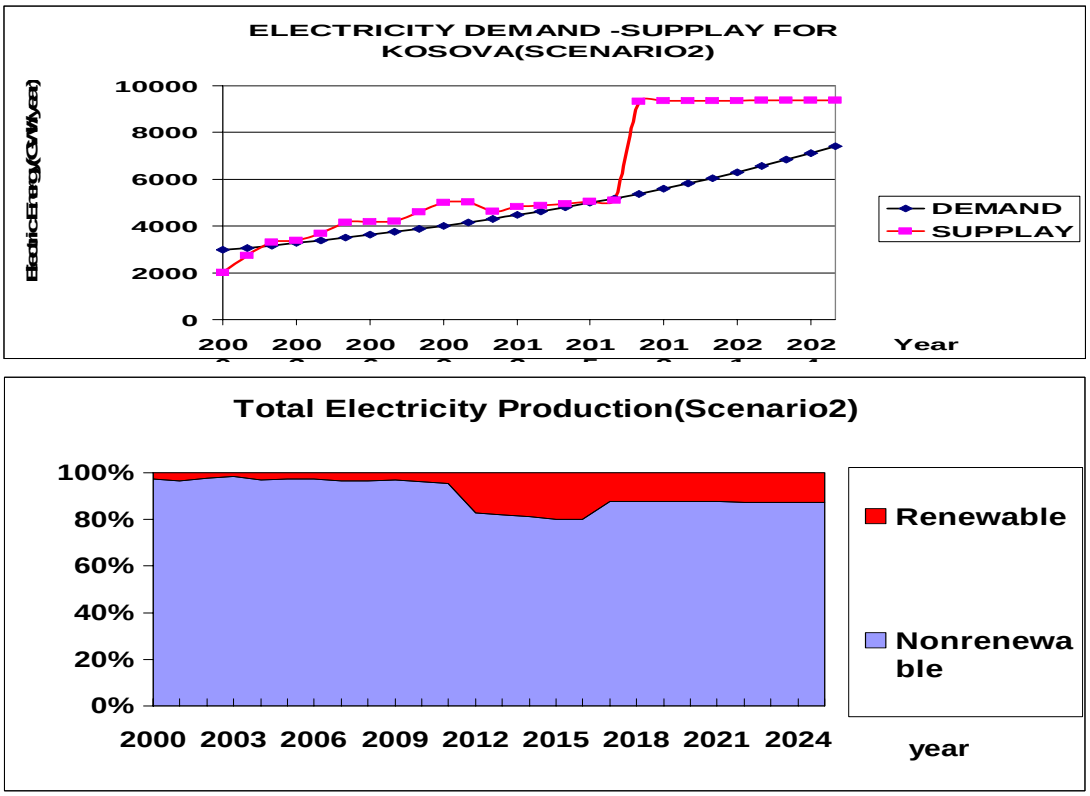

Figure 78: Sustainable Demand-supply electricity energy in Kosovo (Scenario 2)

In Figure 79 the CO_2 and air pollution emission (NOx, SO_2 and dust) output is presented

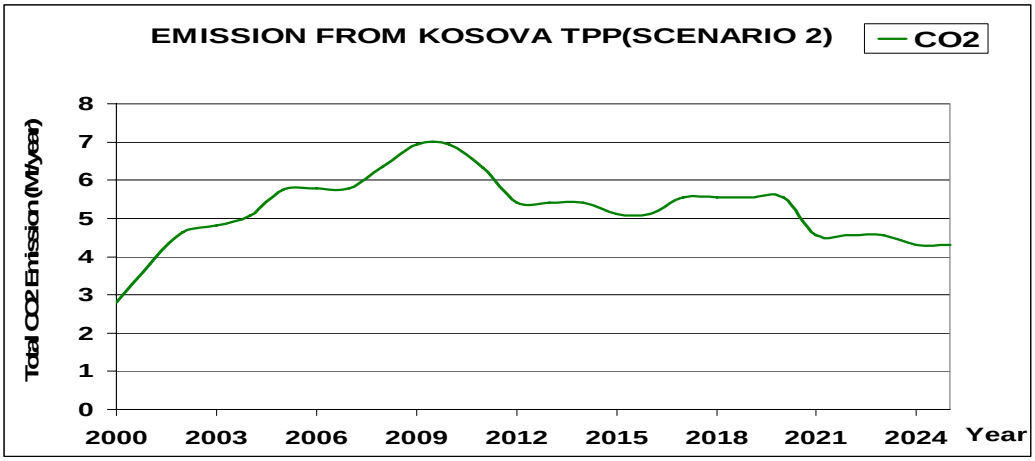

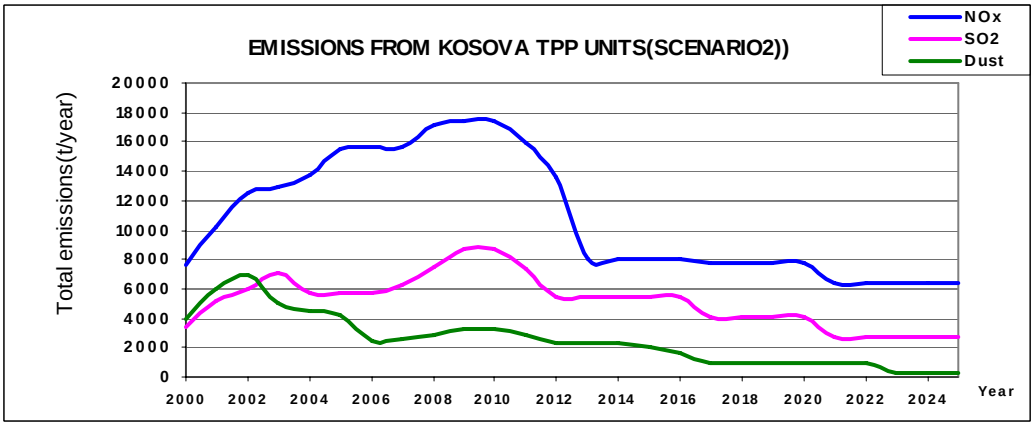

Figure 79: Emissions From Kosovo TPP (Scenario 2)

5 Discussion

Discussion of the Results of the Greenhouse Zero-Dimensional Model With CO_2 Reduction In Emission Due To Renewable Energy Use And New Technologies

For greenhouse zero-dimensional model with CO_2 reduction in emission due to renewable energy use and new technologies we have obtained the results shown by Figures 50-57.

What is important to recognize in this model is that the reduction rate of CO_2 emission for 20% and 50% does not lead to a reduction in the CO_2 accumulation in atmosphere (we have only slowing of the rate of growth in CO_2) (Figure 54).

This means that the global temperature would not decline but only slower its rate of increase (Figure 56). Only if we will simulate a high rate of reducing of CO_2 emissions associated with a unit of energy production activity over a 50 year period from 2005 to 2055 (Figure 55), we will stabilize the accumulation of CO_2 in atmosphere (Figure 54. and 56.) on the constant value and the Earth's surface temperature until the year 2055 will slightly decrease until the constant value T=288.8 K (Figure 57).

This aggressive rate of CO_2 reduction per unit of fossil energy consumption (ppm/Q) for about 80% will be achieved if inflow oriented policies focusing on drastically decreasing fossil fuel energy production and use in alternative renewable energy sources including solar energy in a variety of forms as biomass, wind, hydro energy and in new technological innovation in energy production and consumption.

Modeling the Electrical Energy Demand–Supply and CO_2 Reduction- Discussion of the Results.

In Figures 63, 64 and 66 the electric power production from the lignite and renewable energy is shown. According to this scenario, the renewable energy from the year 2012 to the year 2025 will consist in 12%-15% of the total energy production in Kosovo. With this percentage of the renewable energy, Kosovo as e signatory of the Community of Energy Treaty will accomplish the requirements of this treaty which demands that the energy needs should be fulfilled up to 10-12% from the renewable resources, until the year 2015.

In Figure 68 the CO_2 output is presented. According to the scenario 2, the reduction of CO_2 output will be achieved gradually starting from the year 2017, when the solar energy production with all its modes (HPP, wind, solar, thermal, photovoltaic, etc.) will be 892 GWh, which is 12,79% of the overall annual production of the year 2017. In the year 2017 the TPP A and B_1 as the greatest emitter of CO_2 will be closed, and investments in new technologies in TPP B_2 will make possible the reduction of CO_2 output up to 30% per MWh of energy. The same year the TPP C_2 and C_3 will start with production, with a new technology (zero-emission-technologies and carbon sinks) (Theodore, L and Kunz, R.G., 2003) which enables the sequestration of CO_2 (Miller, B.G, 2005) and the reduction of emission for 40%-50% less than the TPP B emits. Continual application of new technologies until the year 2025 will reduce the CO_2 emission up to 25% of the emitted value form TPP B.

According to the scenario 2, the emission of CO_2 in the year 2025 (5.07 Mt)will be reduced for about 20% in comparison with that of the year 2006 (5.99 Mt)

From the Figure 75 we see that implementing the emission reduction policies and introducing new technologies in transportation, after the year 2015, a continual reduction in air pollution will take place, whereas the CO_2 output till the year 2025 will be reduced by 25% in comparison with the emission values of the year 2007 and will be approximately the same as the values of the year 2001.

In the Figure 76 the scenario of the total annual energy production from the all production units U_j is shown. According to this scenario, the electric power production is dominated with 95% by the energy produced from lignite. From the Figure 76 we see that until the year 2013 (when the C_1 unit is expected to start with production) the Energy Demand – Supply are balanced, whereas from the year 2013 we will witness a great increase in production which will continue until the year 2022, when the C_2 and C_3 units are expected to start production, and a further increase in production. According to this scenario, the renewable energy participates with 2.58%-5.21% of the total energy production for the time period 2000-2012, with an increase of 6.47% - 7.5% for the time period 2013-2022, and a decrease up to 4.8% in the year 2025. This Participation of the renewable energy in the total electric power production does not satisfy the Energy

(Power) Community Treaty (EPCT) demands, a member of which is Kosovo as well. This treaty forecasts that until the year 2015 the total needs for energy must be ensured up to 10-12% from the renewable resources.

In Figure 79 the CO_2 output is presented. According to the scenario 2, the reduction of CO_2 output will be achieved gradually starting from the year 2012, when the solar energy production with all its modes (HPP, wind, solar, thermal, photovoltaic, etc.) will be GWh, which is 19,21% of the overall annual production of the year 2012. In the year 2017 the TPP A as the greatest pollutant and emitter of CO_2 will be closed, and investments in new technologies in TPP B will make possible the reduction of CO_2 output up to 30% per MWh of energy.

The same year the TPP C will start with production, with a new technology (zero-emission-technologies and carbon sinks) (Miller, 2005), which enables the sequestration of CO_2 (Loulou et al., 2005) and the reduction of emission for 50% less than the TPP B emits. Continual application of new technologies until the year 2025 will reduce the CO_2 emission up to 25% of the emitted value form TPP B.

According to the scenario 2, the emission of CO_2 will be reduced for about 25% in comparison with that of the year 2007, as forecasted by EU and Kyoto Protocol. On the other hand, the air pollution emission (NOx, SO_2 and dust) will be significantly reduced, due to the imposed standards of EU, which Kosovo has to apply starting from the year 2015).

6 Conclusions

Because climate change is regionally driven with global consequences and the energy use is central to climate change the harnessing of renewable energy sources is vital to constraining the extent of climate change in global and regional level - in Kosovo in particular.

Firstly the impact of renewable energy in CO_2 reduction in global level (zero dimensional modeling of GHG reduction) is modeled.

What is important to recognize in this model is that the reduction rate of CO_2 emission for 20% and 50% does not lead to a reduction in the CO_2 accumulation in atmosphere (we have only slowing of the rate of growth in CO_2). This means that the global temperature would not decline but only slower its rate of increase. Only if we will simulate a high rate of reduction of CO_2 emissions associated with a unit of energy production activity over a 50 year period from 2005 to 2055, we will stabilize the accumulation of CO_2 in atmosphere on the constant value 413.3 ppm and the Earth's surface temperature until the year 2055 will slightly decrease until the constant value T=288.8 K. This aggressive rate of CO_2 reduction per unit of fossil energy consumption (ppm/Q) for about 80% will be achieved if inflow oriented policies focusing on transitioning away from a fossil fueled energy production and use in alternative renewable energy sources including solar energy in these variety forms as biomass, wind, hydro energy and in new technological innovation in energy production and consumption etc.

Then, the modeling is carried out regionally for Kosovo for two dynamical systems which are the main emitters of GHG (CO_2, N_2O, CH_4, $HCFC_s$, CFS_s, etc), i.e. transport and electricity generation emissions systems.

For mobile source emission system of Kosovo implementing the Options for Reducing Transport Emissions for the total emission of CO, NO_x, SO_2, NH_x, dust (t/year) and CO_2 (M*t*/year after the year 2015, a continuous reduction in air pollution will take place, whereas the CO_2 output till the year 2025 will be reduced by 25% in comparison with the emission values of the year 2007 and will be approximately the same as the values of the year 2001.

For electricity emission system we develop two scenarios. According to scenario 1, electric power is produced 95%-97% from the lignite and only 3-5% from renewable resources for the time period 2000-2025. As a result of the energy production from lignite we have an increase in emission of CO_2.

According to scenario 2, the renewable energy will increase from the year 2015 to the year 2025 from 8% to 14% of total energy production in Kosovo and the reduction of GHG up to 20% in comparison with the year 2005.

In our models we have gradually replaced the fossil fuels energy sources with renewable ones and we introduce the new technology for CO_2 sequestration and high energy efficiency in transport, and also, our models predict the significant reduction on GHG in long term prediction scenarios.

Our models according to participation of renewable energy in total energy, predict high emission of GHG in short term from year 2000 to the year 2010, both in mobile source emission system -transport and electricity power emission system in Kosovo. Because participation of renewable energy in this period is only 2-4%, policy options are status quo and there is no new technology option in both systems.

In the period from 2010 to 2015, stabilization and slight decreases in GHG emission occur. From 2010 to 2015 renewable energy slightly increases from 5- 8% in total electricity power production and in energy use in transport. Policy and technology options for reducing GHG and air pollution take place.

In the long term from year 2015 to 2025 we will have a gradual reduction in GHG by 20% in comparison with the year 2005. During this time renewable energy gradually increases to 14% of the overall energy. Policy and technology options for reducing GHG and air pollution will achieve EU standards which would be compatible with GHG reduction requirements (IPCC, Kyoto Protocol) ensuring a sustainable Energy Demand–Supply for Kosovo that becomes increasingly environmentally compatible.

Emission of sulfur dioxide (SO_2) generated at coal power plants (unit A, B and from new TPP unit C) will be continuously increasing till 2013 and increased concentration of SO_2 due to the new source will potentially affect SO_3^- and SO_4^{2-} at the receptor site that ultimately transforms it into sulfuric acid (H_2SO_4) which is deposited as acid rain. After 2013 in our pollution-transport model we incorporate SO_2 control technology and policy that would reduce SO_2 emissions and as a result acid rains are less possible.

From the results of these models, the variables that drive GHG and air pollutant reduction are

identified.

Acknowledgements

This thesis could not have been written without the support, in different ways, by many people.

First of all, I would like to thank my supervisor Prof. Dr. Ivo Šlaus for many stimulating discussions that have considerably shaped my thinking about the climate change problem. I am deeply indebted to him and Prof. Dr. Aleksander Zidanšek for their support and for the guidance that they have provided to modeling of dynamic systems, as well as for comments on earlier versions of the manuscript which served as very useful guides in preparing the final version.

I am extending special thanks to *Prof. Dr. Robert Blinc*, *Prof. Dr. Naim H. Afgan and Prof. Dr. Lojze Sočan*, who were so kind to serve as evaluators of this thesis, and who will find here some of their ideas and models.

A special gratitude I devote to Prof. dr. Peter Stegnar, to whom belongs the most merit for the opportunity given to me to finish my doctoral studies at the Institute Jozef Stefan in Ljubljana. Thanks to him from my heart.

Particular thanks go to my parents, late Hamit Kabashi and Gjyla Kabashi, who never stopped supporting me on my long and difficult course of education. And, finally, I thank my wife Selvete for the support and patience, and my beloved children Petrit, Yllka and Arianita, who give me courage to attain my aim.

References

JOURNAL ARTICLE:

Abrahamson, D.E (ed.). 1989. The Challenge of Global Warming. Washington: Island Press.
Annual Reviews of Fluid Mechanics, **15** 345-386.

Bekteshi, S.; Kabashi, S. Šlaus, I.; Zidanšek, A.; Najdovski, D. Modeling rapid climate changes and analizing their impacts. *An International Journal Manangement of Environmental quality* **19,** 422-432 (2008)

Blinc, R.; Najdovski, D.; Bekteshi, S.; Kabashi, S.; Šlaus, I.; Zidanšek, A. How to achieve a sustainable future for Europe. *Thermal Science* **12** 19-25 (2008)

Berner, R.; Lasaga, A. Modeling the geochemical carbon cycle. *Scientific American* **260**: 74-81 (1989)

Calvert, J.G. and Sawyer, R.F. Achieving acceptable air quality: some reflections on controlling vehicle emissions. *Science* **261**: 37-45 (1993)

Hays, D.; Imbrie, J.; Shackleton, N.J. Variations in the Earth's orbit: Pacemaker of the ice ages. *Science*, **194**, 1121-1132.

Held, I. Climate models and the astronomical theory of ice ages. *Icarous* **50,** 449-461.

Held, I.; Suarez, M.J. Simple albedo feedback models of the icecaps. *Tellus*, **26**, 613-629 (1974)

Imbrie, J.; Imbrie, J.Z. Modeling the climatic response to orbital variation. *science* 2**07**, (1980)

Kasting, J.; Richardson, S.; Pollack, J..A hybrid model of the CO_2 geochemical cycle and its application to large impact events. *Am.J.Sci*. **286**:361-89

Keeling, C. ; Bacastow, R. ; Carter, S. ; Piper, T.; Whorf, M. ; Mook, W.; Roelofffzen, H.: A three-dimensional model of atmospheric CO_2 transport based on observed winds. 1. Analysis of observation data Geophys. Monogr. D.H. Peterson, ed: *American Geophysical Union*, **55**, 165-236

Klaassen, G.; Miketa, A.; Riahi, K.; Schrattenholzer, L. Targeting technological progress towards sustainable development, *Energy and Environment* **13** (4/5), 553-78 (2002),

Knuston,T.;.Delworth, T.;.Dixon, K.; Stouffer R..Model assessment of regional surface temperature trends (1949-1997) *Journal of Geophysical Research,* 104, **30**, 981-30, 996

Milankovitch, M. Kanon der Erdbestrahlungen und seine Anwendung auf das Eiszeitenproblem.Belgrade; 1941

Newell, R.; Dopplick T. Questions concerning the possible influence of anthropogenic CO_2 on atmospheric temperature. *Journal of Applied Meteorology* **18**, 822-825

Pritchford, M.; Jonson, B. Empirical model of vehicle emissions. Environmental Sci. Tech. **27**: 741-8 (1993)

Ramanathan, V. ; and others, Cloud Radiative Forcing and Climate: Results from the Earth Radiation Budget Experiment, *Science* **243** 57-63 (1989)

Ramanathan, V. ; Barkstrom, B. R. ; Harrison, E. F. Climate and the Earth's radiation budget. *PhysicToday* **42**, 22-33. (1989)

Ramanathan, V.; Coakley, J. A. "Climate Modeling Through Radiative-Convective Models," *Review of Geophysics & Space Physics* **16**,465 (1978):

Raval, A.; Ramanathan, V. Observational determination of the greenhouse effect. *Nature* **342**, 758-761 (1989)

Weitzman, J.; Milankovitch solar radiation variations and ice age ice sheet. *Nature*, **261**, 17-20 (1976).

Zidanšek,A.; Blinc,R.; Jeglič,A.; Kabashi,S; Bekteshi,S.; Šlaus,I. Climate changes, biofuels and the sustainable future. *International Journal of Hydrogen Energy*, doi: 10.1016/j.ijhydene.2008

BOOK:

Beltrami, E. *Mathematics for Dynamic Modeling* (Academic Press, San Diego,1998)

Berkowitz, Norbert. *An introduction to Coal Technology* (Academic Press, San Diego, CA, 1994).

Bruce, H. (ed.) *Dynamic Modeling* (Springer, New York, 1994).

Bunce, N.B. *Environmental Chemistry* (2nd Edition. Winnipeg, Canada: Wooers Publishing 1994).

Davis, S.C.. *Transportation Energy Data book*, (Edition 17. U.S. Department of Energy Report ORNL-6919. Washington, D.C: U.S. Government Printing Office. 1997)

Deaton, M. L. (ed.) *Dynamic Modeling of Environmental Systems* (©2000 Springer Science and Business Media, Inc, New York).

Fay, J. A. (ed.) *Energy and Environment* (New York Oxford University Press Copyright © 2002 M.I.T).

Firor, J. *The changing Atmosphere*: *A Global Challenge*. (New Haven, Yale University Press 1990).

Ford, A. *Modeling the Environment (*Island Press, Washington, 1999).
Franchi, J.R. *Energy in the 21 st Century* (World Scientific Publishing,New Jersy, 2005)
Goldie, J. (ed.) *In Search of Sustainability* (© CSIRO 2005, Collingwood Victoria Australia)
Gribbin, J. *Future Weather and the Greenhouse Effect* (Delacorte Press, New York, 1976).
Griffin, R.D. *Principles of Air Quality Management* (Ann Arbor, MI: Lewis Publishers. 1994).
Haberman, R. *Mathematical Models*: *Mechanical Vibrations, Population Dynamic, and Traffic Flow.*
(New Jersey, Prentice-Hall, Inc,1977).
Hansen, J. (ed.) *Climate sensitivity: Analysis if feedback mechanisms. In Climate Processes and Climate Sensitivity (*Academic Press, New York, 1984)
Hartmann, D.L. *Global Physical Climatology* (Copyright ©1994 by Academic Press, San Diego)
Hobbs. P. V. (ed.) *Aerosols and Climate* (A. Deepak Publishing,New York, 1988,).
Imbrie J.(ed.) *Ice Ages: Solving the Mystery*. (Onslow Publishers, short Hills, NJ. 224 pp. 1979).
John, H. (ed.). *Atmospheric chemistry and physics* (© 1998. by John Wiley & Sons. Inc.New York)
Kraljic, M.A. (ed.).*The Greenhouse Effect* (New York: H.W. Wilson, 1992).
Langer, Josef (ed.) *Forces Shaping the EU(*Frankfurt am Main. Berlin, Bern, Bruxelles, New York, Oxford, Wien, 2008)
Loulou, R. (ed.) *Energy and Environment*(©2005 by Springer Science and Business Media, Inc, New York).
Masters, G.M. *Introduction of Environmental Engineering and Science.*
(Upper Saddle River, NJ: Prentice-Hall, Inc. 1998).
MC Cartney, E. J.*Absorption and Emission by Atmospheric Gases*: *The Physical Processes*.
(Wiley New York, 320 pp,1983)
Meadows, D. (ed.) *Limits to Growth* (Chelsea Green Publishing, White River Junction, Vermont, 2004).
Miller, B.G. *Coal Energy Systems* (Elsevier Academic Press, San Diego, 2005).
Mycock, J.C. (et.) *Handbook of Air pollution Control Engineering and Technology*
(New York: Lewis Publishers,1995)
Peixoto, P. (ed.) *Physics of Climate (*Springer, New York, 1992).
Robinson, A. W. *Modeling Dynamic Climate Systems* (Springer-Verlag, New York 2001) .
Seinfled. J.H. (ed.) *Atmospheric Chemistry and Physics* (New Jersey: Wiley. 1998).
Sorensen, B. *Renewable Energy its physics, engineering, environmental impacts, economics & planning*
(by Elsevier Science .San Diego, 2004).
Theodore, L. *Environmental Technologies at the Nanoscale (*John Wiley, New Jersey, 2003).

ARTICLE IN BOOK/REFERENCE BOOK, CHAPTER IN BOOK:

Boer K. W., ed., pp. 71-159 Solar Energy, Vol 9. (American Solar Energy Society Boulder, CO, 1994).
Houghton J. T. (ed) Climate change: The IPCC Scientific Assessment. (Cambridge University Press, Cambridge, UK, 365 pp.1990).
Houghton, J.T. *Climate Change: The Science of Climate Change*. (Intergovernmental Panel on Climate Change, Cambridge University Press, Great Britain. 1996).
Kabashi, S. *Impacts of Renewable Energy on the Greenhouse Gas Reduction in Kosovo-Dynamic Modeling*. CD proceedings of the 6th Mediterranean Conference and Exhibition on Power Generation,Transmission, Distribution and Energy Conversion - Med Power (Thesaloniki, Greece 2008).
Renewables Global Status Report 2006 Update, *REN21*, published 2007, accessed 2007-05-16 Renewable and Alternative Fuels Basics 101. *Energy Information Administration Retrieved* on 2007-12-17.
Renewables in global energy supply: An IEA facts sheet. *International Energy Agency* (IEA). Global wind energy markets continue to boom – 2006 another record year.
Sočan, L. The European Union in a Global Context. In: A Developmental Approach Lagner J. (Editor), Forces Shaping the EU - Social Science Approaches to Understanding the European Union, Peter Lang Publishing Group, Frankfurt am Main, 2008

WEB PAGE:

EIA (Energy Information Administration) Alternatives to Traditional Transportation Fuels 1994, Volume II, Greenhouse Gas Emissions.
ESTAP (Energy Sector Technical Assistance Project) Kosovo, World Bank Grant No.TF-027791.
http://en.wikipedia.org/wiki/List_of_countries_by_carbon_dioxide_emissions_per_capita
http://enrin.grida.no/htmls/kosovo/SoE/energy.htm
http://www.ec.europa.eu/environment/ipcc/index.htm

http://www.eia.doe.gov/oiaf/1605/techassist.html.
http://www.eia.doe.gov/oiaf/1605/transport.html
http://www.epa.gov/otaq/greenhousegases.htm
IPCC 2007,Al Gore.An Inconvenient Truth: The Planetary Emergency of Global Warming.
IPCC Fourth Assessment Report: Climate Change 2007.
IPCC Scientific Assessment J.T. Houghton G.J Jenkins and J.J. Ephraums, eds, Cambridge University Press, Cambridge UK, vii-xxxiii.
IPCC Second Assessment Report: Climate Change 1995.
IPCC Third Assessment Report: Climate Change 2001.
IPCC Working Group I, 1990: Policymakers summary.
IPPC Directive, the European Commission, 1996.
IPPC Directive, the European Commission, 2006.
Kyoto Protocol: Status of Ratification, 10 July 2006.
MEM (Ministry of Energy and Mining) https://www.ks-gov.net/mem
National Research Council, 1975: Understanding Climate Change: A program for action. National Academy of Sciences, Washington, D. C.
REN21 (2008). Renewables 2007 Global Status Report page 9.
STELLA. Copyright©1985-2007 by ISEE systems, inc. www.iseesystems.com
The Kyoto protocol - A brief summary. European Commission. Retrieved on 2007-04-19
U.S. Environmental Protection Agency. 1998. National Air quality and Emissions Trends Report, 1996. Washington: U.S. Government Printing Office.

Index of Figures

Index of Tables

Index of Algorithms

Appendix

A Difference Equations for Earth Atmosphere Reservoir

Because we used two reservoir variables (one for the Earth one for the atmosphere), we can identify difference equations for each of these variables
In Table 6. and in the preceding discussion, we have defined a situation where the sum of all inflows and outflows are equal. The difference equations that follow are based on those constructs.
Thus, we expect our steady-state solutions to depict a balancing of energy flows into and out of the energy reservoirs.
For the Earth reservoir, E, we have:

$$E(t+\Delta t) = E(t) + (\Phi_3 + \Phi_6 - \Phi_4 - \Phi_5 - \Phi_8)\Delta t \tag{59}$$

In this equations, E(t+ Δt), E(t) represents the amount of energy per area(J/m^2) in the Earth reservoir on time, t+Δt respectively t,
Φ_i,i=3,6,4,5 and 8 represents flux (W/m^2) which inflow and outflow in the Earth reservoir see Table 6.
Than we have:

$$\frac{\Delta E}{\Delta t} = [(1-f_b)(1-a)\Phi_S + R_a A(t) - t_e E(t) - f_a(1-t_e)E(t) - (1-f_a)(1-t_e)E \tag{60}$$

$$\lim_{\Delta t \to 0} \quad \frac{\Delta E}{\Delta t} = \frac{dE}{dt} = (1-f_b)(1-a)\Phi_S + R_a A - E \tag{61}$$

In these equations; E- represents the amount of energy per area in the Earth reservoir(J/m^2) ;Φ_S - represents the solar flux (W/m^2) and A - represents the amount of energy per area in the atmosphere reservoir (J/m^2).
These equations require us to consider the parameters R_a and t_e in units of inverse time (t^{-1}).This is so because we need to achieve units of Watts per meter squared instead of Joules per meter squared for our inflows and outflows. R_a, therefore, is the fraction of the atmosphere's energy density (Joules per meter squared) that is radiated toward the Earth per time, and t_e is the fraction of Earth's energy density (Joules per meter squared) that is transferred to the atmosphere through thermal processes per time.
For the atmosphere reservoir, we have:

$$A(t+\Delta t) = A(t) + (\Phi_2 + \Phi_4 + \Phi_5 - \Phi_7 - \Phi_6)\Delta t \tag{62}$$

A(t+Δt), A(t) is amount of energy per meter squared (J/m^2) in Atmosphere on time t+Δt and t respectively
Φ_i, i=2,4,5,7 and 6 represents flux (W/m^2) which inflow and outflow in the atmospheric reservoir

$$A(t+\Delta t) = A(t) + [f_b(1-a)\Phi_S + t_e E(t) + f_a(1-t_e)E(t) - R_a A(t) - (1-R_a)A(t)]\Delta t \quad (63)$$

$$\lim_{\Delta t \to 0} \quad \frac{\Delta A}{\Delta t} = \frac{dA}{dt} = f_b(1-a)\Phi_S + [t_e + f_a(1-t_e)]E - A \quad (64)$$

In the steady state (equilibrium state) A=const. E=const., T=const=+15˚C.(Figure 32. and 33.)

$\frac{dE}{dt}$ =0, than E= $(1-f_b)(1-a)\Phi_S + R_a A$ (65)

$\frac{dA}{dt}$ =0, than A= $f_b(1-a)\Phi_S + [t_e + f_a(1-t_e)]E$ (66)

These two equations determine the relationship between A and E under Steady-State conditions.

B Difference Equations and Steady-State Solutions for cohort model

In modeling the Mobile source emission system we start from cohort model
Difference equations for cohort models are fairly straightforward. To put it simply, the value of a cohort at a point in time is the amount of inflow from the previous cohort minus the amount of outflow to the next cohort. In addition, if our cohort variables (light and heavy vehicles) have a leakage component, then we need to consider this as an additional outflow.
It should be obvious that these difference equations will be coupled equations. Every inflow to a cohort is an outflow of a previous cohort (except, of course for the first cohort). Every outflow from a cohort is a similarly an inflow to a subsequent cohort.
Let us now suppose that we have a generic cohort model with four cohorts
(X_1, X_2, X_3, X_4) For the time being, let us ignore our leakage component. Each cohort therefore will have an inflow defined as I_1, I_2, I_3,I_4 respectively, and an outflow defined as O_1, O_2, O_3,O_4 respectively. Now recognize that the amount flowing into a cohort is defined as the amount following out of the previous cohort. This in turn was the amount flowing into the pervious cohort at a time to $t - T_{i-1}$ where T_{i-1} is the transit time for the previous cohort. Note also that the outflow for any cohort is equal to the inflow to that cohort at a time equal $t - T_i$. Thus we would have the following series of equations.

For X_1: $X_1(t-\Delta t) = X_1(t) + I_1\Delta t - O_1\Delta t = X_1(t) + I_1(t)\Delta t - I_1(t-T_1)\Delta t$ (67)

$$\lim_{\Delta t\to 0}\frac{\Delta X_1}{\Delta t} = \frac{dX_1}{dt} = I_1(t) - I_1(t-T_{1)} \quad (68)$$

For X_2: $X_2(t-\Delta t) = X_2(t) + I_2\Delta t - O_2\Delta t = X_2(t) + I_1(t-T_1)\Delta t - I_2(t-T_2)\Delta t$ (69)

$$\lim_{\Delta t\to 0}\frac{\Delta X_2}{\Delta t} = \frac{dX_2}{dt} = I_1(t-T_1) - I_1(t-T_2-T_1) \quad (70)$$

For X_3: $X_3(t+\Delta t) = X_3(t) + \Delta t - O_3\Delta t = X_3(t) + I_2(t-T_2)\Delta t - I_3(t-T_3)\Delta t$ (71)

$$\lim_{\Delta t\to 0}\frac{\Delta X_3}{\Delta t} = \frac{dX_3}{dt} = I_1(t-T_2-T_1) - I_1(t-T_3-T_2-T_1) \quad (72)$$

For X_4: $X_4(t+\Delta t) = X_4(t) + I_4\Delta t - O_4\Delta t = X_4(t) + I_3(t-T_3)\Delta t - I_4(t-T_4)\Delta t$ (73)

$$\lim_{\Delta t\to 0}\frac{\Delta X_4}{\Delta t} = \frac{dX_4}{dt} = I_1(t-T_3-T_2-T_1) - I_1(t-T_4-T_3-T_2-T_1) \quad (74)$$

One observation that can be made for these rate equations is that they can all be simplified down to functions of I_1, the inflow into the first cohort. The difference equations simply track this initial inflow through each of the individual cohorts. If we know what the value for I_1 is for a given point in time then we can calculate the expected values of each of these rate equations. Thus if we have a spike or lull in our initial inflow we expect to see that spike or lull transported through each of the cohorts over time
The steady-state conditions occur at the point where all of the following are true:

$$\lim_{\Delta t \to 0} \frac{\Delta X_1}{\Delta t} = \frac{dX_1}{dt} = I_1(t) - I_1(t - T_{1)} = 0 \quad (75)$$

$$\lim_{\Delta t \to 0} \frac{\Delta X_2}{\Delta t} = \frac{dX_2}{dt} = I_1(t - T_1) - I_1(t - T_2 - T_1) = 0 \quad (76)$$

$$\lim_{\Delta t \to 0} \frac{\Delta X_3}{\Delta t} = \frac{dX_3}{dt} = I_1(t - T_2 - T_1) - I_1(t - T_3 - T_2 - T_1) = 0 \quad (77)$$

$$\lim_{\Delta t \to 0} \frac{\Delta X_4}{\Delta t} = \frac{dX_4}{dt} = I_1(t - T_3 - T_2 - T_1) - I_1(t - T_4 - T_3 - T_2 - T_1) = 0 \quad (78)$$

Each of the cohorts will thus be at steady state when,

$$I_1(t) = I_1(t - T_1) = I_1(t - T_2 - T_1) = I_1(t - T_3 - T_2 - T_1) = I_1(t - T_4 - T_3 - T_2 - T_1) \quad (79)$$

SUSTAINABLE ELEKTRICITY DEMAND-SUPPLAY FOR KOSOVA (SCENARIO 2)

C Model in CO_2 reduction emission due to renewable energy use in Kosovo

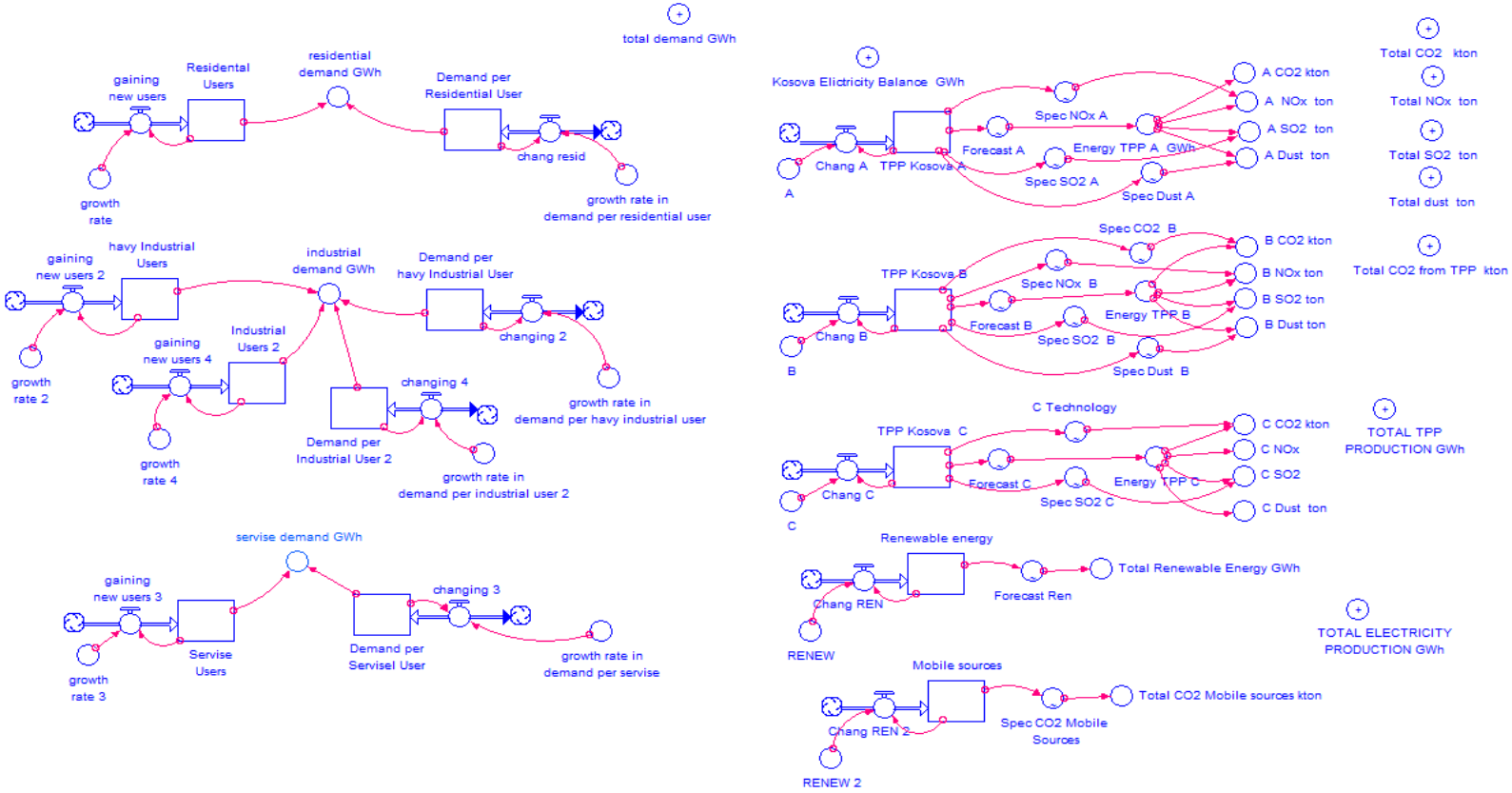

Modeling the Electrical Energy Demand–Supply and CO_2 Reduction

Table 14: Sustainable Electricity Demand-Supply for Kosova

D SUSTAINABLE ELEKTRICITY DEMAND-SUPPLAY FOR KOSOVA (SCENARIO2)																							
year	Total Demand	Kosova electricity production forecast(GWh)	Kosova electricitiy production units									Total Renewable	Total Nonrenewable Energy Production(GWh)	Percentage increase of renewable energy production in Kosovo	CO2 Emission factor(t/MWh)				CO2 From A(Mt/year)	CO2 From B(Mt/year)	CO2 From C(Mt/year)	Total CO2 Emission A+B+C(Mt/year)	Total CO2 Emission from Mobile Sources(Mt/year)	Total CO2 Emission From Transport and Energy Production
			Non renewable(TPP)			Renewable(HPP,WIND,SOLAR, BIOMAS)																		
						HPP AND litle HPP				Wind	Solar													
			A	B	C	R1	R2	R3	R4	R5	R6	R	A+B+C		EFA	EFB	EFC	EFR						
2000	3766	2014	628	1334		52						52	1962	2.58	1.5	1.4	0.8	0	0.94	1.87	0	2.81	0.64	3.45
2001	3876	2690	1138	1485		68						68	2623	2.51	1.5	1.4	0.8	0	1.71	2.08	0	3.79	0.70	4.48
2002	3991	3233	1294	1855		84						84	3148	2.61	1.5	1.4	0.8	0	1.94	2.60	0	4.54	0.74	5.27
2003	4111	3408	1536	1781		92						92	3317	2.69	1.5	1.4	0.8	0	2.30	2.49	0	4.80	0.78	5.57
2004	4235	3080	904	2089		86						86	2994	2.80	1.5	1.4	0.8	0	1.36	2.93	0	4.28	0.80	5.08
2005	4366	3786	860	2847		78						78	3708	2.06	1.5	1.4	0.8	0	1.29	3.99	0	5.28	0.82	6.10
2006	4501	4273	998	3212		63						63	4210	1.47	1.5	1.4	0.8	0	1.50	4.50	0	5.99	0.85	6.84
2007	4643	3928	825	3033		70			0			70	3858	1.77	1.5	1.4	0.8	0	1.24	4.25	0	5.48	0.88	6.36
2008	4792	4393	965	3320		107			0			107	4285	2.45	1.5	1.4	0.8	0	1.45	4.65	0	6.10	0.91	7.00
2009	4947	4436	999	3320		118			0			118	4319	2.65	1.5	1.4	0.8	0	1.50	4.65	0	6.15	0.94	7.08
2010	5109	4854	1418	3320		116			0	0	0	116	4738	2.40	1.5	1.4	0.8	0	2.13	4.65	0	6.77	0.97	7.75
2011	5279	5187	1760	3320		107			0	0	0	107	5080	2.07	1.5	1.4	0.8	0	2.64	4.65	0	7.29	1.01	8.30
2012	5457	5187	1760	3320		107	0	0	0	0	0	107	5080	2.06	1.5	1.4	0.8	0	2.64	4.65	0	7.29	1.05	8.34
2013	5643	7561	746	3068	3000	107	320	78	209	18	15	747	6814	9.88	1.5	1.4	0.8	0	1.12	4.30	2.4	7.81	1.05	8.86
2014	5839	7571	746	3068	3000	107	320	78	209	28	15	757	6814	10.00	1.5	1.4	0.8	0	1.12	4.30	2.4	7.81	1.05	8.86
2015	6044	7576	746	3068	3000	107	320	78	209	28	20	762	6814	10.06	1.5	1.4	0.8	0	1.12	4.30	2.4	7.81	1.01	8.82
2016	6259	7586	746	3068	3000	107	320	78	209	33	25	772	6814	10.18	1.5	1.4	0.8	0	1.12	4.30	2.4	7.81	0.99	8.81
2017	6485	6960	0	3068	3000	107	320	78	294	38	55	892	6068	12.82	1.5	1.4	0.8	0	0.00	4.30	2.4	6.70	0.97	7.67
2018	6722	6965	0	3068	3000	107	320	78	294	43	55	897	6068	12.88	1.5	1.4	0.8	0	0.00	4.30	2.4	6.70	0.95	7.65
2019	6972	6970	0	3068	3000	107	320	78	294	48	55	902	6068	12.94	1.5	1.4	0.8	0	0.00	4.30	2.4	6.70	0.93	7.63
2020	7234	8305	0	1368	5900	107	320	78	332	100	100	1037	7268	12.49	1.5	1.12	0.6	0	0.00	1.53	3.54	5.07	0.91	5.98
2021	7511	8305	0	1368	5900	107	320	78	332	100	100	1037	7268	12.49	1.5	1.12	0.6	0	0.00	1.53	3.54	5.07	0.87	5.94
2022	7802	8305	0	1368	5900	107	320	78	332	100	100	1037	7268	12.49	1.5	1.12	0.6	0	0.00	1.53	3.54	5.07	0.83	5.90
2023	8108	8305	0	1368	5900	107	320	78	332	100	100	1037	7268	12.49	1.5	1.12	0.6	0	0.00	1.53	3.54	5.07	0.79	5.86
2024	8431	8299	0	1368	5900	101	320	78	332	100	100	1031	7268	12.42	1.5	1.12	0.6	0	0.00	1.53	3.54	5.07	0.75	5.82
2025	8771	8299	0	1368	5900	101	320	78	332	100	100	1031	7268	12.42	1.5	1.12	0.6	0	0.00	1.53	3.54	5.07	0.70	5.78

Appendix

B List of publications

Papers 1, 2 and 3 and conference proceedings 8 and 9 are part of the Doctoral Dissertation

1. Robert Blinc, Dimitrij Najdovski, Sadik Bekteshi, Skender Kabashi, Ivo Šlaus, Aleksander Zidanšek, How to achieve a sustainable future for Europe, Thermal Science 12, 19-25, 2008 (Indexed in Science Citation Index Expanded)

2. Skender Kabashi, Sadik Bekteshi, Shukri Klinaku, Treatment of some electric properties in carbon nanotube, Kërkime - Research 14, 191-197, 2006

3. Aleksander Zidanšek, Robert Blinc, Anton Jeglič, Skender Kabashi, Sadik Bekteshi, Ivo Šlaus, Climate Changes, Biofuels and the Sustainable Future. Accepted to International Journal of Hydrogen Energy, doi: 10.1016/j.ijhydene.2008 (IF = 2.725)

4. Sadik Bekteshi, Skender Kabashi, Ivo Šlaus, Aleksander Zidanšek, Dimitrij Najdovski, Modeling rapid climate changes and analyzing their impacts. Management of Environmental Quality, Bradford: Emerald, 2008, vol. 19, no. 4, pp. 422-432

5. Skender Kabashi, Sadik Bekteshi, Shukri Klinaku, Analysis of some properties of nuclear interactions from nucleon-nucleon elastic scattering data, Kërkime - Research 14, 199-207, 2006

6. Skender Kabashi, Ymer Halimi, Sadik Bekteshi, Level density in interacting boson-fermion-fermion model (IBFFM) of the odd-odd nucleus 196Au, Albanian Journal of Natural and Technical Sciences, 2006, vol. XI (19 – 20), pp. 3-12

7. Skender Ahmetaj, Skender Kabashi, Sadik Bekteshi, Gravitational field in a 5-dimensional manifold of space-time-mass, Kërkime - Research 15, 191-197, 2007

8. Kabashi, S. Impacts of Renewable Energy on the Greenhouse Gas Reduction in Kosovo-Dynamic Modeling. CD proceedings of the 6th Mediterranean Conference and Exhibition on Power Generation,Transmission, Distribution and Energy Conversion - Med Power, Thesaloniki, Greece, 2008

9. Skender Kabashi, Sadik Bekteshi, G. Kabashi, Environmental and Climate Change Impacts on Sustainable Energy Demand-Supply in Kosovo. V: GUZOVIĆ, Zvonimir (ur.), DUIĆ, Neven (ur.), BAN, Marko (ur.). 4th Dubrovnik Conference on Sustainable Development of Energy, Water and Environment Systems, Dubrovnik, Croatia, June 2007, CD proceedings

10. Sadik Bekteshi, Skender Kabashi, Burim Kamishi, Advanced in Nucleon-Nucleon Scattering Experiments and their Theoretical Consequences, Sixth International Conference of the Balkan Physical Union American Institute of Physics Proc.-April 23,2007-Volume 899, pp.93-94

11. Sadik Bekteshi, Skender Kabashi Modeling Abrupt Climate Changes and Analysis of Their Impacts, Sustainable Development of Energy, Water and Environment systems: Proceedings of the 4th Dubrovnik Conference SDEWES, Dubrovnik, Croatia (2007)

12. Dimitrij Najdovski, Robert Blinc, Sadik Bekteshi, Skender Kabashi, Ivo Šlaus, Aleksander Zidanšek, Standardisation, Environmentally Friendly Technologies and Sustainable Development, in Sustainable Development of Energy, Water and Environment Systems: Proceedings of the 3rd Dubrovnik Conference, Dubrovnik, Croatia, 5-10 June 2005, Naim Afgan, Zeljko Bogdan, Neven Duic (Eds), World Scientific, 2007, ISBN 9812706402, 9789812706409

Submitted:

Skender Kabashi, Sadik Bekteshi, Dimitrij Najdovski, Robert Blinc, Ivo Šlaus, Aleksander Zidanšek, Dynamic Modeling the Climate Change Impacts on Sustainable Energy Demand-Supply in Kosovo, submitted to Global Environmental Change

Sadik Bekteshi, Skender Kabashi, Ivo Šlaus, Aleksander Zidanšek, Dimitrij Najdovski, Modeling and Analysis of Post-2012 Scenarios for Medium and Longer Term Pollution Emission Reduction, submitted to Climate Policy